ASSESSING THE ROLE OF WARM-SEASON MESOSCALE CONVECTIVE COMPLEXES IN SUBTROPICAL SOUTH AMERICAN PRECIPITATION VARIABILITY

by

JOSHUA D. DURKEE

(Under the Direction of Thomas L. Mote)

ABSTRACT

An investigation of the climatology and rainfall from warm-season (October-May) mesoscale convective complexes (MCCs) for subtropical South America (SSA) revealed the unique nature of these systems. Characteristic changes in MCCs in relation to the South Atlantic Convergence Zone (SACZ) were also explored.

For the austral warm seasons of 1998-2007, 330 MCCs were documented across SSA. An average of 37 MCCs occurred each season and reached a maximum cloud-shield size of 256,500 km^2, and lasted 14 hours. The highest frequency and concentration of MCCs was centered east of the Andes Mountains between 20°S and 30°S over Paraguay, northern Argentina, and southern Brazil. Compared to the United States, MCCs in SSA are significantly larger with longer durations.

An analysis of MCC rainfall was conducted with the use of the Tropical Rainfall Measuring Mission satellite 3B42 (v.6) three-hourly blended precipitation data. The average MCC produces 15.7 mm of rainfall across 381,000 km^2, with a volume of 7.0 km^3. MCCs accounted for 15-21% of the total rainfall across portions of northern

Argentina and Paraguay during 1998-2007. MCCs accounted for 20-30% of the total rainfall between November-February, and 30-50% in December, primarily across northern Argentina and Paraguay. MCCs also produced 25-66% of the total rainfall in portions of west-central Argentina.

Results further showed that for October-March, the SACZ occurred during 23% of the warm season days, during which 75 MCCs formed, versus 216 on non-SACZ days. Most of the interannual variation (89%) in the number of MCCs during periods of SACZ was simply due to changes in the frequency of SACZ. A composite analysis of several lower and middle tropospheric data fields show the large-scale atmospheric patterns favorable for MCCs in preferred areas of the study region during SACZ and non-SACZ periods. This study is unique in showing a link in a preferred region of MCC activity to forms of low-level circulation other than advections of heat and moisture from Amazonia.

INDEX WORDS: Mesoscale Convective Complex, Precipitation, Rainfall Contribution, South Atlantic Convergence Zone, Climatology

ASSESSING THE ROLE OF WARM-SEASON MESOSCALE CONVECTIVE COMPLEXES IN SUBTROPICAL SOUTH AMERICAN PRECIPITATION VARIABILITY

by

JOSHUA D. DURKEE

B.S., Western Kentucky University, 2000

M.S., University of Georgia, 2003

A Dissertation Submitted to the Graduate Faculty of The University of Georgia in Partial Fulfillment of the Requirements for the Degree

DOCTOR OF PHILOSOPHY

ATHENS, GEORGIA

2008

ASSESSING THE ROLE OF WARM-SEASON MESOSCALE CONVECTIVE COMPLEXES IN SUBTROPICAL SOUTH AMERICAN PRECIPITATION VARIABILITY

by

JOSHUA D. DURKEE

Major Professor: Thomas L. Mote

Committee: J. Marshall Shepherd
Andrew J. Grundstein
Todd C. Rasmussen

Electronic Version Approved:

Maureen Grasso
Dean of the Graduate School
The University of Georgia
August 2008

DEDICATION

I dedicate this dissertation foremost to my wife Becky, son Hunter, and two daughters Sierra and Bella. I am infinitely grateful to have such a supportive family. Your continuous love, laughter, and encouragement sincerely helped me in the successful completion of this degree. This dissertation is for you. Thank you.

I dedicate this dissertation also to my mom and dad. I have always looked up to you as role models who continue to succeed from hard work and determination. Without hard work and determination, I never would have succeeded in the completion of this degree. Thank you.

And to my grandma, my sister Kristen and her husband Jim, my brother Colin, thank you for your love and support throughout the years.

I dedicate this dissertation also to my parents-in-law, Dave and Lorraine. You have always provided me and my family with love and support. And to my brother and sister-in-law, Dean and Lisa, thank you for your support throughout my years in graduate school. Thank you.

ACKNOWLEDGEMENTS

First, I would like to acknowledge my wife, Becky. Thank you for encouraging me to pursue my dreams. All of the tiring days and long stressful nights that I encountered do not compare to the sacrifices you have made for me and our family to help me finish. You inspired me to push through the tougher times and to see this degree through. I simply could not have done this without you. Thank you!

I would also like to thank my children, Hunter, Sierra, and Bella for just being wonderful kids. You have brought nothing but joy to me. Thank you especially for tolerating my absence at times when you would rather have had me home.

I would like to acknowledge the immeasurable support from my entire family. Raising a new family during graduate school was quite challenging at times and you have helped the five of us here in Athens keep our heads held high throughout the years. You have my sincerest gratitude. Thank you.

And to my advisor, Dr. Thomas L. Mote, for sharing his expertise and mentoring me through my research, and guiding me toward an exciting career. Thank you. I would also like to acknowledge my committee members, Drs. J. Marshall Shepherd, Andrew J. Grundstein, and Todd C. Rasmussen, for their extensive advice and guidance throughout the years. And to Dr. Chor P. Lo, who also contributed as a committee member before passing away. Thank you.

I would also like to acknowledge Dr. John A. Knox (UGA), for sharing his expertise and continuous guidance, and for many wonderful collaborative research opportunities. Thank you.

I would like to thank Drs. George Huffman (NASA), Leila M. V. Carvalho (University of São Paulo), John Janowiak (NOAA), and Arlene Laing (UCAR) for their extensive guidance and patience with my questions during the early stages of my dissertation research. Thank you.

And to my colleagues and friends who never failed to inspire me to have a good time and to never back down. Your support is greatly appreciated. Thank you.

TABLE OF CONTENTS

Page

ACKNOWLEDGEMENTS v

LIST OF TABLES viii

LIST OF FIGURES ix

CHAPTER

1 INTRODUCTION AND LITERATURE REVIEW 1

1.1 Introduction 1

1.2 Literature review 2

1.3 Research questions 9

1.4 Summary 12

2 A CLIMATOLOGY OF WARM-SEASON MESOSCALE CONVECTIVE COMPLEXES IN SUBTROPICAL SOUTH AMERICA 17

2.1 Introduction 19

2.2 Background 20

2.3 Data and Methodology 24

2.4 Results 27

2.5 Conclusions 33

2.6 References 35

3 THE CONTRIBUTION OF MESOSCALE CONVECTIVE COMPLEXES TO RAINFALL ACROSS SUBTROPICAL SOUTH AMEERICA 58

3.1 Introduction 60
3.2 Data 63
3.3 Methodology 66
3.4 Results 68
3.5 Summary and Conclusions 73
3.6 References 76
4 CHARACTERISTIC CHANGES IN SOUTH AMERICAN MESOSCALE CONVECTIVE COMPLEXES IN RELATION TO THE SOUTH ATLANTIC CONVERGENCE ZONE 93
4.1 Introduction 95
4.2 Data and Methods 99
4.3 Statistical Analysis 101
4.4 Synoptic Analysis 105
4.5 Summary and Conclusions 110
4.6 References 115
5 SUMMARY AND CONCLUSIONS 134
5.1 Overview 134
5.2 Summary 136
5.3 Conclusions 141
REFERENCES 143

LIST OF TABLES

Page

Table 1.1. Mesoscale convective complex definition based on analysis of infrared satellite imagery 14

Table 2.1. Mesoscale convective complex definition based on analysis of infrared satellite imagery 39

Table 3.1. Mesoscale convective complex definition based on analysis of infrared satellite imagery 80

Table 3.2. Comparison of MCC precipitation characteristics between South America (SA), Africa (AF) (Laing et al. 1999), and (3) the United States (US) (McAnelly and Cotton 1989) 81

Table 4.1. Mesoscale convective complex definition based on analysis of infrared satellite imagery 118

Table 4.2. Summary of MCCs, and SACZ and non-SACZ periods during October-March for 1998-2997 119

Table 4.3. MCC composite characteristics based the presence and absence of the SACZ. 120

Table 4.4. The difference between the number of MCCs per SACZ day and non-SACZ day for each warm season 121

Table 4.5. Monthly percent of SACZ days (total number of SACZ days/ total number of days in a month) and the percent of MCCs that occurred during SACZ days (total number of MCC SACZ days/total number of SACZ days), respectively, given by the ordered pairs in each cell.....122

LIST OF FIGURES

Page

Fig. 1.1. (a) Land use/land cover and (b) elevation maps of South America 15

Fig. 1.2. Subtropical South America, including the states of Brazil and the provinces of Argentina.....16

Fig. 2.1. Elevation map of South America 40

Fig. 2.2. Sample scene from 11 January 2007 illustrating cloud shields that met the MCC "size" criterion, with the longitude and latitude location of the cloud-shield centroid and the -52°C cloud-shield area (km^2) 41

Fig. 2.3. MCC frequency per austral warm-season (October-May) for 1998-2007 42

Fig. 2.4. Box and whisker plot of warm-season MCC frequency by month for (a) the years 1998-2007 and (b) 1981-1983 (constructed from data given in Velasco and Fritsch 1987). 43

Fig. 2.5. Frequency for all MCCs during storm initiation, maximum size, and termination times 44

Fig. 2.6. As in Fig. 2.4 except for the maximum cloud-shield size.....45

Fig. 2.7. As in Fig. 2.6 except monthly 46

Fig. 2.8. As in Fig. 2.4 except for MCC lifecycle duration 47

Fig. 2.9. As in Fig. 2.8 except monthly 48

Fig. 2.10. The locations of the cloud shields (a) and centroid locations (b) from the 330 MCCs observed between the warm season months of October-May during 1998-2007 ..49

Fig. 2.11. MCC cloud shields during critical stages observed between the warm season months of October-May during 1998-2007 50

Fig. 2.12. Box plots of the latitudinal distribution of MCC cloud-shield centroid locations during each stage, where "I" is the initiation, "ME" is the maximum extent, and "T" is termination 51

Fig. 2.13. As in Fig. 2.12 except by warm season.....52

Fig. 2.14. As in Fig. 2.10 except by warm season.....53

Fig. 2.15. As in Fig. 2.10 except by month.....54

Fig. 2.16. As in Fig. 2.12 except by month.....55

Fig. 2.17. (a) Scatter plots showing relationships between latitude and cloud-shield area and (b) duration.....56

Fig. 2.18. Histograms and normal curves of MCC (a) duration and (b) maximum cloud-shield extent, and (c) scatter plot showing relationship between MCC duration and maximum extent.....57

Fig. 3.1. Bold outline delineates the La Plata Basin located in the subtropics of South America.....82

Fig. 3.2. Schematic diagram illustrating (a) cloud shields of an MCC overlaid onto a TRMM 3B42 precipitation grid, (b) the convex-hull calculation to determine the area within the MCC storm track, and (c) the final convex hull for the entire MCC duration and retaining only precipitation values within the storm-track area.....83

Fig. 3.3. Schematic representation of the precipitation summation for a hypothetical event.....84

Fig. 3.4. Sample output illustrating the outline of the area (i.e., convex hull) of an MCC storm track overlaid accumulated 3B42 TRMM precipitation.....85

Fig. 3.5. Flow diagram demonstrating the MCC identification and tracking, and precipitation schemes.....86

Fig. 3.6. MCC frequency during the warm season (October-May) for 1998-2007 (N = 330) determined by the number of times a grid point was located inside an MCC storm track.....87

Fig. 3.7. Distribution of the percentage of warm-season rainfall from MCCs during 1998-2007.....88

Fig. 3.8. As in Fig. 3.7 except by month.....89

Fig. 3.9. As in Fig. 3.7 except by warm season.....90

Fig. 3.10. Warm-season precipitation anomalies using 1998-2007 TRMM 3B42 as the baseline.....91

Fig. 3.11. MCC Impact Factors (MIFs) are in 0.5 standard deviation-unit intervals ranging from 1-6 92

Fig. 4.1. Subtropical South America, including the states of Brazil and the provinces of Argentina.....123

Fig. 4.2. Schematic diagram illustrating the SACZ region (hatched box) across South America.....124

Fig. 4.3. Spatial distribution of the 291 MCCs between October-March for 1998-2007 during the time of maximum extent.....125

Fig. 4.4. The number of MCCs (bold line) and the number of days during (a) SACZ and (b) non-SACZ periods (bars) 126

Fig. 4.5. MCC frequency (only during the presence of the SACZ) and the number of SACZ days in each warm season.....127

Fig. 4.6. Spatial distribution of MCCs that occurred during SACZ periods 128

Fig. 4.7. Locations of composite SACZ MCC subsets for the northwest and southwest quadrants (squares and circles, respectively; see Fig. 4.6), SACZ region (North-SACZ, triangles), high-latitude region (South-SACZ, circles with dots), and core MCC region (pentagons with dots), and non-SACZ MCCs in the core region (stars) and systems located inside the primary MCC region (see Fig. 4.2).....129

Fig. 4.8. Schematic diagram illustrating composite synoptic environment for MCCs that occurred during SACZ periods.....130

Fig. 4.9. As in Fig. 4.8 except for systems located inside the MCC region (see Fig. 4.1) during non-SACZ days 131

Fig. 4.10. 925 hPa wind vectors and the locations of MCCs (shaded areas) that occurred during (a) 1-8 January 2000, (b) 24-28 November 2005, (c), 27 January-2 February 2006, and (d) 27 December 2006-16 January 2007 SACZ periods.....132

Fig. 4.11. As in Fig. 12 except for “South” MCCs that took place during (a) 17-25 November 1999, (b) 1-8 January 2000, (c) 27 January-2 February 2006, and (d) 27 December 2006-16 January 2007 SACZ periods 133

CHAPTER 1

INTRODUCTION AND LITERATURE REVIEW

1.1 Introduction

Patterns of South American weather and climate are largely driven by interactions between the atmosphere, adjacent oceans, and the continent's complex physiographic landscapes and land cover characteristics (Figs. 1.1 and 1.2). The Andes are the longest, and one of the world's tallest mountain ranges with very steep elevation gradients. The Amazon region contains the world's largest rain forest and river basin. The combination of the position of the Andes, the cold Peruvian Humboldt current in the eastern Pacific, and the Pacific subtropical high pressure help create the Atacama Desert in northern Chile. The Atacama Desert receives < 10 mm of rainfall on average each year, making this region one of the most arid in the world (Thompson et al. 2003). In contrast, the Amazon basin provides a continuously rich moisture source for thunderstorms through the combination of evapotranspiration and return flow from subtropical Atlantic high pressure. The Andes channel the northeasterly low-level flow of tropical heat and moisture south of Amazonia into the La Plata Basin and subtropical Plains where some of the world's most extreme thunderstorms have been documented (Fig. 1.3) (Zipser et al. 2006).

1.2 Literature review

In subtropical South America (SSA), individual thunderstorms often conglomerate into single organized large-scale thunderstorm systems capable of producing damaging winds, destructive hail, tornadoes, and flooding rains. These thunderstorm complexes, or mesoscale convective systems (MCSs), are frequently observed across SSA during the warm season (October-May), and threaten to disrupt the communities that make up this relatively densely populated region of South America. The largest, longest-lived subclass of MCS is known as the mesoscale convective complex (MCC). MCCs were originally classified by Maddox (1980) from cloud-top characteristics of MCSs over the United States. These systems were observed by Maddox (1980) using infrared (IR) satellite imagery and defined based on explicit temperature, size, and duration criteria (Table 1.1). Since the foundational study provided by Maddox (1980), many researchers have adopted his MCC criteria to understand the characteristics of MCCs, particularly with respect to rainfall production and distribution across the U.S.

a. Characteristics of MCCs

MCCs have been studied all over the world including Africa (Laing and Frisch 1993a; Laing et al. 1999), India (Laing and Fritsch 1993b), China (Miller and Fritsch 1981), Australia (James 1992), Europe (Laing and Fritsch 1997), and most extensively in North America (Maddox 1980; Rogers et al. 1983; Merritt and Fritsch 1984; Kane et al. 1987; Tollerud et al. 1987; Cotton et al. 1989; McAnelly and Cotton 1989; Tollerud and Rogers 1991; Tollerud and Collander 1993; Anderson and Arritt 1998; Ashley et al.

2003, among others). Laing and Fritsch (1997) provided an analysis of MCC characteristics based from a global subset containing 714 MCCs. In that study, the typical MCC developed in the late afternoon, the maximum cloud-shield reached its maximum size in the early morning hours of the following day, and the system dissipated just after sunrise. MCCs were also identified primarily as a warm-season phenomenon, which indicates their connection to the seasonal radiative cycle. Laing and Fritsch (1987) also found that the typical MCC lifecycle lasts 10 hours with a contiguous ≤ -32°C cloud-shield size of 354,000 km^2 at the time of maximum extent.

b. Characteristics of MCC rainfall

McAnelly and Cotton (1989) found that MCCs in the U.S. distribute, on average, at least 1 mm of rainfall over nearly 500,000 km^2. Much of MCC rainfall is found beneath the colder cloud shield (≤ -52°C cloud top temperature), with precipitation maxima located within the equatorward flank of the storm system (McAnelly and Cotton 1989; Kane et al. 1987). Specifically, Kane et al. (1987) showed that the southeast quadrant typically accounts for more than half of the heaviest precipitation area beneath the anvil. The asymmetric rainfall distribution is largely due to the position of the southerly low-level jet relative to the storm's mean eastward motion in the U.S. (Bartels and Rockwood 1983; Merritt and Fritsch 1984; Kane et al. 1987; McAnelly and Cotton 1989; Collander and Tollerud 1993). Ashley et al. (2003) showed MCC rainfall accounts for 8-18% of the annual rainfall across portions of the central U.S.

c. Impacts of MCC rainfall

While MCCs have the ability to generate a variety of severe convective weather phenomena (e.g., damaging winds, large hail, and tornadoes), torrential rains and flooding must also be regarded as a major constituent of the hazards produced from these systems (Houze et al. 1990; Maddox 1983). Previous studies asserted that MCC rainfall has considerable social and economic impacts, particularly agricultural, across the Great Plains and Midwest of the U.S. In particular, Rogers et al. (1983) showed that a single MCC occurrence can produce detrimental effects in terms of injuries and casualties, and property and crop damage.

Annual MCC summaries for the U.S. (Maddox 1980; Rogers et al. 1983; Augustine and Howard 1988; Anderson and Arritt 1998) illustrate the devastating societal impacts of heavy persisted rainfall produced from MCCs. According to Maddox (1980), one in five MCCs during 1978 resulted in injury or death. Rogers et al. (1983) found several injuries and fatalities were associated with 27 of the 37 reported flash-flood-producing MCCs. Of the 28 MCCs observed during 1993, 18 were associated with extensive flooding in the central Plains and Midwest and also resulted in numerous casualties (Anderson and Arritt 1998). These summaries highlight the magnitude of caution that must be taken during regarding MCC rainfall.

Aside from damaging floods, MCCs can produce widespread beneficial precipitation during the growing season in the region between the Rocky and Appalachian Mountains of the U.S. (Maddox 1979; Fritsch et al. 1986; Tollerud and Collander 1993 Ashley et al. 2003). Because MCC activity dominates this region during the warm season, the resultant precipitation can be valuable to the large agricultural

community that thrives in this region (Ashley et al. 2003). Specifically, Kane (1985) indicated that MCCs produce crucial July and August precipitation for the corn-growing season in Iowa. Fritsch et al. (1986) also suggested that MCC precipitation could hinder the onset of drought for portions of the central U.S.

d. South American MCCs

Velasco and Fritsch (1987) provided one of the earliest investigations of South American MCCs. In that study, the highest concentration of MCC activity was found between 20°-40°S in the subtropical region. Results from their two-year analysis also showed that MCCs in SSA were predominantly nocturnal events that lasted 11.5 hours, and reached maximum cloud-shield extents (≤ -52°C cloud-shield temperature) of 188,000 km^2. Similar to the hazards associated with North American MCCs, the spatial and temporal MCC characteristics found by Velasco and Fritsch (1987) indicates that heavy rainfall should also be regarded as one of the primary hazards produced from MCCs in South America. Specifically, Velasco and Fritsch (1987) found 47 of the 78 MCCs that occurred between November-April during 1981-1983 were associated with heavy rains (≥ 25 mm), while 11 MCCs were associated with floods from rainfall totals ≥ 100 mm. Four MCCs resulted in three injuries and 13 deaths in association with heavy rains from MCCs (Velasco and Fritsch 1987).

It is clear rainfall from extreme thunderstorms events poses a number of hazardous outcomes for humankind and the economy of SSA (IPCC 2007; Jonkman 2005; Carvalho et al. 2002; Mechoso et al. 2001; Velasco and Fritsch 1987). One of the most prominent hazards that results from heavy rainfall is flooding. Compared to a wide

spectrum of global natural disasters, freshwater flooding events are the most substantial in terms of the number of affected people (Jonkman 2005). Jonkman (2005) found that flash floods, which commonly occur in the wake of heavy precipitation events, have the highest mortality rate of any flood type. Lastly, Jonkman (2005) found on average, 100 people are killed per flooding event across the American continents.

However, there are beneficial impacts of rainfall produced from large, long-lasting thunderstorm complexes. For example, Mechoso et al. (2001) stated that the La Plata Basin is one of the largest food-producing regions in the world. The economy of the region is largely supported from agriculture, which is highly dependent on rainfall. Many of the waterways inside the region are navigable for the transport of commodities. Nearly 80% of the electricity demand inside the basin is met with the use of hydropower (Mechoso et al. 2001). Thus, the precipitation feeds one of the leading natural resources of SSA.

From these assessments, MCCs are potentially one of the most influential weather systems for SSA in terms of adverse and/or beneficial outcomes in relation to rainfall production and distribution. However, there is a paucity of research focusing on South American MCCs. Much of our current understanding of MCCs in SSA is based on results from a single study by Velasco and Fritsch (1987), which is now two decades old. The primary limitation of that study is that it only contains a two-year sample. While much of the MCC characteristics documented in Velasco and Fritsch (1987) are similar to previous studies of MCC in other regions around the world, it is possible that under-sampling may have influenced their findings. This is especially true given the years of investigation: 1981-1983. Velasco and Fritsch (1987) point out that part of their study

period includes one of the strongest El Niño events on record. The frequency of MCCs increased from 22 during 1981-1982 to 56 during the El Niño year of 1982-1983. Numerous other studies have demonstrated that the interannual variability in South American weather and climate patterns are strongly influenced by the El Niño/Southern Oscillation (Curtis 2008; Silva and Ambrizzi 2006; Carvalho et al. 2004 and 2002; Lau and Zhou 2003; Nieto-Ferreira et al. 2003; Barros et al. 2002; Berbery and Barros 2002; Liebmann and Marengo 2001; Grimm et al. 2000 and 1998; Ropelewski and Halpert 1987; among others). Other studies of South American MCCs limited the focus to specific events or concentrated on MCC occurrences across relatively smaller areas within the continent (e.g., Figueiredo and Scolar 1996; Duquia and Silva Dias 1994; Rocha 1992; Scolar and Figueiredo 1990; Silva Dias 1987; Guedes 1985; Guedes and Silva Dias 1984). Therefore, a longer period of record is necessary in order to better understand and describe the physical characteristics of MCCs in SSA.

Another limitation in South American MCC literature is the lack of research regarding rainfall from MCCs. The only known study to explicitly focus on MCC rainfall in South America is provided by Viana (2006). In that study, 31 rain-gauges were used to quantify the contribution of MCCs to the total rainfall across the state of Rio Grande do Sul, Brazil, between October-December during 2003. Viana (2006) determined that MCCs contributed an average of 63% of the total rainfall across the state during that period. Nevertheless, our knowledge of South American MCC rainfall remains limited.

Perhaps the lack of MCC rainfall studies is due to sparse data availability across SSA. There is no sufficiently dense, quality-controlled rain-gauge or radar network with

a long-term period of record to accurately quantify precipitation across all of SSA. Furthermore, space and time resolutions of many available gridded precipitation datasets are not adequate to examine precipitation variability of mesoscale phenomena. The advent of space-borne instruments for estimating rainfall offers the opportunity to address these concerns. Satellites offer rainfall data at finer space and time scales, which allows scientists to avoid the difficulties inherent in the existing *in situ* precipitation datasets. A climatological investigation of MCCs in SSA, combined with the availability of fine-scale remotely sensed rainfall data, is exploited in this dissertation to assess MCC rainfall across the region. Ultimately, the goal of this work is to provide a unique climatological understanding of the physical and rainfall characteristics of MCCs for SSA.

e. MCCs and the South Atlantic Convergence Zone

One important climatological feature that has been shown to influence precipitation patterns across South America is the South Atlantic Convergence Zone (SACZ) (Liebmann et al. 2004 and 1999; Carvalho et al. 2004 and 2002; Jones and Carvalho 2002; Barros et al. 2002; Lenters and Cook 1999; Nogués-Paegle and Mo 1997; Figueroa et al. 1995; Kodama 1992). The SACZ is a subjectively defined warm-season phenomenon, whereby a quasi-stationary northwest-southeast oriented band of convection is located over central Amazonia, extending toward southeastern Brazil and the western Atlantic Ocean. Research has shown that the SACZ strongly influences the direction of the low-level tropical heat and moisture transport from the Amazon Basin via the low-level jet (LLJ), which results in a geographical displacement of maximum precipitation (Carvalho et al. 2004; Liebmann et al. 2004 and 1999; Nieto-Ferreira et al.

2003; Barros et al. 2002; Nogués-Paegle and Mo 1997). Other studies have shown that long-lived organized thunderstorms are strongly connected to the location of the exit region of the LLJ (Saulo et al. 2007; Salio et al. 2007; Vera et al. 2006; Silva and Berbery 2006; Liebmann et al. 2004; Zipser et al. 2004; Nieto Ferreira et al. 2003; Marengo et al. 2002; Berbery and Collini 2000; Laing and Fritsch 2000; Nicolini and Saulo 2000, among others). Therefore, it is plausible to consider that the SACZ may affect MCC activity. Consequentially, changes in the spatial distribution of precipitation during the SACZ may be partly explained by changes in the frequency and location of MCCs.

1.3 Research questions

MCCs have been shown to contribute substantially to rainfall totals in various regions of the world (e.g., Ashley et al. 2003; Laing et al. 1999, McAnelly and Cotton 1989, Fritsch et al. 1986). The motivation for this dissertation stems from the dearth of South American MCC research, and addresses this issue in a three-part investigation.

The first manuscript (Chapter 2) provides a climatological assessment of MCCs in SSA during the austral warm-season (October-May) for 1998-2007. Physical attributes such as MCC duration, cloud-shield area, and cloud-system centroid locations are documented throughout the lifecycle of each event. Given the abundance of heat and moisture advected from the Amazon rainforest and Atlantic Ocean, in addition to the preliminary results provided by Velasco and Frisch (1987), it is hypothesized that MCCs in SSA are considerably large, long-lasting events, particularly compared to those in the U.S. Part of the motivation for this manuscript was to also identify differences among

the findings between Velasco and Fritsch (1987) and the current study. In order to investigate these differences, this study addresses the following questions:

- What are the annual and monthly MCC spatial distributions throughout SSA?
- How does MCC frequency vary throughout the warm season?
- What is the typical MCC diurnal cycle?
- Are there preferred areas within SSA for MCCs throughout the warm season?
- What is the relationship between the latitude and MCC size and duration?
- How do MCCs in SSA compare to those in the U.S.?

The second manuscript (Chapter 3) assesses the role of MCCs in warm-season rainfall variability across SSA for 1998-2007. A unique examination of MCC rainfall is conducted from the use of Tropical Rainfall Measuring Mission Multi-Satellite Precipitation Analysis (TMPA) 3B42 version 6 data (Huffman et al. 2007). This particular TRMM product provides global three-hourly rain rate estimates with latitudinal coverage between 50°N-S (0.25° x 0.25° grid) for the period of record. Following the hypothesis from the previous study, it is expected that MCCs contribute substantially to rainfall totals across SSA. It is further hypothesized that given MCCs are larger, longer-lasting events compared to those in the U.S., MCCs contribute larger fractions of the total rainfall across SSA when compared to the U.S. A combination of the MCC dataset and TMPA precipitation data allows for the following questions to be addressed:

- What are typical MCC rainfall characteristics, particularly with respect to aerially average rainfall totals, rainfall areas, and rain-rates?

- What are the annual and monthly distributions of MCC rainfall contribution for SSA?
- What part of SSA receives the greatest fractions of precipitation from MCCs?
- How does the contribution of MCCs to the total rainfall change throughout the warm season?
- What is the impact of MCC rainfall with respect to regional precipitation anomalies?
- How do rainfall characteristics for MCCs in SSA compared to MCCs in Africa and U.S.

The final manuscript (Chapter 4) examines the relationship between the SACZ and MCC activity between October-March of 1998-2007. Previous research has shown that MCCs are connected to the position the LLJ, and that the Amazonian LLJ is strongly influenced by the SACZ. It hypothesized that the SACZ modulates MCC activity through changes in synoptic environments conducive to MCC development. The remaining questions that will be addressed in this study include the following:

- How often is the SACZ present?
- How does the frequency and location of MCCs across SSA change during the presence of the SACZ?
- How often to MCCs occur during SACZ periods?
- Where in SSA is the variability in MCC activity greatest during SACZ periods?
- Are there significant differences in MCC physical characteristics between active and non-active SACZ periods?

- How do MCC rainfall characteristics change between active and non-active SACZ periods?
- What are typical synoptic environments conducive to SACZ and non-SACZ MCCs?
- Are there situations where MCC development is not associated with the Amazonian LLJ during active SACZ periods?

Velasco and Fritsch (1987) noted the similarities between the physiographic and atmospheric environments conducive to MCCs across the American continents. Specifically, MCCs are commonly found in the mid-latitudes, over very large river basins (i.e., Mississippi and La Plata) located on the lee sides of major mountain ranges (i.e., Rockies and Andes). Synoptically prime environments for both locations include ample influx of low-level heat and moisture transport, weak mid-level shortwave trough, and upper-level divergence. MCCs typically initiate in the warm sector or on the cool side of a quasi-stationary frontal boundary near the exit region of the LLJ. Given such similar environments, any differences found in the physical and rainfall MCC characteristics between the two continents may enhance our understanding of the behavior of MCCs.

1.4 Summary

South American weather and climate has been a particular topic of interest for scientists and research groups from around the world during the past two decades. Due to the social and economic relevance regarding the frequent occurrence of extreme thunderstorms and heavy precipitation, many researchers have narrowed their focus on

warm-season precipitation variability across the tropics and subtropics. A number of studies of South America have examined large, long-lived MCSs, and few have quantified MCS rainfall. Despite these research efforts, there remain only few studies of South American thunderstorms pertaining to the largest class of organized convection, the mesoscale convective complex.

The purpose of this dissertation is to enhance our limited understanding of South American MCCs by incorporating contemporary methods with the use of innovative remote sensing techniques to help fill the gap of South American MCC research. Results from this dissertation will provide a better understanding of South American MCCs in a global context, particularly with respect to the role of MCCs as contributors to the global hydrologic cycle (Laing et al. 1999).

Table 1.1 Mesoscale Convective Complex definition based on analyses of infrared satellite imagery.

Mesoscale Convective Complex (MCC) Definition	
Criterion	**Physical Characteristics**
Size	Interior cold cloud region with temperature of ≤ -32°C must have an area ≥ 100,000 km^2
	Interior cold cloud region with temperature of ≤ -52°C must have an area ≥ 50,000 km^2
Initiation	Size definition first satisfied
Duration	Size definition must be met for a period of ≥ 6 hours.
Maximum Extent	Contiguous cold-cloud shield (IR temperature -52°C) reaches maximum size.
Shape	Eccentricity (minor axis/major axis) ≥ 0.7 at time of maximum extent.
Terminate	Size definition is no longer satisfied
original MCC definition developed by Maddox (1980)	

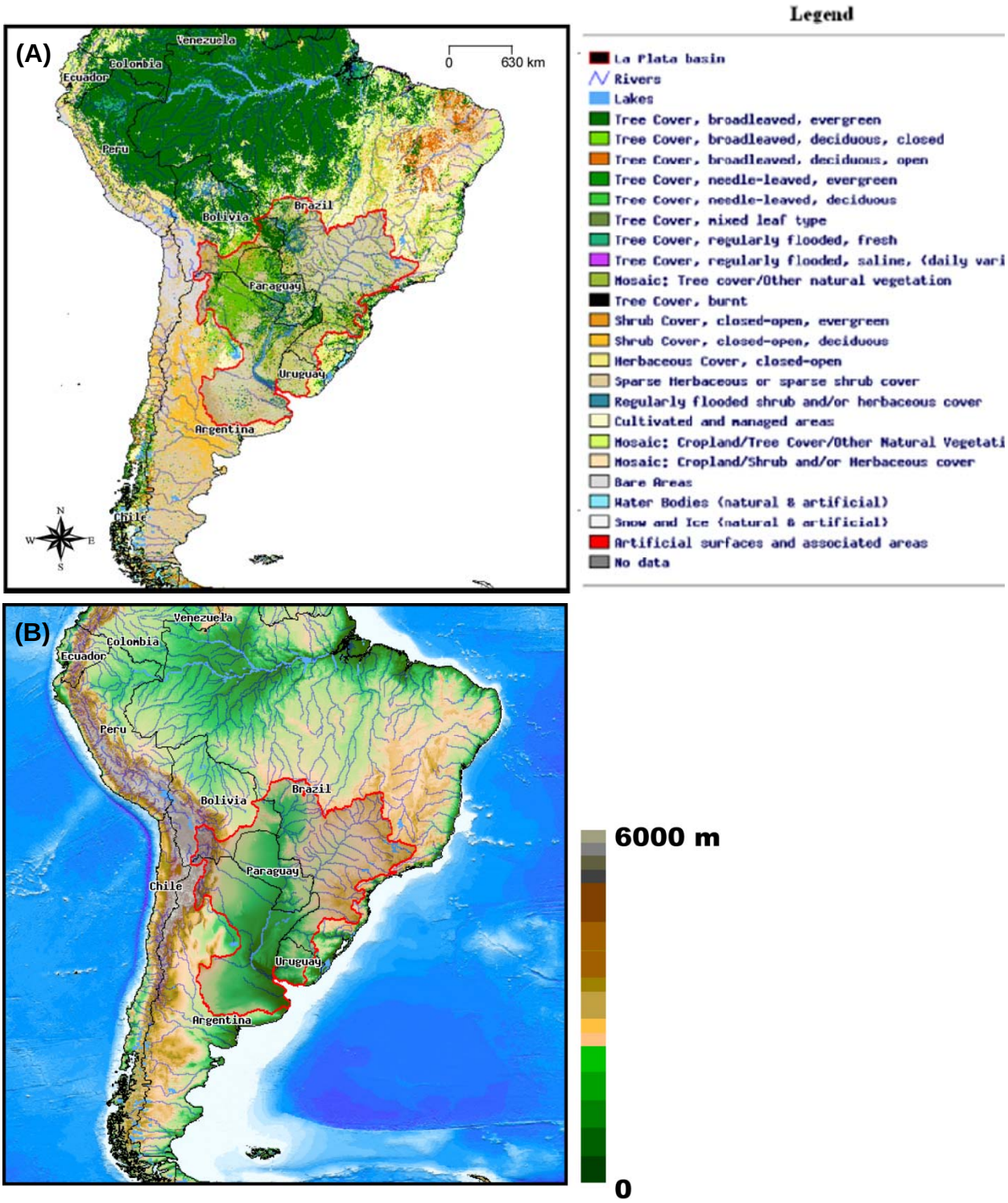

Fig. 1.1. **(**a) Land use/land cover and (b) elevation maps of South America. Map created from the National Center for Atmospheric Research Earth Observing Laboratory. Source: National Center for Atmospheric Research Earth Observing Laboratory.

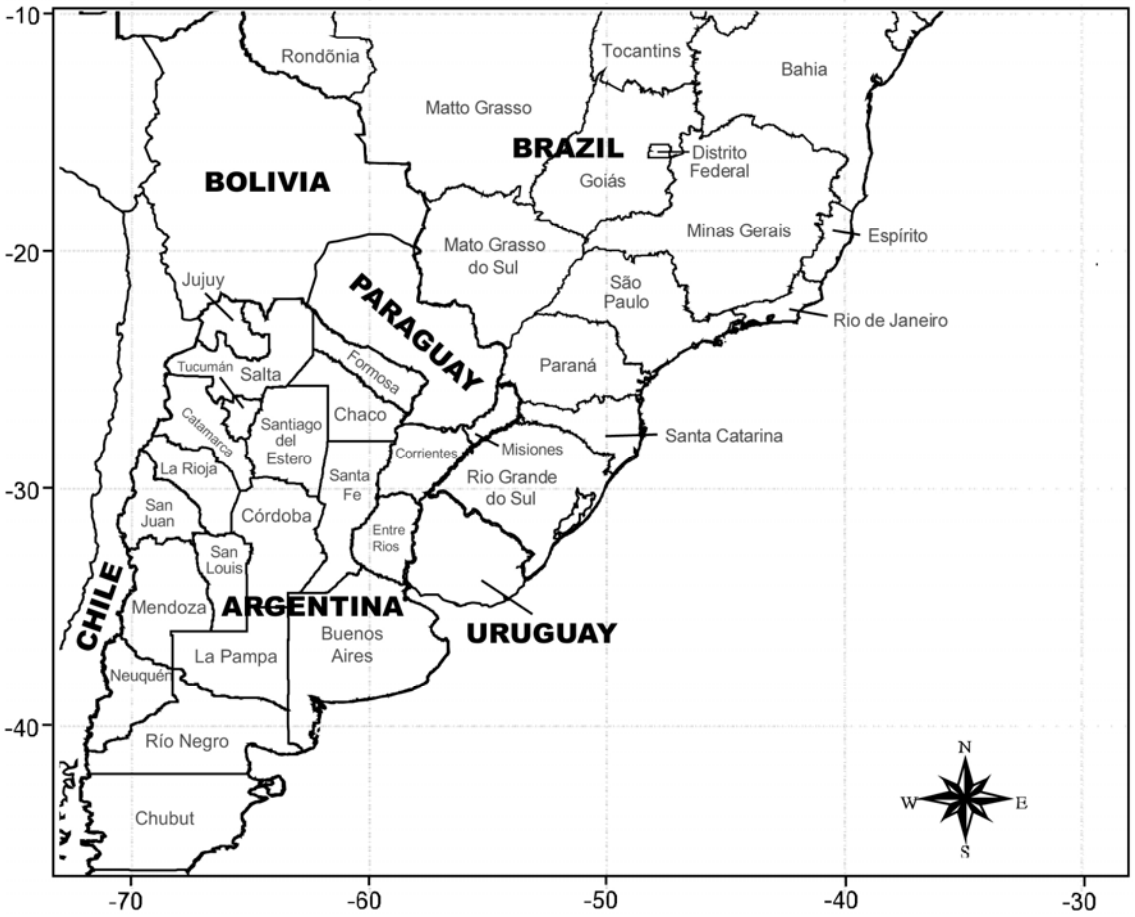

Fig. 1.2. Subtropical South America, including the states of Brazil and the provinces of Argentina.

CHAPTER 2

A CLIMATOLOGY OF WARM-SEASON MESOSCALE CONVECTIVE COMPLEXES IN SUBTROPICAL SOUTH AMERICA[1]

[1] Durkee, J. D. and T. L. Mote. Submitted to *International Journal of Climatology*, 03/21/08.

ABSTRACT

This study extends investigations of mesoscale convective complexes (MCCs) over subtropical South America (SSA) by describing the physical characteristics of MCCs during the austral warm season (October-May) for 1998-2007 in SSA. Within the nine warm seasons, 330 events were documented. An average of 37 MCCs occurred each warm season and reached a maximum cloud-shield size of 256,500 km^2, and lasted 14 hours on average. These findings show MCCs in SSA are larger and longer-lived than shown in previous work. Compared to the United States, MCCs in SSA are significantly larger with longer durations. Unlike U.S. systems, these events do not exhibit much poleward migration throughout the warm season. The highest frequency and concentration of MCC cloud shields is centered east of the Andes Mountains between 20°S and 30°S over Paraguay, northern Argentina, and southern Brazil throughout the warm season. As a result, there was little relationship between latitude, and MCC maximum extent or duration ($r = -0.178$ and -0.006, respectively). There is however, a moderate positive relationship ($r = 0.560$) between duration and maximum extent. Ultimately, MCCs in SSA are large, long-lasting events that possess great potential for contributing substantially to precipitation totals across the region.

2.1 Introduction

Subtropical South America (SSA) is a region susceptible to the timing, intensity, distribution, and variability of heavy precipitation events. This region – southern Bolivia, southern Brazil, Paraguay, northern Argentina, and Uruguay – is home to the world's fifth largest river basin, the La Plata Basin (Fig. 2.1). The La Plata Basin comprises 30% of the Earth's fresh water supply and drains one quarter of the entire continent. As one of world's top food producers, the economy of the region largely thrives from livestock and crop harvests. The Paraná, Paraguay, and Uruguay Rivers help supply nearly 80% of the basin's electricity through hydropower technologies. Moreover, the world's largest hydroelectric power plant facility is located along the Paraná River at the Itaipú Dam on the Brazil/Paraguay border. Overall, the La Plata basin generates 70% of the combined Gross National Product of the countries within the basin (Mechoso et al., 2001).

Indeed, one of the greatest threats for SSA is frequent occurrences from some of the world's most intense thunderstorm complexes (e.g., mesoscale convective systems (MCSs)) and their resultant heavy precipitation (Salio and Nicolini, 2007; Vera et al. 2006; Zipser et al. 2006; Silva and Berbery 2006; Nieto Ferreira et al. 2003; Carvalho et al. 2002; Velasco and Fritsch 1987, among others). MCSs are comprised of individual thunderstorms organized together as a larger-scale weather system with a contiguous precipitation area. Heavy rainfall from MCSs is often associated with floods, which can be disastrous to livestock, crops, and humankind. Undoubtedly, the lack of MCS rainfall could also be detrimental to the region's agricultural communities. Therefore, understanding the characteristics and role MCSs play in the subtropical hydroclimate of South America is imperative.

2.2 Background

Much attention has been devoted toward understanding interactions between the physical landscapes of South America with certain synoptic and mesoscale processes conducive to MCS development (Salio and Nicolini 2007; Zipser et al. 2006; Silva and Berbery 2003; Nieto Ferreira et al. 2003; Mota 2003; Carvalho et al. 2002, among others). Results from many of those studies include descriptions of physical characteristics of MCSs. However, the majority of those studies are limited in temporal scope to a few years or less. Even fewer studies of South American thunderstorms have focused on mesoscale convective complexes (MCCs) (e.g., Laing and Fritsch 1997 and 2000; Figueiredo and Scolar 1996; Duquia and Silva Dias 1994; Rocha 1992; Scolar and Figueiredo 1990; Silva Dias 1987; Velasco and Fritsch 1987; Guedes 1985; Guedes and Silva Dias 1984). MCCs, the largest MCS sub-class, exhibit large quasi-circular cloud shields (i.e., $\geq$ 50,000 km^2) that persist for $\geq$ 6 h (Table 2.1). MCCs have been widely studied in other parts of the world, including Africa (Laing and Frisch 1993a; Laing et al. 1999), India (Laing and Fritsch 1993b), China (Miller and Fritsch 1981), Australia (James 1992), Europe (Laing and Fritsch 1997) and most notably North America (Maddox 1980; Rogers et al. 1983; Merritt and Fritsch 1984; Kane et al. 1987; Tollerud et al. 1987; Cotton et al. 1989; McAnelly and Cotton 1989; Tollerud and Rogers 1991; Tollerud and Collander 1993; Anderson and Arritt 1998; Ashley et al. 2003, among others). A summary of global MCC populations and their large-scale environments was developed by Laing and Fritsch (1997 and 2000).

Previous MCC research has shown these particular systems are capable of producing tornadoes, severe hail, and damaging winds. However, based on the spatial

and temporal thresholds originally set forth by Maddox (1980), heavy precipitation must be regarded as a cause of several of the hazards produced by MCCs (Maddox, 1983; Houze et al. 1990). Perhaps the greatest hazards that result from heavy precipitation are persistent regional flooding, localized flash floods, mudslides, and property and crop damage (Maddox 1979; Maddox 1980; Maddox 1983; Tollerud et al. 1987; McAnelly and Cotton 1989; Houze et al. 1990; Anderson and Arritt 1998).

In addition, Maddox (1980) found one in five MCCs in the U.S led to injuries or deaths, while Rogers et al. (1983) found 27 of the 37 reported flash-flood-producing MCCs in the U.S during 1982 resulted in numerous injuries and casualties. Anderson and Arritt (1998) indicated that the extensive 1993 Midwestern flood was in part, attributed to 18 of the 27 recorded MCCs that resulted in many reports of injuries, deaths, and property and crop damage. In South America, Velasco and Fritsch (1987) found 11 floods and 13 casualties were attributed to 13 of the 78 MCCs during 1981-1983. Little research has documented MCC hazards outside the Americas.

Despite the documented negative impacts of MCC rainfall, numerous studies have also suggested that MCC precipitation is vital for sustaining agriculture and farming industries in the Great Plains and Midwest regions of the U.S. (Fritsch et al. 1986; Tollerud and Collander 1993; Ashley et al. 2003). Fritsch et al. (1986) suggested that MCC rainfall may help sustain balanced soil moisture budgets and possibly prevent the onset of drought. Ashley et al. (2003) and Fritsch et al. (1986) show that MCCs have contributed up to 60% of the total precipitation in portions of the central U.S. Laing et al. (1999) demonstrated that MCCs contributed an average of 22% of the total rainfall during July-September 1987 across portions of the Sahel in Africa. Laing et al. (1999)

suggested that MCCs may even contribute substantially to global hydrologic and energy cycles. Based on the findings and suggestions from previous studies, it is clear that MCCs possess the potential to have a large impact on precipitation patterns of a region. One such region that has been shown to experience recurring MCC activity similar to the U.S. is the subtropics of South America.

Compared to the global population of MCCs, North and South American systems share many similarities. Ashley et al. (2003) and Laing and Fritsch (2000) found the mean location for MCC genesis and initiation for the Americas are located on the lee side of major mountain ranges (Rockies and Andes) over plains regions. MCCs on both continents also commonly develop within similar atmospheric environments; baroclinic zones that contain high values of low-level vertical wind shear ($\geq$ 6-8 m s^{-1}) and convective available potential energy (CAPE) ($\geq$ 1500 J kg^{-1}); areas of maximized warm, moist air transport via a low-level jet; and upper-level divergence superimposed low-level convergence with the advancement of an approaching (and often weak) mid-level short-wave (Maddox 1980; Laing and Fritsch 2000). In one of the few available studies that explicitly focuses on the South American MCC population for a study period greater than one year, Velasco and Fritsch (1987) (hereafter, VAF) documented an average of 39 events during November-April across SSA for 1981-1983. The 15-year MCC climatological dataset put forth by Ashley et al. (2003) shows an average of 35 events for the U.S. annually. Both sets of events display similar diurnal patterns whereby MCC initiation generally occurs during the late afternoon/early evening hours, and reach maximum size near midnight, before dissipating during the morning.

Differences in MCC physical characteristics between the two studies show that, while the annual frequency of all events were similar in North and South America, South America had a much higher frequency of larger systems. These South American MCCs also had mean lifecycles up to two hours longer and average continuous cold cloud-shield areas nearly 23,000 km^2 greater in size[2]. VAF and Laing and Fritsch (2000) attribute these physical differences to greater moisture supply from the Amazon Basin, steeper mid-level lapse rates influenced from the upstream Andes, and higher tropopause heights.

The knowledge base for when and where these events occur and the atmospheric environments conducive to their development has been established for North America. However, in order to advance our understanding of South American MCCs, particularly in the subtropics, a climatological database of a longer duration is needed. The possibility remains that physical traits of the events documented in VAF might be biased given their short period of record (two years). In fact, VAF note the frequency of events between the two years they observed ranges from 22 to 56, the latter which occurred during a strong El Niño event. Numerous studies have shown that South American climate patterns, especially convective patterns, are strongly influenced by the El Niño/Southern Oscillation (ENSO). For example, Nieto Ferreira (2003) found greater MCS frequencies and nearly twice the rainfall amount across SSA during the 1998 El Niño compared to the 1999 La Niña. Therefore, a more complete and accurate description of MCCs in SSA may be established with an examination of a longer period of record.

[2] Note that this difference might be conservative as VAF used an 8°-12°C colder cloud-shield threshold than the original MCC criteria by Maddox (1980) due to modified IR image enhancement.

This investigation sets out to address this issue by providing climatological descriptions of the physical characteristics of subtropical South American MCCs during the austral warm season (defined here as October-May) for 1998-2007. The period of record was chosen based on the inclusion of a wide range of ENSO phases and magnitudes in an attempt to avoid potential bias in the dataset. Furthermore, high resolution precipitation products from low-orbiting satellites (e.g., the Tropical Rainfall Measuring Mission) are readily available during 1998-2007 for subsequent studies of MCC rainfall. Results from this study provide a more comprehensive understanding of South American MCCs and the characteristics that underlie these heavy rain producers. This is particularly important for the La Plata Basin, given its dependency on rainfall from events such as MCCs.

2.3 Data and Methodology

This study adheres to a strictly defined set of MCC cloud-shield criteria observable in infrared (IR) satellite imagery (see Table 2.1). Full disc GOES-8 and GOES-12 4 km IR satellite data, primarily at three-hourly time intervals, were provided by the National Oceanic Atmospheric Administration Comprehensive Large-array data Stewardship System (NOAA CLASS data available at: http://www.class.ncdc.noaa.gov). The nominal times for the 3-hourly satellite images were 0245, 0545, 0845, 1145, 1445, 1745, 2045, and 2345 UTC. There were occasional instances when nominal images were missing, but were available during other times (e.g., 1015 or 0315 UTC).

MCCs were documented using an automated cloud-top identification procedure similar to Augustine (1985). The procedure used here first consists of an automated

routine to identify all cloud shields in each satellite image that satisfy the "size" criterion in Table 2.1. Each group of pixels identified by this criterion was outlined by a polygon to delineate the peripheral border of the cloud shield. In order to determine the orientation and eccentricity of the contoured cloud shield(s), the authors used an empirical orthogonal function (EOF) analysis of pixel coordinates (see Jackson, 1991 and Carvalho and Jones, 2001). The output for each image time was threefold. First, in one output file each cloud shield was assigned a unique identification based on the year, Julian day, and time of occurrence. Each unique occurrence contains basic output of its physical properties including horizontal area, eccentricity, and longitude/latitude coordinates of the system centroid. Second, the longitude/latitude vertices of the polygon defining the cloud shield were output. The final output was an image of a scene illustrating the contoured outlines of all cloud shields that met MCC "size" criteria (Fig. 2.2).

The first step for tracking the cloud shields was to manually observe a sequence of scenes. System evolution was handled similar to the Machado et al. (1998) approach. When a system was observed to split, the cloud shield that closely resembled the previous scene (often the largest cloud shield within the split) was logged as a continuation of the lifecycle of that system. The remaining cloud shield was documented as system initiation and tracked separately as a new event. Merging cloud shields were handled in two ways. If a cloud shield was observed to merge with another smaller system, the lifecycle of the larger system was considered active. In contrast, if a cloud shield was observed to merge with another larger system, the smaller system's lifecycle was considered to terminate at the time of the merge. Manual observation of sequential scenes ensured confidence that

the rubrics of splitting and merging systems were handled properly. Once a cloud shield was identified with initiation and termination times, that group of cloud shields was flagged as one event and given a unique system identification. Because the regional focus was on the subtropical region, only systems where any portion of the cloud shield occurred south of 20°S at any point during its lifecycle were considered. What remained was a catalog of MCSs for SSA. The final step was to extract only those events which met the "duration" and "shape" thresholds in Table 2.1 in order to complete the requirements for MCC classification. This process was repeated over October-December and January-May blocks for each warm season spanning 1998-2007.

Other published examples of automated procedures designed to identify mesoscale convection include FORTRACC (Machado et al., 1998) and MASCOTTE (Carvalho and Jones, 2001). These procedures are also designed to track and document system lifecycles, thereby eliminating manual observation of successive satellite imagery. Two primary advantages for tracking convective systems using fully automated methods are that the analyses are consistently performed and are time efficient. However, one disadvantage includes the manner in which these routines handle the evolution of a given system (i.e., splitting and merging systems). Machado et al. (1998) compared the results between their fully automated method and approaches similar to this study (i.e., hybrid approach). They found that although hybrid approaches tends to handle the propagation trajectories better, the differences between the two methods are minimal for larger datasets. Despite the advantage for one technique over another, the authors of this study believe while the current approach can be somewhat subjective and labor intensive, it

provided an important opportunity to visually determine and verify the splitting or merging of cloud systems.

2.4 Results

Previous studies provided by Salio and Nicolini (2007), Vera et al. (2006), Zipser et al. (2006), Nieto Ferreira et al. (2003) Carvalho et al. (2002), and Machado et al. (1998) have shown that SSA is highly susceptible to MCS activity. The findings from this study provide support for the results from VAF that the largest and often longest-lived MCS class, the MCC, is no exception.

a. Temporal analysis

For the nine warm seasons during 1998-2007 there were 330 observed MCCs, with a median (average) of 33 (37) events (Fig. 2.3). Although mean warm-season frequencies between VAF and this study are similar, there are notable differences in monthly frequencies (cf. Fig. 2.4a and b). VAF show November as the month of peak MCC occurrence, while our study shows a peak during December and January. Also, the results of this study show a strong connection between the monthly MCC frequency pattern and the seasonal solar cycle, contrary to the results in VAF.

One disadvantage of analyzing 3-hourly satellite images is accurately identifying MCC diurnal patterns and other storm statistics, such as maximum cloud-shield size and system duration. For instance, it is likely the critical stages outlined in Table 2.1 (i.e., storm initiation, when the cloud shield reaches maximum extent, and storm termination) occurred between image times. While this is true regardless of the time interval between

images, uncertainty in the interpretation of the diurnal pattern increases with decreasing temporal resolution.

Fig. 2.5 illustrates MCC diurnal frequency for each critical stage. The greatest frequency of occurrence for initiation, maximum extent, and termination occurred between 1745, 2045, and 0245 UTC, respectively. Nearly 75% of all MCCs started between 1745 and 0245 UTC. Meanwhile, 78% reached maximum size between 2045 and 0845 UTC, and 77% dissipated between 2045 and 1145 UTC. Despite the temporal overlap in each stage, MCCs in SSA appear to occur more often at night (between 1745 and 0245 UTC).

The average size of all 330 MCCs at maximum extent was 256,500 km^2 – 27% larger than shown by VAF. The warm-season distribution of maximum cloud-shield sizes shows the 2002-03 and 2004-05 seasons had considerably larger MCCs (medians of 252,800 km^2 and 263,400 km^2, respectively), while MCCs in the remaining seasons were closer to 200,000 km^2 (Fig. 2.6). The largest MCCs occurred during late spring to early summer and late fall, while the smallest systems occurred during late summer (Fig. 2.7). The average duration for all events was 14 hours -2.5 hours greater than the duration given by VAF. There is a high degree of variability in MCC duration from year to year (Fig. 2.8). However, it appears that longer-lived storms tend to occur during spring to early summer and fall (Fig. 2.9).

b. Spatial analysis

From the nine warm seasons examined in this study, it is clear that MCCs in SSA are particularly large, long-lasting and relatively frequent events. This section illustrates the spatial distribution of MCCs in SSA.

By examining the location of the cloud shields and cloud-shield centroids, one can see MCCs are most frequent over Paraguay, northern Argentina, and portions of southern Brazil (Fig. 2.10). The same area also had the highest concentration of MCC cloud shields during each stage of their evolution (Fig. 2.11). Specifically, MCCs were mostly located within the 20°S-30°S latitude band during all stages (Fig. 2.12). These findings are especially important because the highest MCC precipitation rates are most likely to occur between storm initiation and maximum extent, while the greatest precipitation areas tend to occur near maximum extent (McAnelly and Cotton, 1989). In all warm seasons, the bulk of MCC activity was located between 20°S and 30°S (Fig. 2.13), with the highest concentrations of MCCs over much of Paraguay and northern Argentina (Fig. 2.14). The monthly analysis shows MCC frequency and concentration was greatest between 20°S and 30°S over Paraguay and northern Argentina during spring and summer. However, MCCs decreased in frequency and concentration, and exhibited a poleward shift in fall compared to summer (Figs. 2.15 and 2.16).

In summary, VAF showed the preferred hub of MCC activity throughout the warm season over Paraguay and neighboring areas of bordering countries. Results from this study lend support to that conclusion. From October through December, the frequency of MCCs increased at the same time they became more concentrated over Paraguay, northern Argentina, and portions of southern Brazil. In January, the frequency

was similar to December but MCCs became more widespread throughout the region. Both the extent and frequency of MCCs diminished throughout the remainder of the warm season. However, from February to April a slight poleward shift in the highest concentration of MCCs occurred, which placed the maximum over northern Argentina. The primary difference between the final two months is that the cloud shields became less concentrated in May.

c. Comparison to previous work

One of the only available studies that documented MCCs across SSA prior to this work has been provided by VAF. Although their study is presented in a climatological framework, their results only include two years of MCCs, one of which was collocated in time with a particularly strong ENSO warm event. The goal of this study was to extend their work and provide a more comprehensive analysis by examining the physical characteristics and spatial variability of MCCs across SSA for nine austral warm seasons during 1998-2007.

Overall, the findings between the two studies are similar, but there are a few notable differences. The first difference is in the monthly frequency of MCCs. While our study shows a monthly frequency pattern closely resembling a normal distribution centered on a peak during December and January, VAF showed a distinct peak in November, nearly double the frequency in any other month. Given that this study found that 80% of all MCCs occurred during November through March, we must conclude MCCs in SSA are tied to favorable synoptic environments (such as those described in section 2.2).

Another difference between this work and VAF is MCC duration and maximum extent. Our results show MCCs in SSA have longer lifecycles than previously documented –a mean duration of 14 hours (2.5 hours longer than VAF). Our study also found MCCs reach an average maximum size of 256,500 km^2, or 27% larger than VAF. On the other hand, VAF used an 8°-12°C colder cloud-top temperature threshold, which likely accounts for the smaller systems found in their study. Nevertheless, both studies highlight the fact that MCCs are very large, long-lasting, and frequently occurring events in SSA that possess great potential for contributing substantially to precipitation across the region.

d. Comparison between North and South American MCCs

This study utilized the 15-year. U.S. MCC database developed by Ashley et al. (2003) for a comparison of MCC characteristics between the American continents. As described in section 2.2, North and South American MCCs share many similar physiographic and atmospheric environments. However, key differences in their environments may partially explain differences in the characteristics of North and South American MCCs. These are the clues that can enhance our understanding of these prolific rain-producing events.

It is important to note while Ashley et al. (2003) considered the entire year, comparisons made hereafter are based only on their warm season (April-August) statistics. Ashley et al. (2003) found an average warm-season frequency of 33 events in the U.S., compared to the average 37 events for SSA. The lower U.S. frequency might be explained by an examination of eight months in this study compared to five months in

Ashley et al. (2003). This study chose a longer period based on the relatively higher frequency of MCCs into the fall. VAF suggested the extended warm season in SSA may be accounted for by the influence of the oceans on the relatively smaller land mass. VAF also added that MCCs in SSA have a higher frequency at relatively lower latitudes compared the U.S. Another difference exists within the monthly migratory patterns. Our study shows that MCC activity shows only a slight poleward migration toward the end of the warm season, whereas MCCs in the U.S. display distinct poleward displacement throughout each month. VAF suggested that these differences are likely explained by the migration pattern of the westerlies in both regions. The poleward shift in the westerlies is considerably greater over North America and MCC development tends to follow this pattern (VAF).

When comparing the differences between lifecycle durations and maximum sizes, the South American systems show remarkable differences from their North American counterparts. The maximum MCC cloud-shield size for the U.S. during the warm season is 164,600 km^2. An independent samples difference of means t-test was used to determine significant differences between North and South American MCC characteristics. Our results show MCCs in SSA are significantly larger, with an average size of 256,500 km^2 ($p = 0.01$). The results are similar for system durations. MCCs in SSA ($\bar{x}$ = 14 hours) last significantly longer than those of their North American counterpart ($\bar{x}$ = 10 hours) ($p = 0.01$).

Furthermore, Ashley et al. (2003) found MCCs had larger cloud shields and longer durations during the early warm season in the U.S. As the warm season progresses, MCCs often develop smaller cloud shields with shorter durations. Ashley et

al. (2003) suggested that these changes are tied to evolving synoptic and dynamic processes throughout the warm season. Tollerud and Rogers (1991) add that larger, longer-lived MCCs are more common during the early warm season due to proximities to moisture from the Gulf of Mexico. This study shows MCCs in SSA are somewhat larger and longer lasting during spring to early summer and fall compared to late summer systems. However, because a large proportion of MCC activity occurred between 20°S and 30°S, the relationship between latitude and MCC maximum extent or duration was weak ($p = 0.01$) (Fig. 2.17). However, there was a significantly moderate relationship that showed longer-lived MCCs in SSA are often larger ($p = 0.01$) (Fig. 2.18).

2.5 Conclusions

The subtropical region of South America is common place for intense thunderstorm activity. Over the recent decade, a great deal of research has been done to get a better understanding of the convective events that occur there, and the physical environments that influence their behavior. Subtropical South America is a region highly susceptible to heavy rains often produced from frequent occurrences of MCSs. This study extends the knowledge of South American MCS activity by focusing on the MCC, a particular subset of MCS that can produce prodigious precipitation.

Velasco and Fritsch (1987) provided the first examination of South American MCCs. That study was limited to a two-year analysis, with results that may reflect bias from a strong El Niño event that occurred during the sample period. Nevertheless, the results found by Velasco and Fritsch (1987) highlight the importance of utilizing a longer period of record in order to gain a better understanding of South American MCCs.

This study used a hybrid automated/manual approach to identify and track 330 MCCs across SSA between October-May during 1998-2007. On average, there are 37 MCCs each warm season with peak frequencies in December and January. These are predominantly nocturnal events that largely take place east of the Andes between 20°S and 30°S. MCCs in SSA typically last 14 hours and reach maximum sizes of 256,500 km^2. Due to the use of 3-hourly satellite data, some physical traits (e.g., lifecycle duration and maximum extent) are likely conservative estimates. Moreover, results from this work show considerable seasonal and monthly variability in the spatial distribution and physical characteristic of these MCCs.

The monthly frequency and spatial distribution suggest MCCs over SSA are likely connected to certain synoptic and mesoscale processes favorable for their development. Specifically, peak MCC frequency and concentration patterns in Paraguay, northern Argentina, and southern Brazil during summer are indicative of minimum static stability common during this time of year. From the results found in VAF, Laing and Fritsch (2000), and Vera et al. (2006), steep lapse rates develop from ample low-level heat and moisture supply from the Amazon Basin, and cold-air advection from the high terrain of the upstream Andes. Upper-level disturbances rotate through a quasi-stationary subtropical jet-stream, which provide enhanced ascent for the onset of convection. The mean position of the subtropical jet relative to areas of maximized low-level heat and moisture via the low-level jet helps explain the dominance of MCC activity between 20°S and 30°S.

A comparison between MCCs in the Americas shows that the systems in the Southern Hemisphere are significantly larger and longer-lasting events. Ashley et al.

(2003) found that larger and longer-lasting MCCs also produce the greatest and most widespread rainfall. Few studies have examined MCS precipitation across SSA. However, the majority of the analyses of those studies are limited in scope to a few years or less. The effort should be made to provide a quantitative assessment of MCC rainfall in SSA. The dominant presence of MCC activity in Paraguay, northern Argentina, and southern Brazil suggests these systems possess great potential for contributing substantially to precipitation totals across the region. The current study provides an excellent foundation for such a study.

2.6 References

Anderson, C. J., and R. W. Arritt, 1998: Mesoscale convective complexes and persistent elongated convective systems over the United States during 1992 and 1993. *Mon. Wea. Rev.*, **126**, 578–599.

Ashley, W. S., T. L. Mote, P. G. Dixon, S. L. Trotter, J. D. Durkee, E. J. Powell, and A. J. Grundstein, 2003: Effects of mesoscale convective complex rainfall on the distribution of precipitation in the United States. *Mon. Wea. Rev.*, **131**, 3003-3017.

Augustine, J. A., 1985: An automated method for the documentation of cloud-top characteristics of mesoscale convective systems. NOAA Tech. Memo. ERL ESG-10, NOAA/FSL, Boulder, CO, 121 pp.

Carvalho, L. M. V., C. Jones 2001: A satellite method to identify structural properties of mesoscale convective systems based on maximum spatial correlation tracking technique (MASCOTTE). *J. Appl. Meteor*., **40**, 1683–1701.

Carvalho, L. M. V., C. B. Jones, and B. Liebmann, 2002: Extreme precipitation events in southern South America and large-scale convective patterns in the South Atlantic Convergence Zone. *J. Climate,* **15**, 2377-2394.

Collander, R. S., and E. I. Tollerud, 1993: Characteristics of extreme rainfall in mesoscale convective complexes: a phenomenological study. Preprints, *13th Conference on Weather Analysis and Forecasting*, August 2-6, 1993: Vienna, Virginia, 393-396.

Cotton, W. R., R. L. McAnelly, and C. J. Tremback, 1989: A composite model of mesoscale convective complexes. *Mon. Wea. Rev.,* **117**, 765 -783.

Fritsch, J. M., R. J. Kane, and C. R. Chelius, 1986: The contribution of mesoscale convective weather systems to the warm-season precipitation in the United States. *J. Appl. Meteor.*, **25**, 1333-1345.

Houze, R. A., B. F. Smull, and P. Dodge, 1990: Mesoscale organization of springtime rainstorms in Oklahoma. *Mon. Wea. Rev.,* **118**, 613-654.

James, J., 1992: A preliminary study of mesoscale convective complexes over the mid-latitudes of eastern Australia. Tech. Report 66, Bureau of Meteorology, Melbourne, Australia, 30 pp.

Jackson, J. E., 1991: A user's guide to principal component analysis. Wiley-Interscience, 569 pp.

Kane, R. J., C. R. Chelius, and J. M. Fritsch, 1987: Precipitation characteristics of mesoscale convective weather systems. *J. Appl. Meteor.*, **26**, 1345–1357.

Laing, A. G., and J. M. Fritsch, 1993a: Mesoscale convective complexes in Africa. *Mon. Wea. Rev.,* **121,** 2254–2263.

Laing, A. G., and J. M. Fritsch, 1993b: Mesoscale convective complexes over the Indian monsoon region. *J. Climate*, **6**, 911–919.

Laing, A. G., and J. M. Fritsch, 1997: The global population of mesoscale convective complexes. *Quart. J. Roy. Meteor. Soc.,* **123**, 389–405.

Laing, A. G., J. M. Fritsch, and A. J. Negri, 1999: Contribution of mesoscale convective complexes to rainfall in Sahelian Africa: Estimates from geostationary infrared and passive microwave data. *J. Appl. Meteor.*, **38**, 957–964.

Laing, A. G., and J. M. Fritsch, 2000: The large-scale environments of the global populations of mesoscale convective complexes. *Mon. Wea. Rev.,* **128**, 2756-2776.

Machado, L. A. T., W. B. Rossow, R. L. Guedes, and A. W. Walker, 1998: Life cycle variations of mesoscale convective systems over the Americas. *Mon. Wea. Rev.,* **126**, 1630-1654.

Maddox, R. A., 1979: A methodology for forecasting heavy convective precipitation and flash flooding. *Natl. Wea. Dig.*, **4**, 30-42.

Maddox, R. A., 1980: Mesoscale convective complexes. *Bull. Amer. Meteor. Soc.*, **61**, 1374-1387.

Maddox, R. A., 1983: Large-scale meteorological conditions associated with mid-latitude mesoscale convective complexes. *Mon. Wea. Rev.* **111**, 1475-1493.

McAnelly, R. L., W. R. Cotton, 1989: The precipitation life cycle of mesoscale convective complexes over the central United States. *Mon. Wea. Rev.*, **117**, 784-808.

Mechoso, R. C., P.S. Días, W. Baetghen, V. Barros, E.H. Berbery, R. Clarke, H. Cullen, C. Ereño, B. Grassi and D. Lettenmaier, 2001: Climatology and Hydrology of the La Plata Basin. *Document of VAMOS/CLIVAR document*, 56 pp. [available online: http://www.clivar.org/organization/vamos/index.htm].

Merritt, J. H., and J. M. Fritsch, 1984: On the movement of the heavy precipitation areas of mid-latitude mesoscale convective complexes. Preprints, *10th Conf. Weather Forecasting and Analysis,* AMS, Tampa, FL, 529, 536.

Miller, D. and J. M. Fritsch, 1991: Mesoscale convective complexes in the western Pacific region. *Mon. Wea. Rev.*, **119**, 2978–2992.

Mota, G. V., 2003: Characteristics of rainfall and precipitation features defined by the Tropical Rainfall Measuring Mission over South America. Ph.D. dissertation, University of Utah, 215 pp.

NOAA, Comprehensive Large-Array Stewardship System, 2007: Silver Spring, MD. [available online: http://www.class.noaa.gov].

Nieto Ferreira, R. N., T. M. Rickenbach, D. L., Herdies, and L. M. V. Carvalho, 2003: Variability of South American Convective Cloud Systems and Tropospheric Circulation during January–March 1998 and 1999. *Mon. Wea. Rev.*, **131**, 961–973.

Rodgers, D. M., K. W. Howard, and E. C. Johnston, 1983: Mesoscale convective complexes over the United States during 1982. *Mon. Wea. Rev.,* **111**, 2363-2369.

Salio, P. and Nicolini M., 2007: Mesoscale convective systems over southeastern South America and their relationship with the South American low-level jet. *Mon. Wea. Rev.*, **135**, 1290-1308.

Sapiano, M. R. P. and P. A. Arkin, (2008): An inter-comparison and validation of high resolution satellite precipitation estimates with three-hourly gauge data. Submitted to *J. Hydr. Meteor.*

Silva, V. B. S. and E. H. Berbery, 2006: Intense rainfall events affecting the La Plata Basin. *J. Hydr. Meteor.,* **7**, 769-787.

Tollerud, E. I., D. Rodgers, and K. Brown, 1987: Seasonal, diurnal, and geographic variations in the characteristics of heavy-rain-producing mesoscale convective complexes: A synthesis of eight years of MCC summaries. Preprints, *11th Conf. Weather Modification*. Edmonton, Alta., Canada, 143-146.

Tollerud, E. I. and D. M. Rodgers, 1991: The seasonal and diurnal cycle of mesoscale convection and precipitation in the central United States: Interpreting a 10-year satellite-based climatology of mesoscale convective complexes. Preprints, *7th Conference on Applied Meteorology*. Salt Lake City, Utah, 63-70.

Tollerud, E. I. and R. S. Collander, 1993: Mesoscale convective systems and extreme rainfall in the central United States. *Extreme Hydrological Events: Precipitation, Floods and Droughts, International Association of Hydrological Sciences* Number *213*, 11-19.

Velasco, I., and J. M. Fritsch, 1987: Mesoscale convective complexes in the Americas. *J. Geophys. Res*., **92**, 9591–9613.

Vera, C., J. Baez, M. Douglas, C. B. Manuel, J. Marengo, J. Meitin, M. Nicolini, J. Nogués-Paegle, J. Paegle, O. Penalba, P. Salio, M. A. Silva Dias, P. Silva Dias, and E. Zipser, 2006: The South American Low-Level Jet Experiment. *Bull. Amer. Meteor. Soc.,* **87**, 63–77.

Zipser, E. J., D. J. Cecil, C. Liu, S. W. Nesbitt, and D. P. Yorty, 2006: Where are the most intense thunderstorms on Earth?. *Bull. Amer. Meteor. Soc*., **87**, 1057–1071.

Table 2.1. Mesoscale Convective Complex definition based on analyses of enhanced IR satellite imagery.

Mesoscale Convective Complex (MCC) Definition	
Criterion	**Physical Characteristics**
Size	Interior cold cloud region with temperature of ≤ -52°C must have an area 50,000 km^2
Initiation	Size definition first satisfied
Duration	Size definition must be met for a period of ≥ 6 hours.
Maximum Extent	Contiguous cold-cloud shield (IR temperature -52°C) reaches maximum size.
Shape	Eccentricity (minor axis/major axis) ≥ 0.7 at time of maximum extent.
Terminate	Size definition is no longer satisfied
MCC definition originally developed by Maddox (1980)	

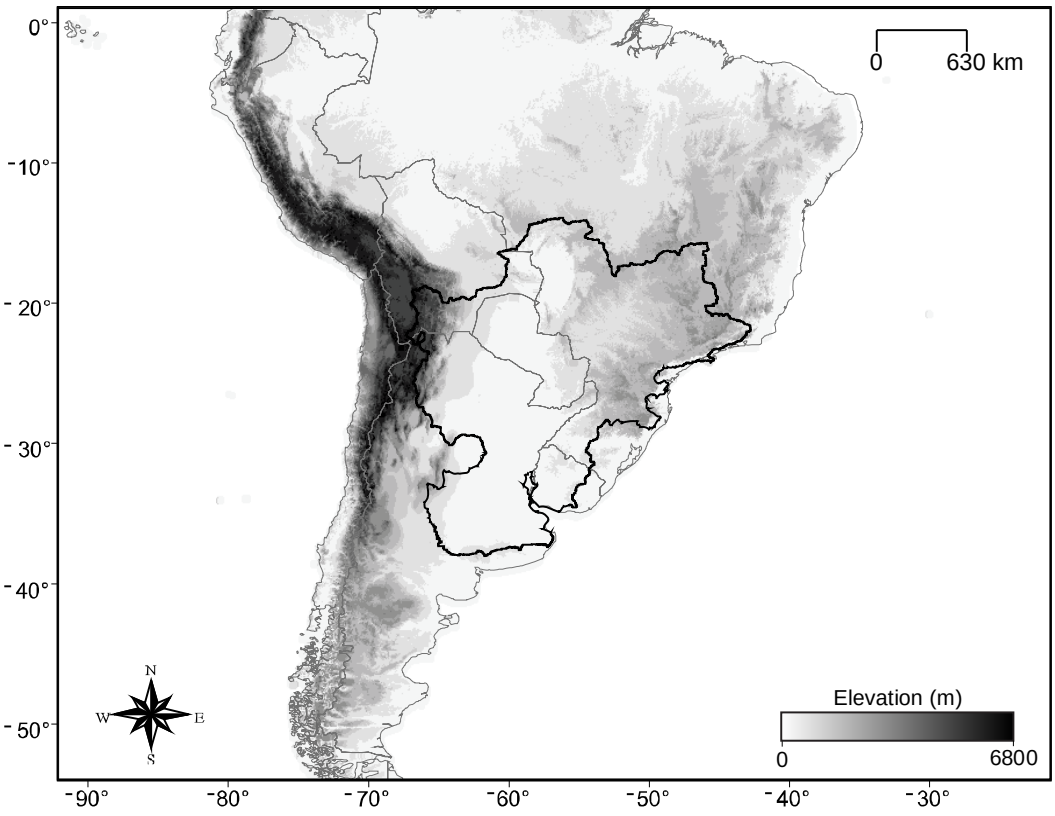

Fig. 2.1. Elevation map of South America. The perimeter of the La Plata Basin is indicated by the bold outline.

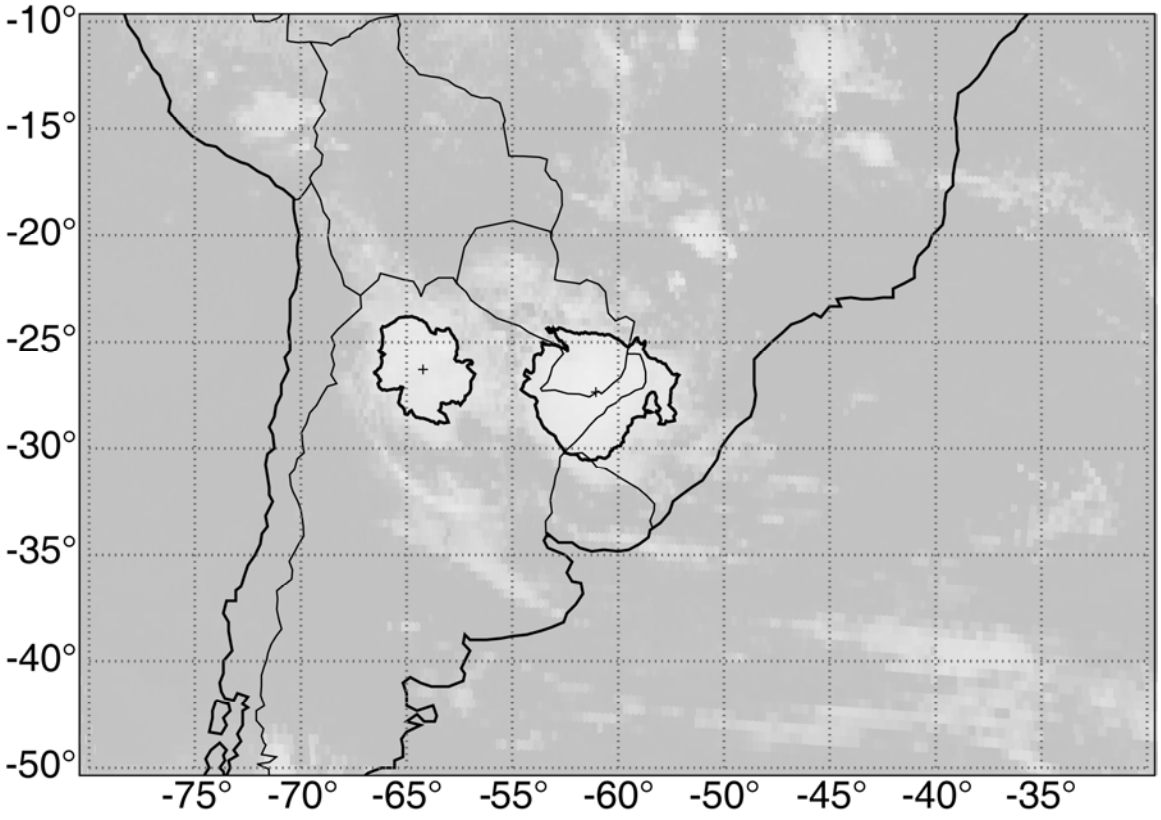

Fig. 2.2. Sample scene from 11 January 2007 illustrating cloud shields that met the MCC "size" criterion, with the longitude and latitude location of the cloud-shield centroid and the -52°C cloud-shield area (km^2). The "+" indicates the cloud-system centroid.

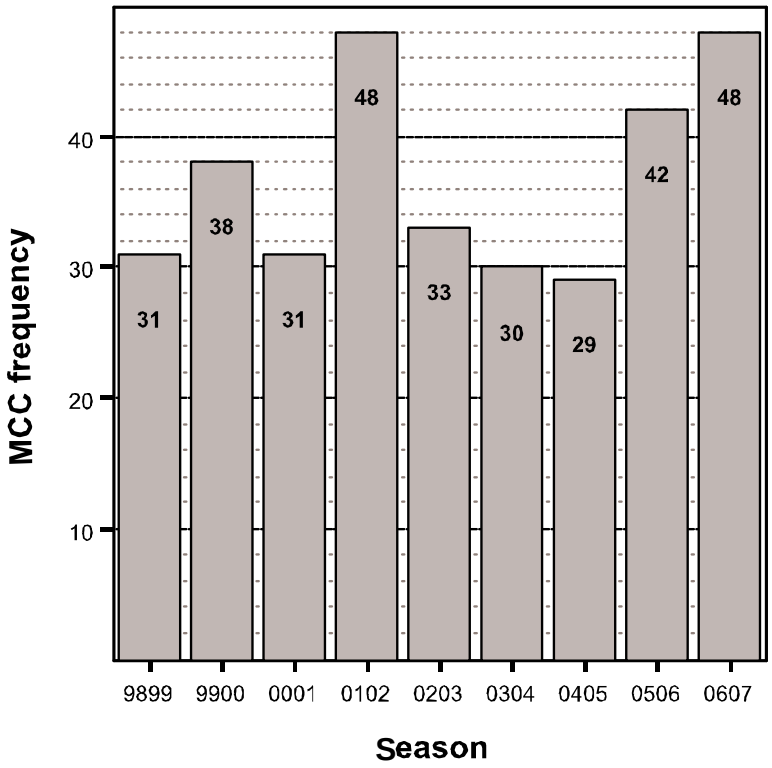

Fig. 2.3. MCC frequency per austral warm-season (October-May) for 1998-2007.

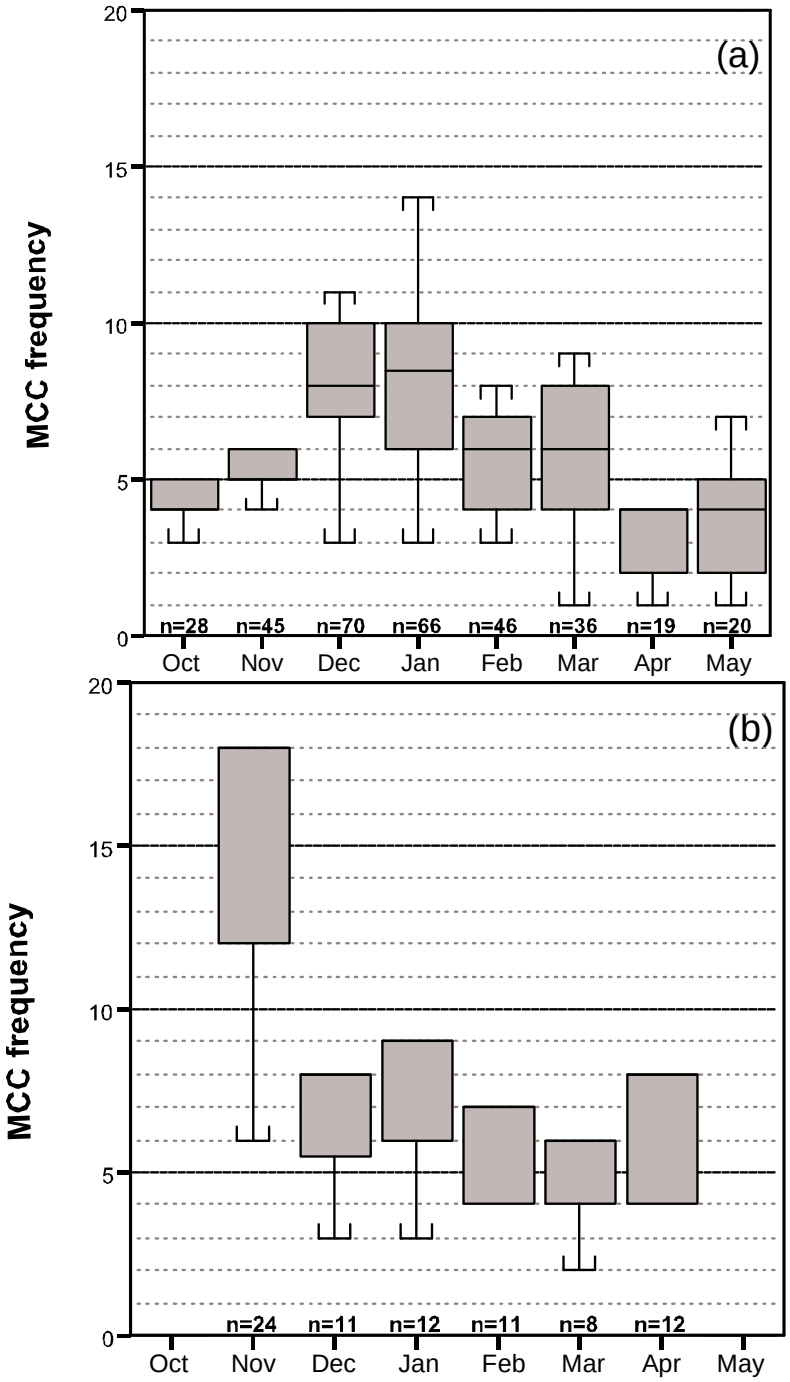

Fig. 2.4. Box and whisker plot of warm-season MCC frequency by month for (a) the years 1998-2007 and (b) 1981-1983 (constructed from data given in Velasco and Fritsch 1987). The boxes show the inter-quartile range, the whiskers show the 10th and 90th percentiles, and the solid line indicates the median. N is equal to the total frequency of events for a given month for the entire period of record.

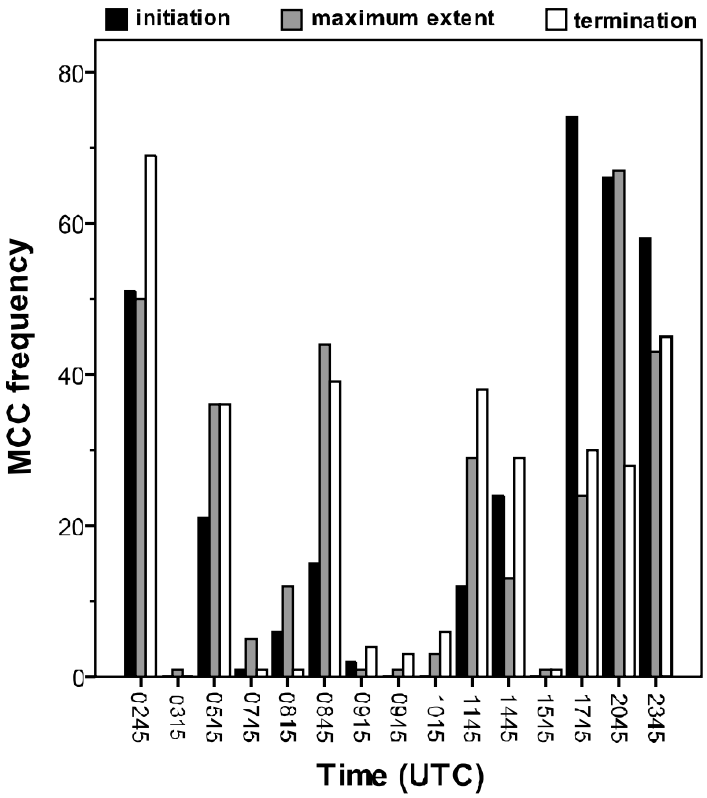

Fig. 2.5. Frequency for all MCCs during storm initiation, maximum size, and termination times.

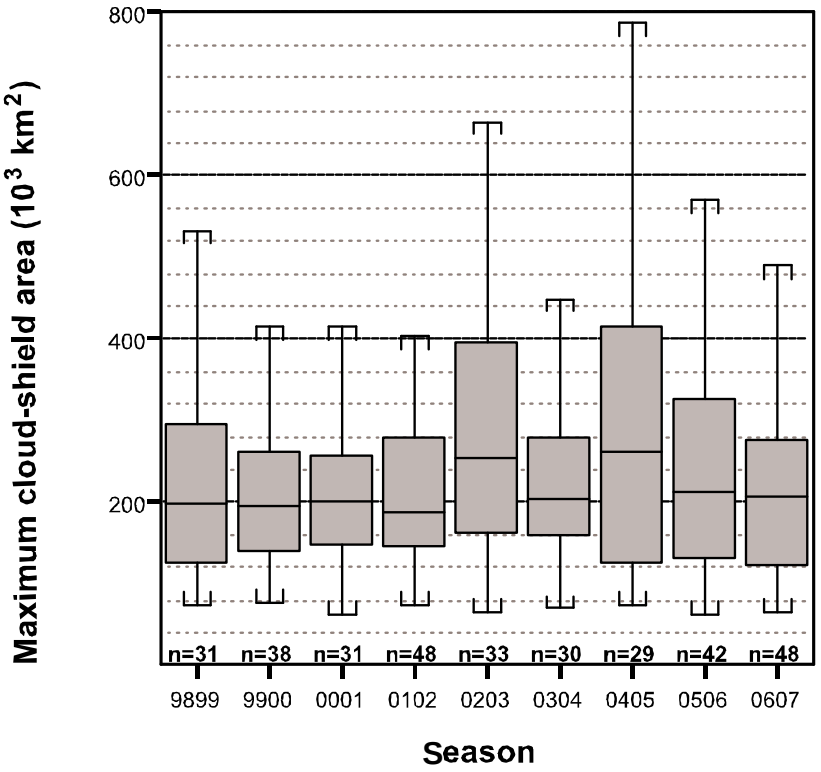

Fig. 2.6. As in Fig. 2.4 except for the maximum cloud-shield size.

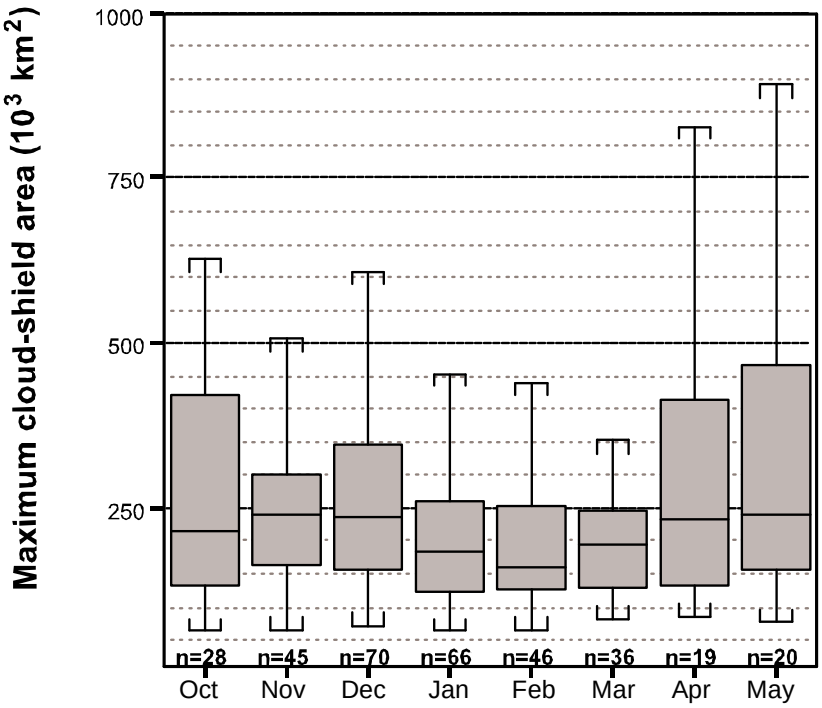

Fig. 2.7. As in Fig. 2.6 except monthly.

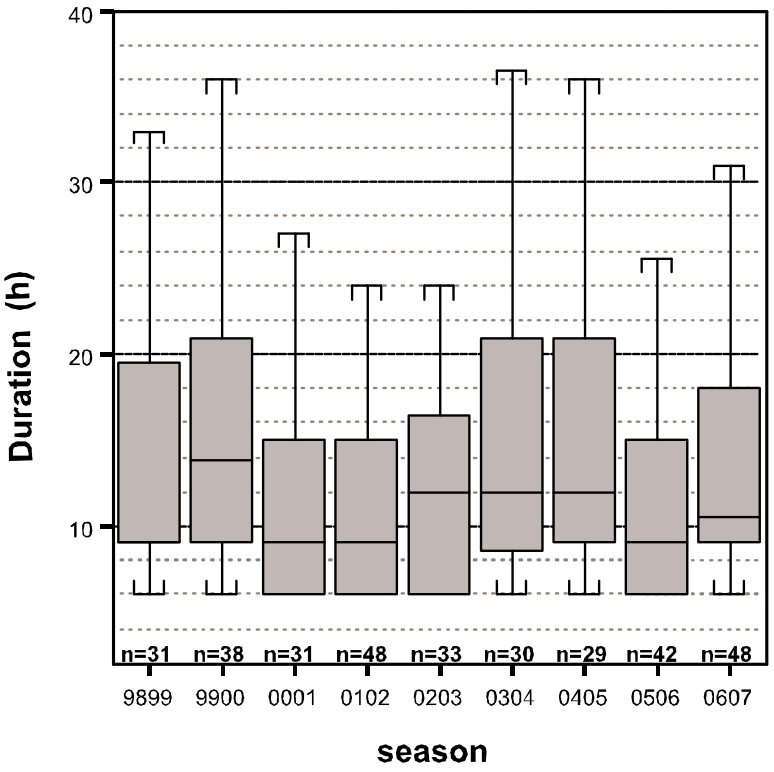

Fig. 2.8. As in Fig. 2.4 except for MCC lifecycle duration.

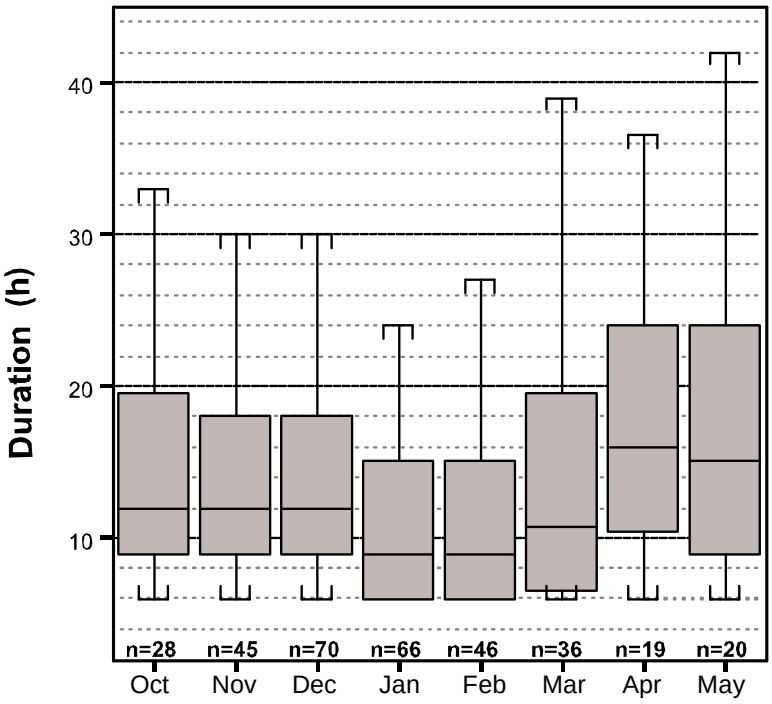

Fig. 2.9. As in Fig. 2.8 except monthly.

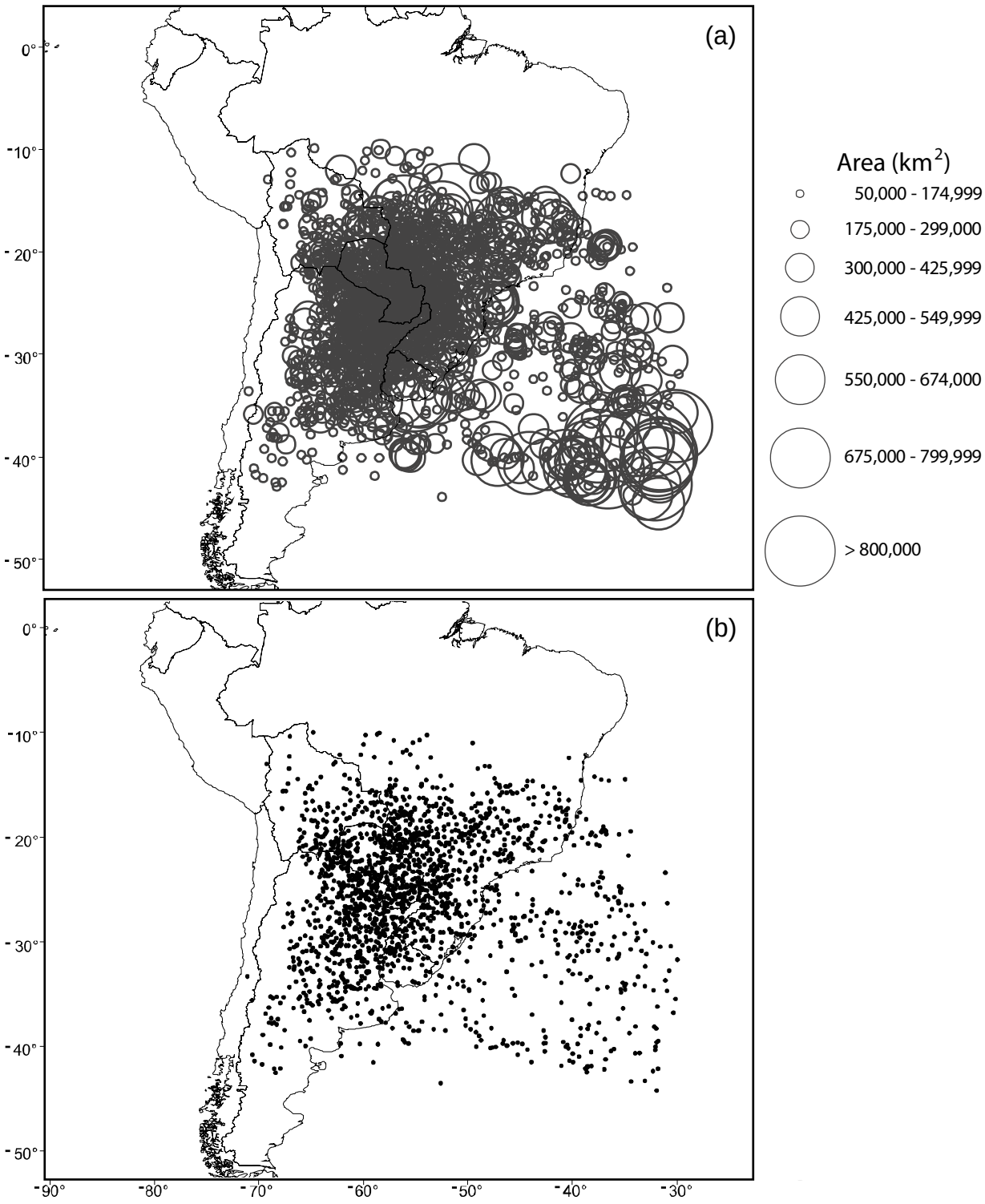

Fig. 2.10. The locations of the cloud shields (a) and centroid locations (b) from the 330 MCCs observed between the warm season months of October-May during 1998-2007.

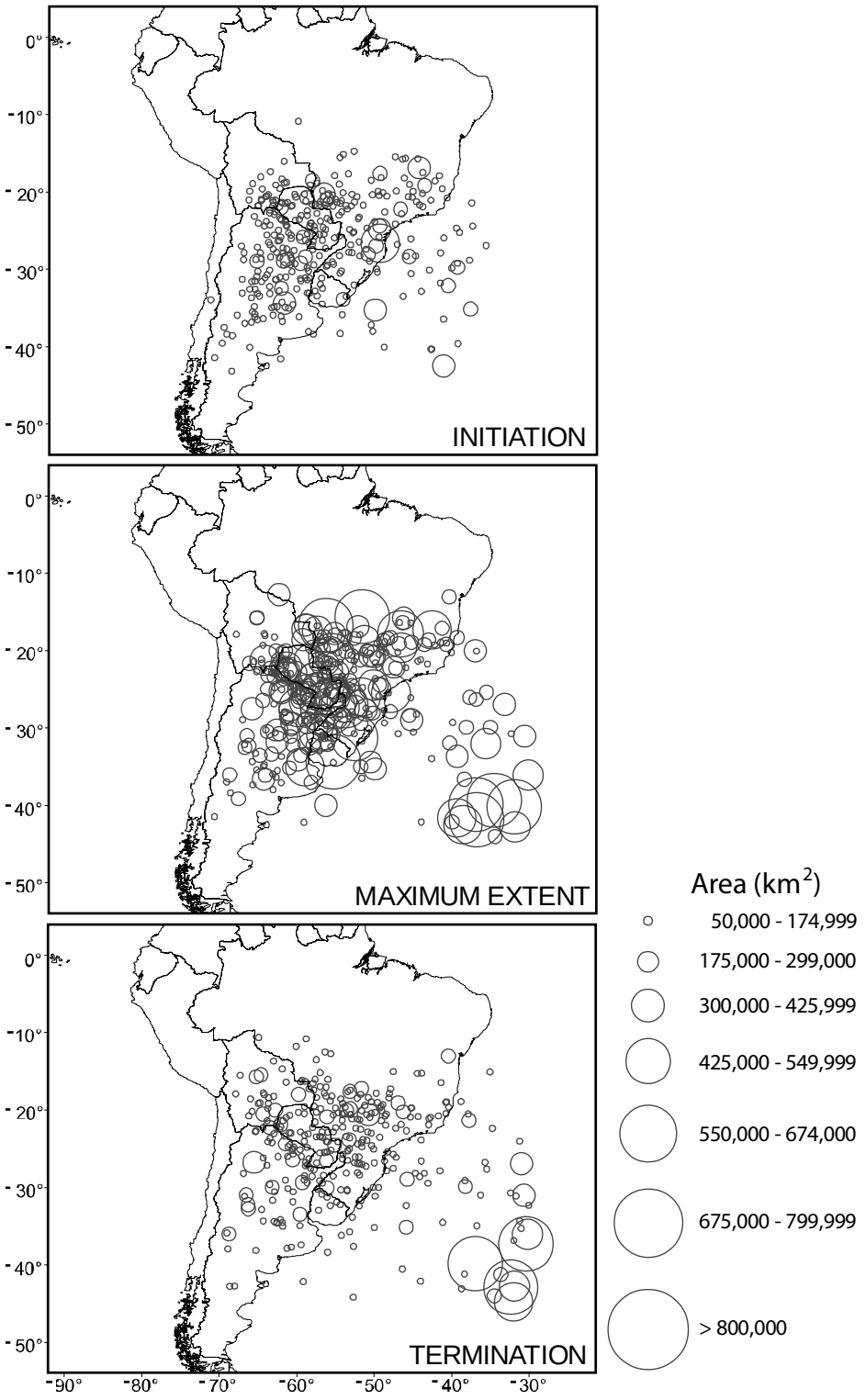

Fig. 2.11. MCC cloud shields during critical stages observed between the warm season months of October-May during 1998-2007.

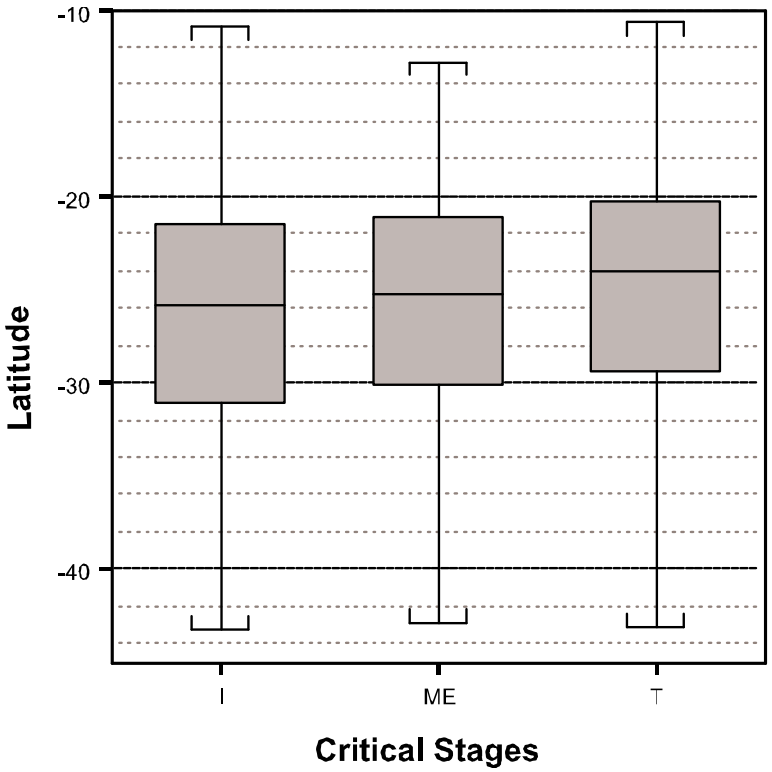

Fig. 2.12. Box plots of the latitudinal distribution of MCC cloud-shield centroid locations during each stage, where "I" is the initiation, "ME" is the maximum extent, and "T" is termination.

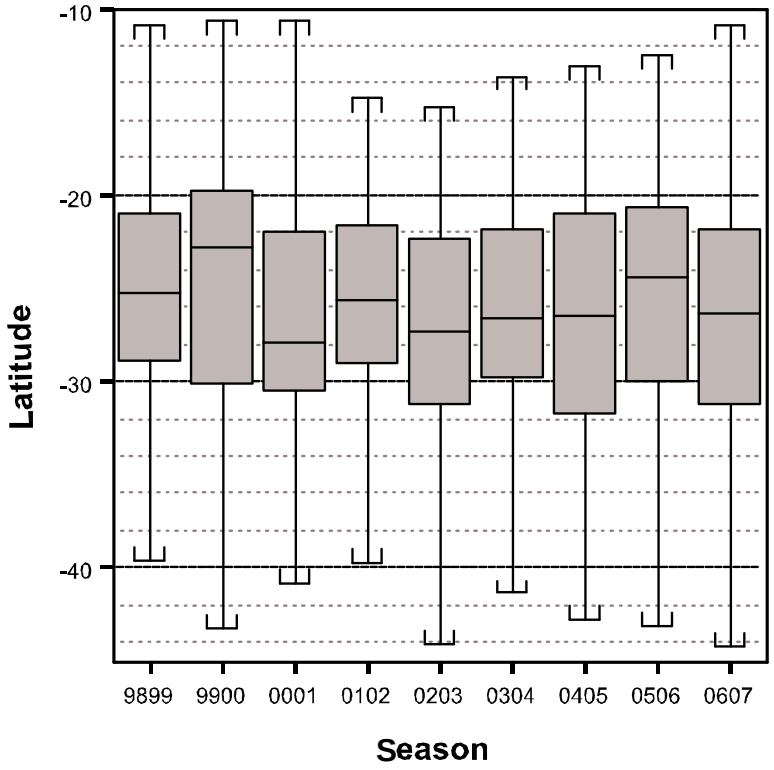

Fig. 2.13. As in Fig. 2.12 except by warm season.

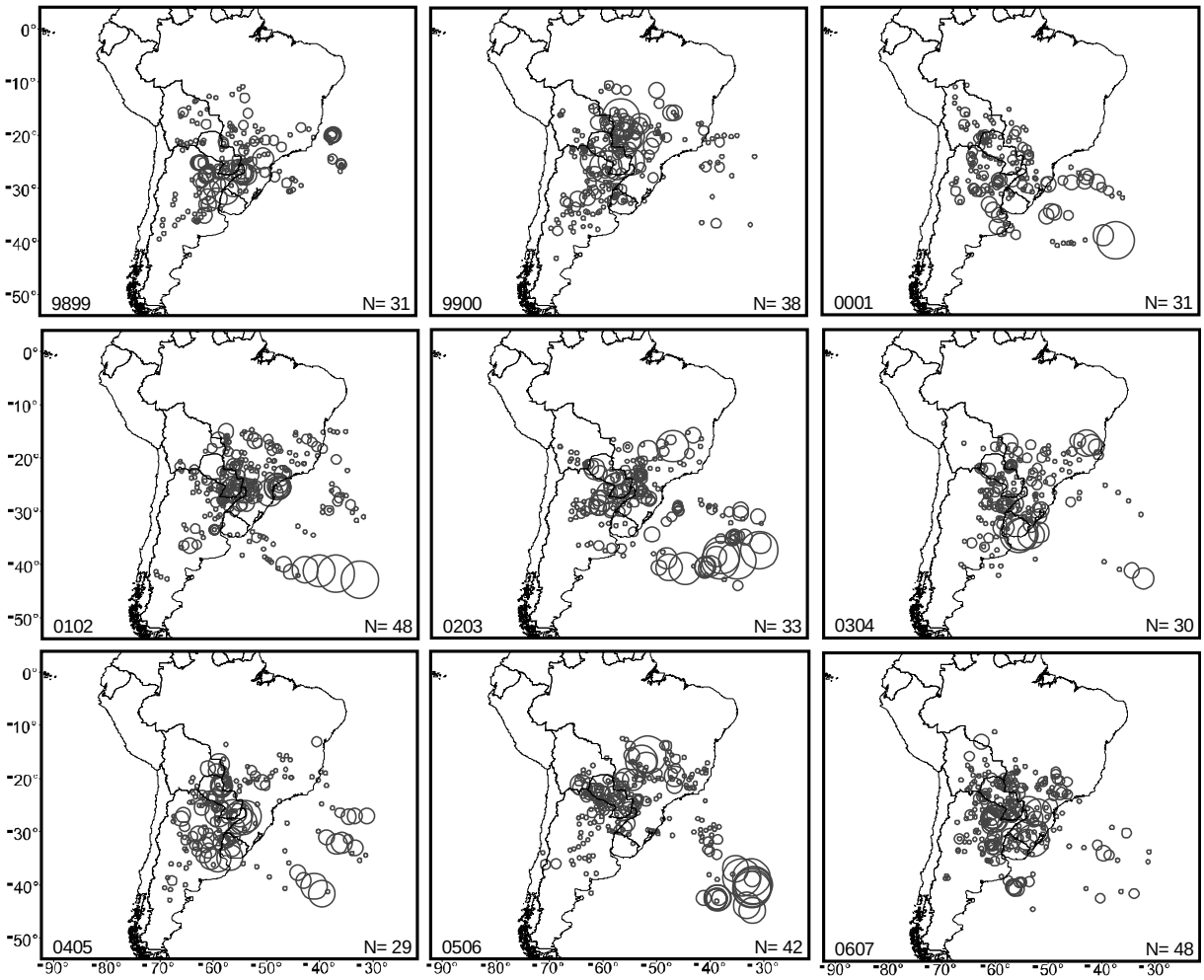

Fig. 2.14. As in Fig. 2.10 except by warm season. Note that N is equal to the number of MCC events during a given season and not the number of cloud shields.

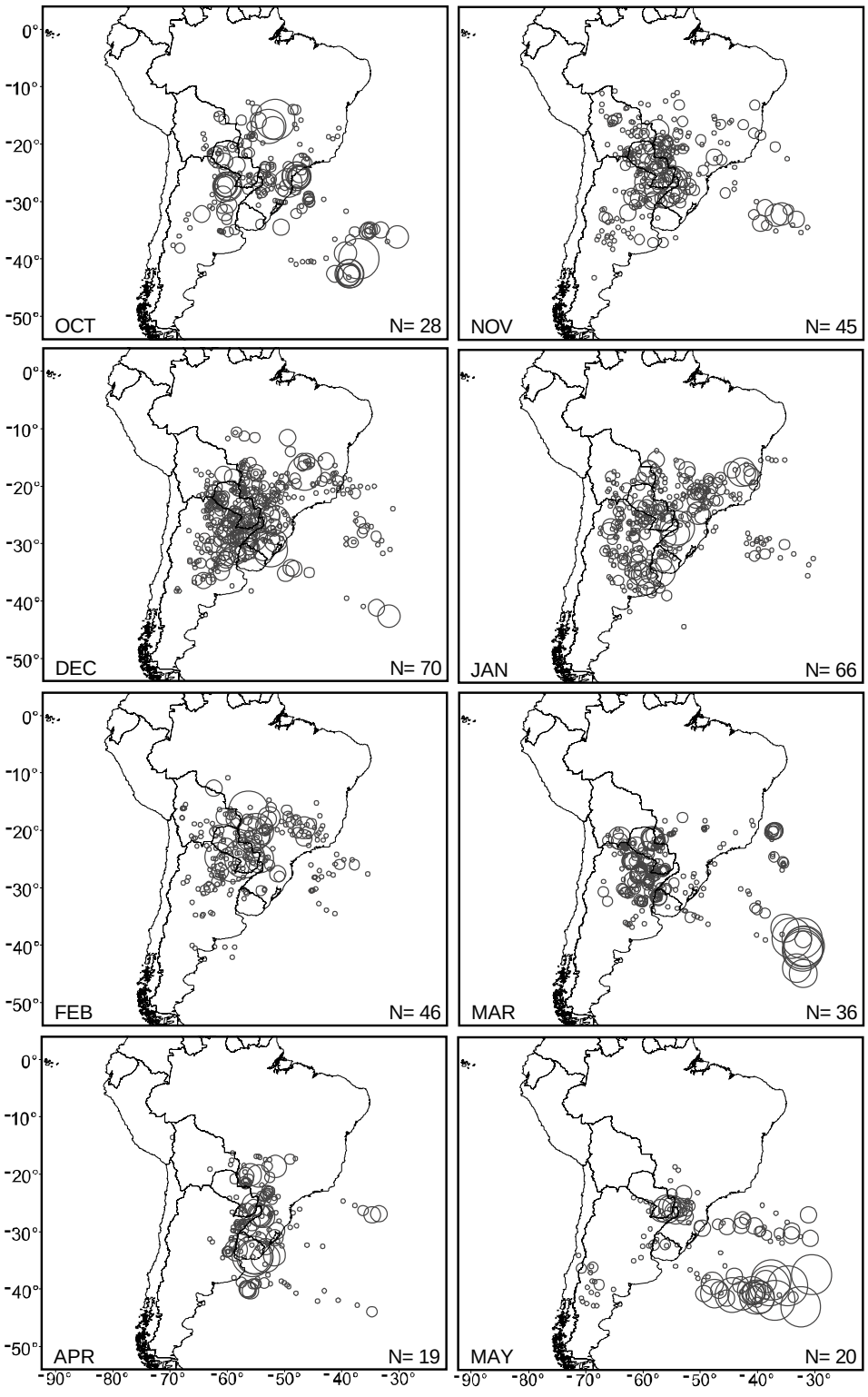

Fig. 2.15. As in Fig. 2.10 except by month.

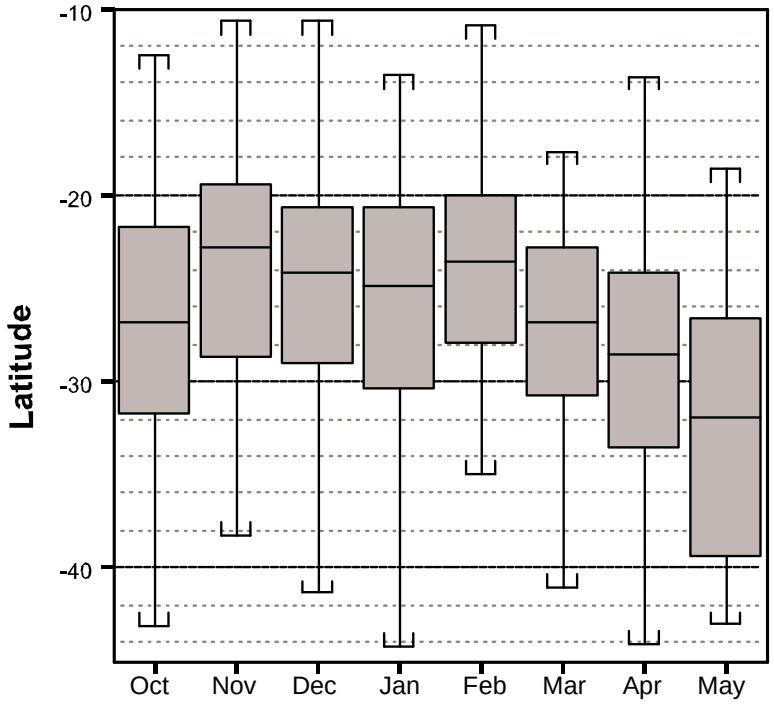

Fig. 2.16. As in Fig. 2.12 except by month.

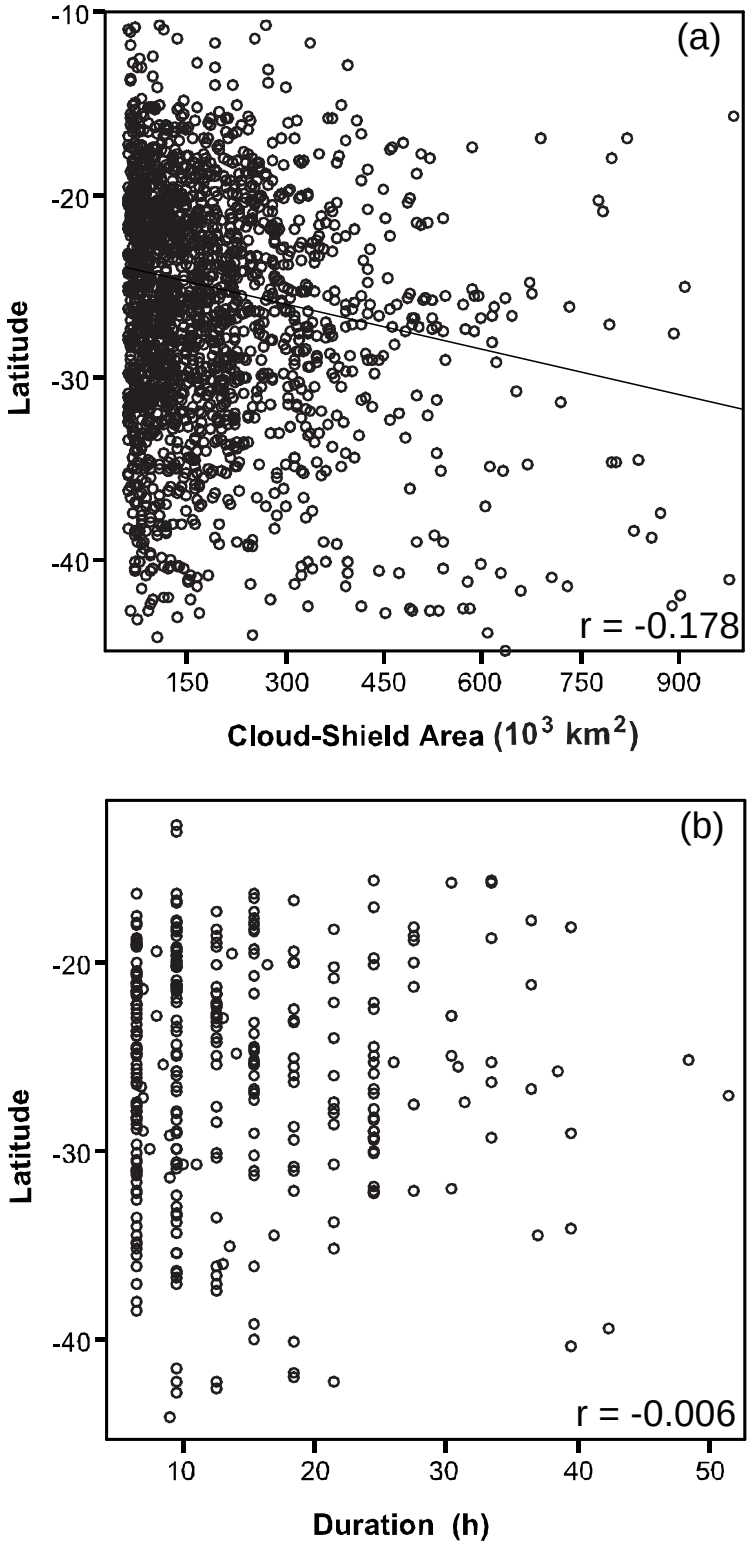

Fig. 2.17. (a) Scatter plots showing relationships between latitude and cloud-shield area and (b) duration.

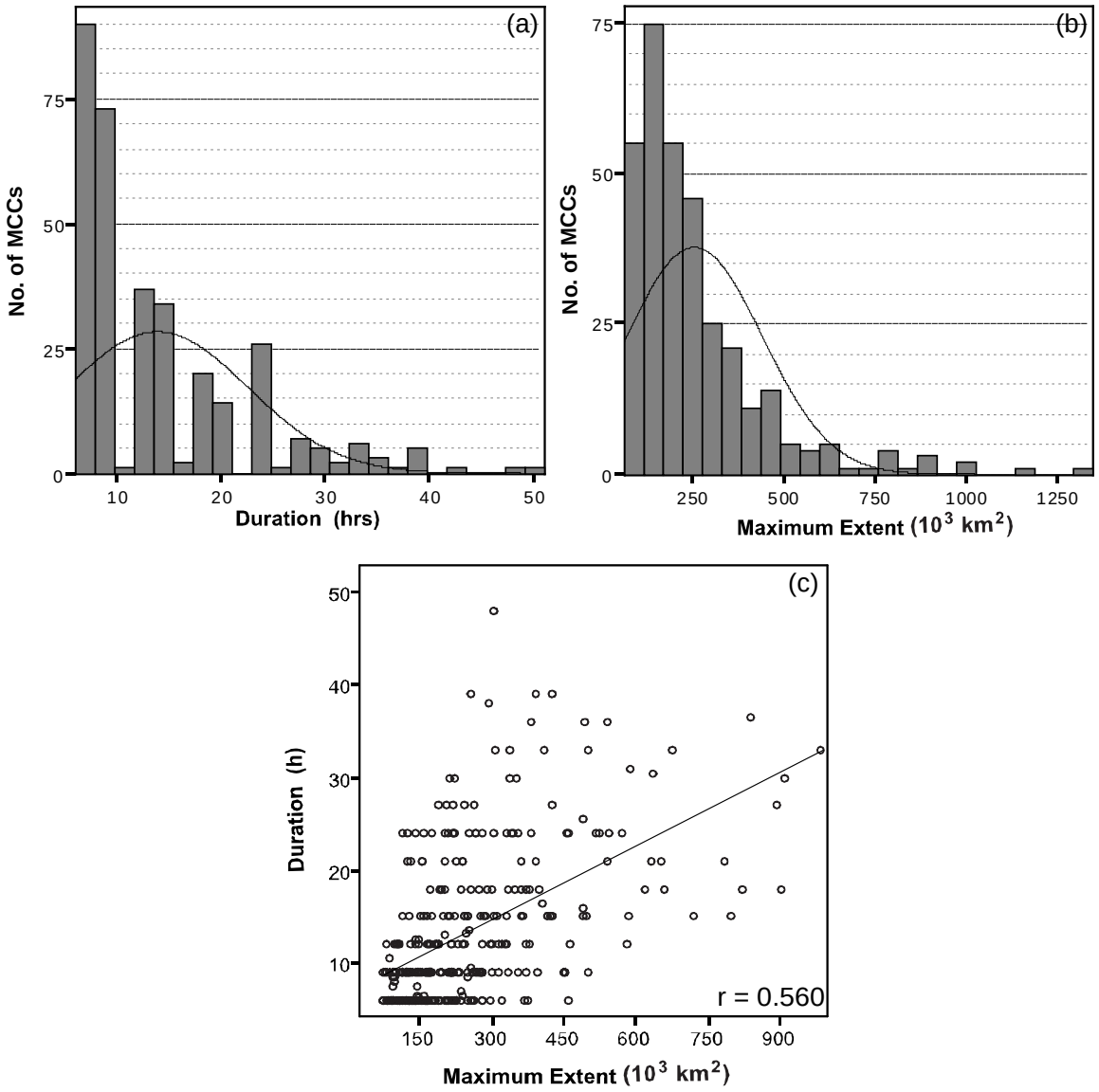

Fig. 2.18. Histograms and normal curves of MCC (a) duration and (b) maximum cloud-shield extent, and (c) scatter plot showing relationship between MCC duration and maximum extent.

CHAPTER 3

THE CONTRIBUTION OF MESOSCALE CONVECTIVE COMPLEXES TO RAINFALL ACROSS SUBTROPICAL SOUTH AMERICA[3]

[3] Durkee, J. D., T. L. Mote, and J. M. Shepherd. To be submitted to *Journal of Climate.*

ABSTRACT

This study uses a database consisting of 330 austral warm-season (October-May) mesoscale convective complexes (MCCs) during 1998-2007 to determine the contribution of MCCs to rainfall across subtropical South America (SSA). A unique precipitation analysis is conducted using Tropical Rainfall Measuring Mission (TRMM) 3B42 v.6 data. The average MCC produces 15.7 mm of rainfall across 381,000 km^2, with a volume of 7.0 km^3. MCCs in SSA have the largest precipitation areas compared to North American and African systems. MCCs accounted for 15-21% of the total rainfall across portions of northern Argentina and Paraguay during 1998-2007. However, MCCs account for larger fractions of the total precipitation when analyzed on monthly and warm-season time scales. Widespread MCC rainfall contributions of 11-20% were observed in all months. MCCs accounted for 20-30% of the total rainfall between November-February, and 30-50% in December, primarily across northern Argentina and Paraguay. MCCs also produced 25-66% of the total rainfall across portions of west-central Argentina. Similar MCC rainfall contributions were observed during warm seasons. An MCC Impact Factor (MIF) was developed to determine the overall impact of MCC rainfall on warm-season precipitation anomalies. Results show the greatest impacts on precipitation anomalies from MCC rainfall were located near the center of the La Plata Basin. This study demonstrates that MCCs in SSA produce widespread precipitation that contributes substantially to the total rainfall across the region.

3.1 Introduction

Mesoscale convective complexes (MCCs) are a frequently occurring subclass of mesoscale convective systems (MCSs) widely observed around the globe. These large, long-lasting organized systems are comprised of an ensemble of thunderstorms that together, often yield intense rain rates within contiguously sizeable precipitation areas and can greatly influence the hydroclimate of a region. One such region that has been shown to have a high frequency and concentration of MCCs during the austral warm season (defined here as October-May) is the La Plata Basin (Fig. 3.1). The La Plata Basin is the fifth-largest drainage basin in the world (3.2×10^6 km^2) located east of the Andes Mountains primarily between 20°S-40°S (also referred as subtropical South America; hereafter SSA), which drains the Paraná, Paraguay, and Uruguay River systems. Much of the economy of this densely populated region comes from agriculture and hydroelectric power demand, which is exceedingly reliant upon and vulnerable to heavy precipitation events (Mechoso et al. 2001).

Previous studies have shown that MCCs can account for large fractions of rainfall (e.g., up to 60% during the warm season in the central United States (Ashley et al. 2003 and Fritsch et al. 1986; 22% in Sahelian Africa, Laing et al. 1999). However, SSA is largely void of any observational evidence of the role of MCCs in the region's warm-season rainfall. Therefore, more studies of mesoscale precipitation are necessary in order to gain a better understanding of the role of convective rainfall in the precipitation climatology of SSA.

Warm-season precipitation in SSA largely exhibits a nocturnal maximum (Berbery and Collini 2000). Berbery and Barros (2002) identified a precipitation

maximum over portions of Paraguay, northeastern Argentina, and southeastern Brazil throughout much of the warm season. Numerous studies have shown the timing and location of precipitation maxima across SSA are modulated through the exchange tropical heat and moisture via the northerly low-level jet (Saulo et al. 2007; Vera et al. 2006; Silva and Berbery 2006; Liebmann et al. 2004; Zipser et al. 2006; Nieto Ferreira et al. 2003; Marengo et al. 2004; Berbery and Collini 2000; Laing and Fritsch 2000; Nicolini and Saulo 2000). Many of these studies have demonstrated that the low-level jet plays a vital role in the development and maintenance of predominantly nocturnal mesoscale convective systems (MCSs) within the subtropical region. Zipser et al. (2006) found these subtropical South American MCSs are among the world's most intense thunderstorms.

The foundational study of South American MCCs from Velasco and Fritsch (1987) provided the initial evidence of MCC activity in SSA, but did not assess MCC rainfall. Viana (2006) examined MCCs in the southern state of Rio Grande do Sul, Brazil and found these events contributed an average of 63% of the total rainfall between October-December in 2003. Mota (2003) examined large MCSs from December 1997-Novmeber 2000 and found these events contributed up to half of the total rainfall across portions of SSA. Salio and Nicolini (2007) suggested MCSs are the dominant contributor to precipitation totals across the region. Although many of these studies provide initial evidence of these large thunderstorm complexes producing considerable proportions of the total rainfall across SSA, a climatological understanding of rainfall contributions from these systems have remained unknown.

Chapter 2 described the climatological characteristics of 330 warm-season MCCs across SSA for 1998-2007. The results from Chapter 2 established that the region with the greatest frequency and highest concentration of MCCs coincides well with the location of the precipitation maximum described by Berbery and Collini (2000). Chapter 2 also showed that these systems are predominantly nocturnal, which also matches well with the night-time precipitation maximum highlighted by Berbery and Barros (2002). Consequently, one may ask if the precipitation patterns found throughout the warm season across SSA may be ascribed in part, to relatively frequent and concentrated MCC activity near the center of the La Plata Basin.

The findings from Chapter 2 showed on average, these austral systems are statistically significantly larger and longer-lived than MCCs in the U.S. They showed that MCCs in SSA reach an average maximum size of 256,500 km^2 and last 14 hours (compared to 164,600 km^2 and 10 hours in the U.S.; $p = 0.01$). Moreover, the smaller, shorter-lived South American systems are commonly similar in size and duration with the larger, longer-lasting events in the U.S. (cf. Chapter 2 and Ashley et al. 2003). Tollerud et al. (1987) and Ashley et al. (2003) found that larger, longer-lived MCCs commonly produce the greatest precipitation amounts. These results raise the question regarding MCC precipitation across SSA: Do the physical characteristics described in Chapter 2 suggest that relative to the U.S., MCCs in SSA contribute more to the total warm-season rainfall?

In support of the findings and suggestions of previous work described above, the findings from Chapter 2 provide strong evidence that the precipitation variability across SSA is connected with MCC rainfall. The initial work of Viana (2006) and Mota (2003)

further supports this hypothesis. However, there are no available studies that provide a long-term examination of MCC rainfall contributions across SSA. Therefore, the overarching goal of this study is to determine the contribution of MCCs to warm-season rainfall across SSA for 1998-2007.

3.2 Data

To determine precipitation characteristics of warm-season MCCs across SSA, this study utilized the dataset assembled in Chapter 2, which contains 330 MCCs. These systems were identified and tracked from full disc GOES-8 and GOES-12 4 km infrared (IR) satellite data, which were provided by the National Oceanic Atmospheric Administration Comprehensive Large-Array data Stewardship System (NOAA CLASS data available at: http://www.class.ncdc.noaa.gov). The nominal times for the satellite images were 0245, 0545, 0845, 1145, 1445, 1745, 2045, and 2345 UTC. There were occasional instances when nominal image times were missing, but were available during other times (e.g., 0915 UTC).

Analyzing precipitation characteristics for specified thunderstorm events across South America presents a number of challenges. The primary difficulty is finding an available dataset that contains a consistently quality controlled long-term record with a sufficient temporal sampling resolution and network density to capture the mesoscale precipitation variability within all 330 MCCs. For example, the Global Precipitation Climatology Centre (GPCC) provides global land-based accumulated rainfall data for the period of record, but only at monthly time scales with one-degree resolution (http://www.dwd.de). The World Climate Research Program's (WCRP) Global

Precipitation Climatology Project (GPCP) provides rainfall data for the period of record from merged passive microwave and land-based estimators, but only at daily time scales with one-degree resolution (ftp://rsd.gsfc.nasa.gov/pub/1dd/).

One of the objectives of Tropical Rainfall Measuring Mission (TRMM) during its inception in December 1997 was to provide relatively high temporal and spatial rainfall data, particularly for poorly sampled regions (Kummerow et al. 2000). This study uses TRMM Multi-Satellite Precipitation Analysis (TMPA) 3B42 Version 6, which provides global 3-hourly precipitation rate estimates with latitudinal coverage between 50°N-S (0.25° grid) from 1998 January - near real time (http://disc.sci.gsfc.nasa.gov/data/datapool/TRMM). The 3B42 product is derived from an amalgamation of passive microwave estimates from the onboard TRMM microwave imager (TMI), Special Sensor Microwave Imager (SSM/I), Advanced Microwave Sounding Unit (AMSU), Advanced Microwave Scanning Radiometer (AMSR), and calibrated IR estimates from geostationary platforms (consult Huffman et al. (2007) and Huffman and Bolvin (2007) for explicit details on the TMPA algorithm and 3B42 processing).

Huffman and Bolvin (2007) discuss two concerns with the 3B42 dataset. First, the orbital altitude of the TRMM platform was increased from 350 to 401.5 km in August 2001. Due to the success of TRMM, the boost was carried out for fuel reduction to increase the longevity of the project. The advantage was an increase in the latitudinal coverage from 40°N-S to 50°N-S. However, changes in the footprint and minimum detectable precipitation rates occurred. Although version 6 of the dataset attempts to account for these discrepancies, some differences in the minimum detectable rain rates

can still be found. Second, the latitude bands 40°S-50°S only contain passive microwave estimates between 1 January 1998 - 6 February 2000. This is particularly problematic given the limited availability of passive microwave data during this time (i.e., few passes a day that systematically missed precipitation). Therefore all MCCs with cloud-shield areas beyond 40°S were flagged for potential precipitation errors during this time.

Another important consideration is the robustness of passive microwave rainfall estimates of mesoscale phenomena over land areas. First, the use of passive microwave data to distinguish rain over land is ambiguous using low frequency (i.e., < 22 GHz) absorption methods due to similar emissivities of land and rainfall. Therefore, scattering techniques using high frequency channels (i.e., 85 GHz) are used to associate the concentration of ice particles with precipitation. According to Ebert et al. (2007), scattering techniques are particularly useful in estimating precipitation from mid-latitude convective systems. Furthermore, Ebert et al. (2007) provide a land-based comparative analysis of TMPA data against relatively dense rain-gauge networks across the U.S., Australia, and northwest Europe. Results from their study showed that the accuracy of satellite-derived rainfall totals is greatest during the warm season and increases toward lower latitudes, particularly with respect to deep convective precipitation regimes. Ebert et al. (2007) also found that in the U.S., TMPA rainfall estimates were near that of radar estimates for daily precipitation bias and frequency. Sapiano and Arkin (submitted) showed that TMPA exhibited little bias in warm-season convective precipitation estimates over the Great Plains in the U.S, when compared to rain gauge estimates. Second, 3B42 data have been suggested as suitable metrics for long-lived meso-α

systems[4], particularly when analyzed in a climatological framework. Considering the relative minimum bias in TMPA warm-season rainfall estimates, and that this study focuses on warm-season MCCs over the subtropical land mass of South America for the period 1998-2007, 3B42 data is considered a unique viable source for quantifying MCC rainfall (Huffman personal communication; Huffman et al. 2007).

3.3 Methodology

The MCC identification and tracking method outlined in Chapter 3 included a hybrid automated/manual observation approach that conformed to specific MCC criteria (Table 3.1) (see that study for more details). There were two outputs from that work necessary for this study. The first is a list of events where each observed cloud shield was tagged with a unique identifier based on the event number for a given year, Julian day, and time of occurrence. These cloud shields included data on horizontal area, eccentricity, and centroid coordinates. The second output contained the longitude/latitude coordinates that make up the outer perimeter of the continuous cold cloud-shield.

The first step toward quantifying MCC precipitation was to use data from the output files to determine the aerial swath of each event's storm track. For this study, MCC precipitation was assumed to fall solely within this swath. In order to demarcate the storm-track aerial coverage, a convex hull was calculated throughout each event's lifecycle (see Barber and Huhdanpaa 1996) and overlaid onto 3B42 precipitation grids. For example, Fig. 3.2 shows a hypothetical MCC observed across a sequence of four

[4] meso-α scale: length scales of 250-2500 km and duration of ≥ 6 h (Orlanski 1975).

satellite images. For the series of cloud shields, a convex hull is computed to determine the aerial storm-track swath for the first and second observations, followed by the second and third, and third and fourth. The end product is a mask that represents the location of the total surface area beneath an MCC during its lifecycle.

The next step was to use the convex hull mask to determine accumulated precipitation for each event. Fig. 3.3 shows a schematic diagram of the precipitation summation scheme of a hypothetical event. It is important to note that 3-hourly TRMM 3B42 precipitation data represent instantaneous values centered on synoptic times (i.e., 0000, 0300, 0600, 0900, 1200, 1500, 1800, and 2100 UTC). Given the nominal times of the imagery, a weighting factor of 0.5 was applied to all precipitation values within 1.5 hours on either side the system's initiation and termination (1745 and 0845 UTC in Fig. 3.3, respectively,). The solid gray box signifies precipitation values weighted unity. Accumulated rainfall is simply the average of all weighted rain rates multiplied by the number of hours in the event.

The output contained aerially-averaged precipitation totals and total precipitation areas associated with each of the 330 events. The accumulated rainfall was also tabulated for each grid point within the convex hull for each event, and summed into monthly and warm-season totals. An output file where each scene contained the outline of the convex hull mask and accumulated precipitation was produced as a verification check of this process (Fig. 3.4). Lastly, monthly and seasonal summations of 3B42 data were determined for all precipitation (i.e., from MCCs and all other rainfall events). The contribution of MCC rainfall is expressed as the ratio of MCC precipitation to the total rainfall at each grid point. A summary of the entire process is illustrated in Fig. 3.5.

3.4 Results

MCCs between 1 January 1998 – 6 February 2000 were screened for cloud-shield areas south of 40°S to assess for potential precipitation discrepancies (see section 3.2). Four events had distinct discontinuities in precipitation data between 40°-50°S. The data in question only accounted for less than two percent of the total precipitation observed for these events. Therefore, precipitation south of 40°S for these events was removed from further analysis.

a. Period of record

The average MCC in SSA produces 15.7 mm of rainfall over an area of 381,000 km^2, with a volume of 7.0 km^3. A comparison of mean precipitation characteristics for MCCs in South America, Africa (Laing et al. 1999), and the U.S. (McAnelly and Cotton 1989) is shown in Table 3.2. MCC precipitation depths and volumes found in this study fall between African and U.S. systems, but produce the largest precipitation areas. These larger precipitation areas are accounted for by larger MCCs in South America (cf. Chapter 2, McAnelly and Cotton 1989, and Laing and Fritsch 1993). However, the precipitation characteristics described by McAnelly and Cotton (1989) might be conservative given they only considered late warm-season events. Ashley et al. (2003) showed that late-season MCCs in the U.S. are commonly much smaller, shorter-lived systems.

A spatial examination of the 330 MCC storm tracks shows the greatest MCC frequencies over Paraguay, northern Argentina and southern Brazil (Fig. 3.6). The geographic distribution of the fractional contribution of MCC rainfall revealed a similar

pattern (Fig. 3.7). Specifically, 15-21% of the total precipitation in northern Argentina and portions of Paraguay was accounted for by MCCs. These values appear low compared to the results of Mota (2003) and Viana (2006) (40-50% and 63%, respectively). These differences are likely attributed to the period of record and methods used in their studies. For example, Mota (2003) used a precipitation feature algorithm (see Nesbitt et al. 2000) to identify three years of MCSs based on criteria different from Table 3.1, which likely included a considerable sample of events smaller than MCCs. Viana (2006) used 31 rain gauges to determine MCC rainfall contributions. The results found by Viana (2006) may also be reflective of only examining a three-month record (October-December 2003). Furthermore, Viana (2006) used a warmer cloud-top threshold of -32°C. The colder cloud-top threshold of -52°C was used in this study because MCC precipitation areas are mostly confined to areas beneath these colder cloud shields (McAnelly and Cotton 1986 and 1989), and has been widely used in other MCC studies (e.g., Augustine and Howard 1988; Anderson and Arritt 1998, Laing et al. 1999; Anderson and Arritt 2001).

b. Monthly analysis

MCCs contributed 11-20% of the total rainfall across much of SSA in all months (Fig. 3.8). Paraguay and northern Argentina consistently received the largest fraction of total precipitation from MCCs. Between November-February, much of Paraguay and northern Argentina received 20-30% of the total precipitation from MCCs. The maximum contributions of MCCs to rainfall were found across northern Argentina and portions of Paraguay and southeastern Brazil during December (30-50%).

At times, portions of west-central Argentina also received considerable percentages of MCC rainfall. The area largely within the provinces of Mendoza, Neuquén, and La Pampa received 25-44% of the total precipitation from MCCs during October. MCCs contributed 30-66% and 30-40% of the precipitation to the same area during November and May, respectively. The findings from Chapter 2 and Velasco and Fritsch (1987) showed MCCs are infrequent to this particular area. It is likely that areas infrequent to MCCs tend to experience greater fractional rainfall contributions from MCCs when they occur.

This study shows the fraction of precipitation due to MCCs is larger for much of SSA compared to the U.S. Ashley et al. (2003) found that MCCs contributed 10-20% of the monthly rainfall across the central U.S. with maximum values of 28%. Results from this study indicate monthly precipitation patterns across SSA are influenced more from MCCs.

c. Warm-season analysis

An examination of the interannual variability in MCC precipitation contribution basis shows considerable spatial variability (Fig. 3.9). During each of the nine warm seasons, much of Paraguay and its neighboring border areas experienced the most MCC activity. As expected, the majority of the largest fractions of total rainfall due to MCCs were found in these areas. MCCs contributed 11-20% of the warm-season rainfall across much of SSA, but it was not uncommon to find 40-50% across portions northern Argentina, Paraguay, and southern Brazil during most warm seasons.

It is clear that MCCs contribute substantially to warm-season precipitation across SSA. Some studies have suggested MCC rainfall plays a potentially important role in regional rainfall budgets (e.g., Fritsch et al. 1986; Anderson and Arritt 1998; Ashley et al. 2003). However, no such relationships have been shown for SSA. One way to assess the impact of MCC precipitation beyond rainfall contributions is to examine warm-season precipitation anomalies with and without MCC rainfall. For this study, warm-season precipitation anomaly maps were constructed using mean TRMM 3B42 data for January 1998 - December 2007 as a baseline for comparison. Precipitation anomalies were determined as the difference between observed and mean values. Warm-season precipitation anomalies for the period of record are shown in Fig. 3.10.

The warm seasons of 1998-99, 2000-01, and 2002-03 had similar MCC frequencies with maximum fractional contributions of rainfall totaling 33% (see Fig. 3.9). Each of these warm seasons also experienced three different precipitation anomaly conditions. The greatest fractional contributions of MCC rainfall were located in areas that were close to average warm-seasonal rainfall. However, above-average precipitation extended from Argentina into southeastern Brazil in 2002-03, the same area where MCCs contributed the least rainfall. The 2000-01 warm season experienced mostly average and some above-average rainfall, yet MCCs contributed the least amount of the total rainfall during this time. These findings raise the question, how does the spatial variability in warm-season precipitation anomalies for the period of record change in the absence of MCC rainfall? The answer to this question provides a clearer understanding of the influence of MCCs by identifying only those areas with the greatest differences in precipitation anomalies due to MCC rainfall.

Visual assessments of such differences were difficult to discern from a 0.25° grid resolution, even in some areas (e.g., northern Argentina) where MCC fractions were large. In order to determine the extent and magnitude of the effect of MCC rainfall on warm-season precipitation anomalies, a MCC Impact Factor (MIF) was developed. The MIF simply shows the contribution of MCCs to seasonal rainfall anomalies given by,

$$\text{MIF} = \frac{\left(R_y - \overline{R}\right) - R_{mcc}}{2\sigma_{RA}} \qquad \text{Eq. (4.1)}$$

where R_y is the total rainfall for a given year, $\overline{R}$ is the climatological mean rainfall, R_{mcc} is the total MCC rainfall, and σ_{RA} is the standard deviation of the rainfall anomaly. Only grid points that contained differences between the anomaly value and MCC rainfall ($\Delta\sigma_i$) ≥ 0.5 standard deviations were considered. The MIF ranking is scale ranges from 1-6 at 0.5 standard deviation intervals. For example, a MIF-1 indicates a 0.5-1.0 standard-deviation change in the precipitation anomaly, whereas a MIF-6 indicates a ≥ 3.0 standard-deviation change. The locations of the greatest impacts from MCC rainfall during each warm season are illustrated in Fig. 3.11.

The analysis revealed that the impact of MCC precipitation on anomalous precipitation patterns varies considerably in extent and magnitude. MIF-1 was found in all warm seasons. The 2000-01 warm season was unique in that only MIF-1 was observed. However, many MIF-1 locations were found in areas of below-average rainfall (particularly southern Brazil). The extent of the impact was greatest during 1999-2000 with MIF-1 as the dominant magnitude. Anomalously dry conditions were collocated

with zero impact across Uruguay, northeastern Argentina, and southeastern Brazil during 2005-06. Notice how MIF-4 and MIF-5 were collocated with near average rainfall just to the northwest. Additionally, the extent of the overall impact is collocated well with the area of predominantly above-average rainfall during 2006-07. These results demonstrate that MCC rainfall has the capability to alter precipitation totals in ways that are potentially beneficial (drought deterrence) and/or detrimental (floods).

3.5 Summary and Conclusions

This study provides a climatological description of the precipitation characteristics of 330 warm-season MCCs for 1998-2007. Results show MCCs contribute substantially to precipitation totals across SSA. It is clear from these examinations a great degree of variability exists in contributions by MCCs to the total monthly and warm-season rainfall. This study also shows MCCs play a particularly important role in warm-season precipitation anomalies across SSA.

On average, MCCs in SSA distribute 15.7 mm of rainfall across 381,000 km^2, producing a volume of 7.0 km^3. South American systems have the largest precipitation areas compared to published studies for North America and Africa. Previous studies suggest the physiographic arrangement of the Andes Mountains and abundant tropical supply of Amazonian heat and water-vapor flux into the subtropical region are key factors in the development and maintenance of these large heavy precipitation events.

MCC storm-track frequencies and rainfall contributions were generally greatest over Paraguay and the surrounding areas of the neighboring countries. The extent of MCC rainfall was primarily east of the Andes between 10°S-45°S. For the period of

record, portions of northern Argentina and Paraguay received 15-21% of the total precipitation from MCCs. However, MCCs account for larger fractions of the total precipitation when examined on interannual and intraseasonal time scales. Fractional MCC rainfall contributions of 11-20% were found over much of SSA in all months. MCCs accounted for 20-30% of the total rainfall between November-February, and 30-50% in December across northern Argentina and Paraguay. MCCs also contributed 25-66% of the total rainfall across smaller areas within the provinces of Mendoza, Neuquén, and La Pampa in west-central Argentina. It is likely that the larger rainfall contributions from MCCs occurred over a region infrequent to MCC activity. This study also shows that the monthly percentage of rainfall due to MCCs is much larger in SSA compared to the U.S (e.g., 50% vs. 20%, respectively).

MCCs account for slightly larger percentages of rainfall when examined by warm season, relative to monthly rainfall contributions. In each warm season, MCCs contributed ≥ 30% of the total rainfall across many areas within SSA, while some areas received ≥ 50%. Based on these findings, MCCs play an essential role in precipitation totals across SSA. However, these results do not necessarily portray the overall impact of MCC rainfall.

This study developed an MCC Impact Factor (MIF) to determine the effect of MCC rainfall on warm-season precipitation anomalies. The MIF identifies locations where anomaly values changed by ≥ 0.5 standard deviations in the absence of MCC rainfall, and uses a MIF magnitude ranking scale of 1-6. Results show that the extent and magnitude of the impact of MCC rainfall on precipitation anomalies varies considerably. In some instances, the contribution of MCCs to the total rainfall was relatively low (≤

20%) while MIF-1s were collocated with above-average rainfall. In other cases the fractional contribution of MCC rainfall was relatively high (≥ 30%), which had a high impact on an area (MIF-4s and MIF-5s) and normal rainfall totals surrounded largely by extremely below-average values. Results from the MIF analysis demonstrate that MCC rainfall plays in important role in determining regional anomalous precipitation conditions.

In summary, results from this study extend our global understanding of the role of MCCs in regional precipitation totals. MCCs in SSA are large, long-lived events that produce copious amounts of precipitation over sizeable areas. These events account for large percentages of the total precipitation across SSA, which have been shown to have a substantial impact on regional precipitation anomalies. Furthermore, this study provides a new perspective on monthly and warm-season precipitation patterns across SSA. However, due to strict MCC classification criteria used in this study, it is likely that the inclusion of other large MCSs would show higher rainfall contributions. Further investigations could examine differences in fractional contributions of MCC and MCC-like events. These types of studies are becoming increasingly important given that the most recent Assessment Report from the Intergovernmental Panel on Climate Change (IPCC 2007) states heavy precipitation events are very likely to increase throughout the next century, contributing to nearly 20% increased rainfall amounts and up to 40% increased annual runoff across portions of SSA. Increases in flood frequency and magnitude from heavy rainfall events will likely contribute to considerable property loss and disruptions of industry, settlement, and society. Lastly, increases in heavy

precipitation events and their resultant flooding will likely lead to an increased risk of injuries, infectious respiratory and skin diseases, and loss of life (IPCC 2007).

3.6 References

Anderson, C. J., and R. W. Arritt, 1998: Mesoscale convective complexes and persistent elongated convective systems over the United States during 1992 and 1993. *Mon. Wea. Rev.*, **126**, 578–599.

Anderson, C. J., and R. W. Arritt, 2001: Mesoscale convective systems over the United States during the 1997-1998 El Niño. *Mon. Wea. Rev.*, **129**, 2443-2457.

Ashley, W. S., T. L. Mote, P. G. Dixon, S. L. Trotter, J. D. Durkee, E. J. Powell, and A. J. Grundstein, 2003: Effects of mesoscale convective complex rainfall on the distribution of precipitation in the United States. *Mon. Wea. Rev.*, **131**, 3003-3017.

Augustine, J. A., and K. W. Howard, 1988: Mesoscale convective complexes over the United States during 1985. *Mon. Wea. Rev.*, **116**, 685-701.

Barber, D. and H. Huhdanpaa, 1996: The quickhull algorithm for convex hulls. ACM Transactions on Mathematical Software, **22**, 469-483.

Berbery, E. H., and E. A. Collini, 2000: Springtime and water vapor flux over southeastern South America. *Mon. Wea. Rev.*, **128**, 1328–1346.

Berbery, E. H., and V. R. Barros, 2002: The hydrologic cycle of the La Plata Basin in South America. *J. Hydr. Meteor.*, **3**, 630-645.

Ebert, E., J. E. Janowiak, and C. Kidd, 2007: Comparison of near real-time precipitation estimates from satellite observations and numerical models. *Bull. Amer. Meteor. Soc.*, **88**, 47-64.

Fritsch, J. M., R. J. Kane, and C. R. Chelius, 1986: The contribution of mesoscale convective weather systems to the warm-season precipitation in the United States. *J. Appl. Meteor.*, **25**, 1333-1345.

Huffman, G. J., R.F. Adler, D. T. Bolvin, G. Gu, E. J. Nelkin, K. P. Bowman, Y. Hong, E. F. Stocker, D. B. Wolff, 2007: The TRMM Multi-satellite Precipitation Analysis: Quasi-global, multi-year, combined-sensor precipitation estimates at fine scale. *J. Hydrometeor*., **8**, 38-55.

Huffman, G. J., and D. T. Bolvin, 2007: Real-time TRMM multi-satellite precipitation analysis data set documentation. Laboratory for Atmospheres, NASA Goddard Space Flight Center and Science Systems and Applications, Inc. [available online: ftp://meso.gsfc.nasa.gov/pub/trmmdocs/3B42_3B43_doc.pdf].

IPCC, 2007: Climate Change 2007: Synthesis report. Contribution of Working Groups I, II, and III to the Fourth Assessment Report of the Intergovernmental Panel on Climate Change. IPCC, Geneva, Switzerland, 104 pp. [available online: http://www.ipcc.ch/ipccreports/ar4-syr.htm].

Kummerow, C., J. Simpson, O. Thiele, W. Barnes, A. T. C. Chang, E. Stocker, R. F. Adler, A. Hou, R. Kaka, F. Wentz, P. Ashcroft, T. Kozu, Y. Hong, K. Okamoto, T. Iguchi, H. Kuroiwa, E. Im, Z. Haddad, G. Huffman, B. Ferrier, W. S. Olson, E. Zipser, E. A. Smith, T. T. Wilheit, G. North, T. Krishnamurti, and K. Nakamura, 2000: The status of the Tropical Rainfall Measuring Mission (TRMM) after two years in orbit. *J. Appl. Meteor*., **39**, 1965–1982.

Laing, A. G., and J. M. Fritsch, 1993: Mesoscale convective complexes in Africa. *Mon. Wea. Rev.,* **121,** 2254–2263.

Laing, A. G., J. M. Fritsch, and A. J. Negri, 1999: Contribution of mesoscale convective complexes to rainfall in Sahelian Africa: Estimates from geostationary infrared and passive microwave data. *J. Appl. Meteor.*, **38**, 957–964.

Laing, A. G., and J. M. Fritsch, 2000: The large-scale environments of the global populations of mesoscale convective complexes. *Mon. Wea. Rev.,* **128**, 2756-2776.

Liebmann, B., G. N. Kiladis, C. S. Vera, A. C. Saulo, and L. M. V. Carvalho, 2004: Subseasonal variations of rainfall in South America in the vicinity of the low-level jet east of the Andes and comparison to those in the South Atlantic Convergence Zone. *J. Climate*, **17**, 3829-3842.

Maddox, R. A., 1980: Mesoscale convective complexes. *Bull. Amer. Meteor. Soc*., **61**, 1374-1387.

Marengo, J., W. R. Soares, C. Saulo, and M. Nicolini, 2004: Climatology of the LLJ east of the Andes as derived from the NCEP reanalyses: characteristics and temporal variability. *J. Climate,* **17,** 2261–2280.

McAnelly, R. L., W. R. Cotton, 1986: Meso-β-scale characteristics of an episode of meso-α-scale convective complexes. *Mon. Wea. Rev*., **114**, 1740-1770.

McAnelly, R. L., W. R. Cotton, 1989: The precipitation life cycle of mesoscale convective complexes over the central United States. *Mon. Wea. Rev.*, **117**, 784-808.

Mechoso, R. C., P.S. Días, W. Baetghen, V. Barros, E.H. Berbery, R. Clarke, H. Cullen, C. Ereño, B. Grassi and D. Lettenmaier, 2001: Climatology and Hydrology of the La Plata Basin. *Document of VAMOS/CLIVAR document*. 56 pp. [available online: http://www.clivar.org/organization/vamos/index.htm].

Mota, G. V., 2003: Characteristics of rainfall and precipitation features defined by the Tropical Rainfall Measuring Mission over South America. Ph.D. dissertation, University of Utah, 215 pp.

NOAA, Comprehensive Large-Array Stewardship System, 2007: Silver Spring, MD. [available online: http://www.class.noaa.gov].

Nesbitt, E., J. Zipser, and D. J. Cecil, 2000: A census of precipitation features in the tropics using TRMM: radar, ice scattering, and lightning observations. *J. Climate*, **13**, 4087-4106.

Nicolini, M., and A. C. Saulo, 2000: ETA characterization of the 1997–98 warm season Chaco jet cases. Preprints, *Sixth Int.Conf. on Southern Hemisphere Meteorology and Oceanography,* Santiago, Chile, Amer. Meteor. Soc., 330–331.

Nieto Ferreira, R. N., T. M. Rickenbach, D. L., Herdies, and L. M. V. Carvalho, 2003: Variability of South American Convective Cloud Systems and Tropospheric Circulation during January–March 1998 and 1999. *Mon. Wea. Rev*., **131**, 961–973.

Orlanski, I., 1975: A rational subdivision of scales for atmospheric processes. *Bull. Amer. Meteor. Soc*., **56**, 527-530.

Salio, P. and Nicolini M., 2007: Mesoscale convective systems over southeastern South America and their relationship with the South American low-level jet. *Mon. Wea. Rev*., **135**, 1290-1308.

Saulo C., J. Ruiz, and Y. G. Skabar, 2007: Synergism between the low-level jet and organized convection at its exit region. *Mon. Wea. Rev*., **135**, 1310-1326.

Silva, V. B. S. and E. H. Berbery, 2006: Intense rainfall events affecting the La Plata Basin. *J. Hydr. Meteor.,* **7**, 769-787.

Tollerud, E. I., D. Rodgers, and K. Brown, 1987: Seasonal, diurnal, and geographic variations in the characteristics of heavy-rain-producing mesoscale convective complexes: A synthesis of eight years of MCC summaries. Preprints, *11th Conf. Weather Modification*. Edmonton, Alta., Canada, 143-146.

Velasco, I., and J. M. Fritsch, 1987: Mesoscale convective complexes in the Americas. *J. Geophys. Res*., **92**, 9591–9613.

Vera, C., J. Baez, M. Douglas, C. B. Manuel, J. Marengo, J. Meitin, M. Nicolini, J. Nogués-Paegle, J. Paegle, O. Penalba, P. Salio, M. A. Silva Dias, P. Silva Dias, and E. Zipser, 2006: The South American Low-Level Jet Experiment. *Bull. Amer. Meteor. Soc.,* **87**, 63–77.

Viana, D. R., 2006: Avaliação da precipitação e desastres naturais associados a complexos convectivos de mesoescala no Rio Grande do Sul entre Outubro e Dezembro de 2003. M. S. thesis, Universidade Federal do Rio Grande Do Sul, 136 pp.

Zipser, E. J., D. J. Cecil, C. Liu, S. W. Nesbitt, and D. P. Yorty, 2006: Where are the most intense thunderstorms on Earth?. *Bull. Amer. Meteor. Soc.*, **87**, 1057–1071.

Table 3.1. Mesoscale Convective Complex definition based on analyses of enhanced IR satellite imagery.

Mesoscale Convective Complex (MCC) Definition	
Criterion	**Physical Characteristics**
Size	Interior cold cloud region with temperature of ≤ -52°C must have an area 50,000 km^2
Initiation	Size definition first satisfied
Duration	Size definition must be met for a period of ≥ 6 hours.
Maximum Extent	Contiguous cold-cloud shield (IR temperature -52°C) reaches maximum size.
Shape	Eccentricity (minor axis/major axis) ≥ 0.7 at time of maximum extent.
Terminate	Size definition is no longer satisfied
MCC definition originally developed by Maddox (1980)	

Table 3.2. Comparison of MCC precipitation characteristics between South America (SA), Africa (AF) (Laing et al. 1999), and (3) the United States (US) (McAnelly and Cotton 1989).

No. of MCCs		**Mean precipitation characteristics**		
		Depth (mm)	Area (km^2)	Volume (km^3)
SA	330	15.7	381,000	7.0
AF	41	34.0	285,000	11.9
US	122	10.8	320,000	3.5

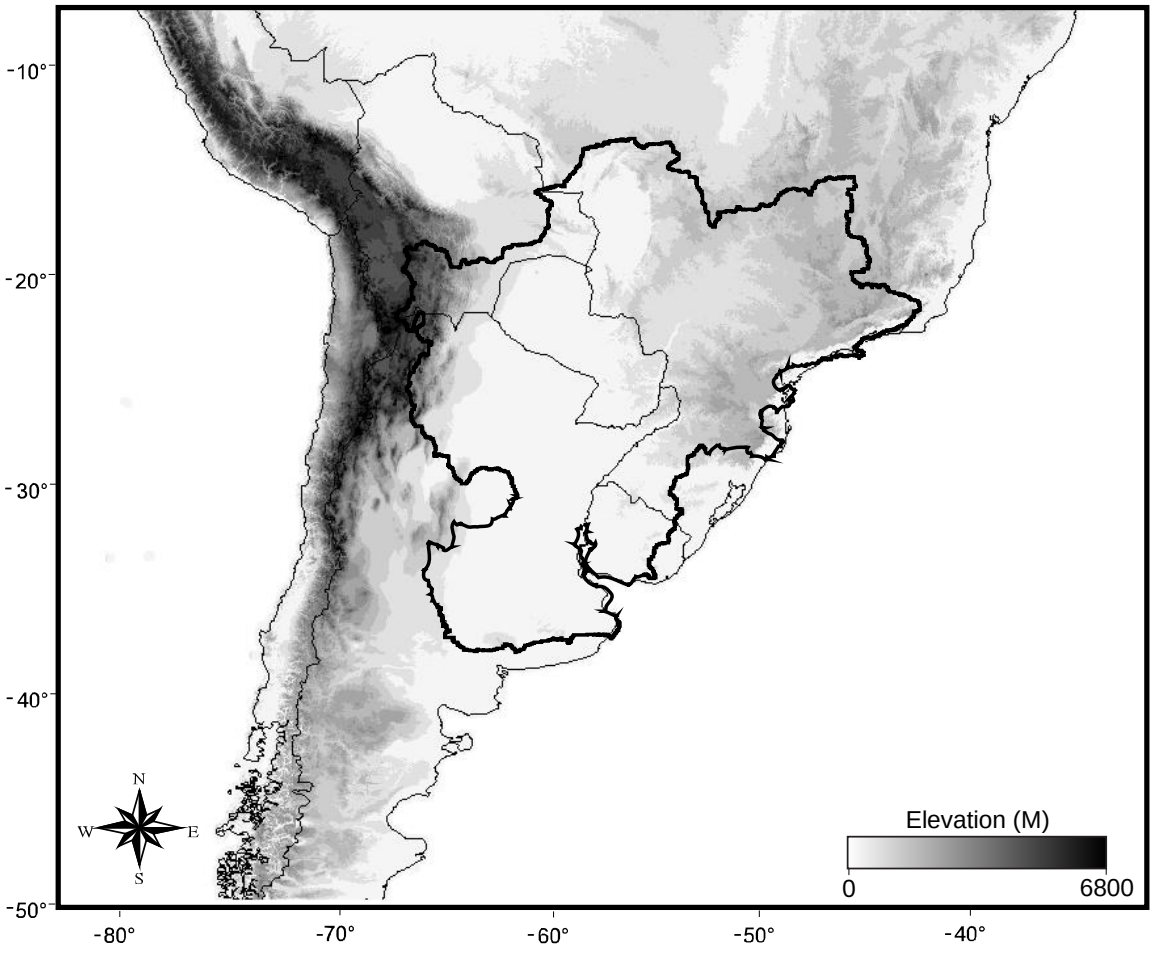

Fig. 3.1. Bold outline delineates the La Plata Basin located in the subtropics of South America.

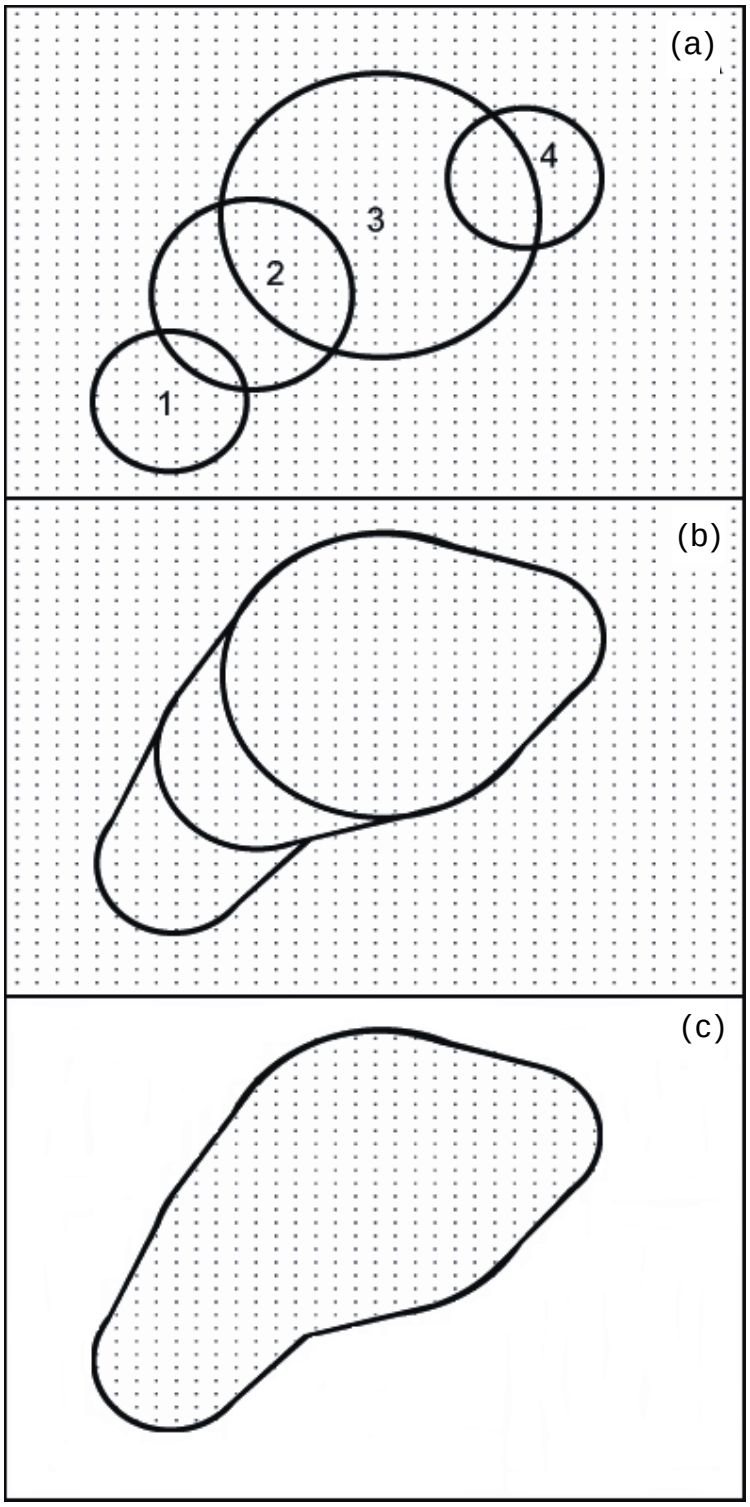

Fig. 3.2. Schematic diagram illustrating (a) cloud shields of an MCC overlaid onto a TRMM 3B42 precipitation grid, (b) the convex-hull calculation to determine the area within the MCC storm track, and (c) the final convex hull for the entire MCC duration and retaining only precipitation values within the storm-track area.

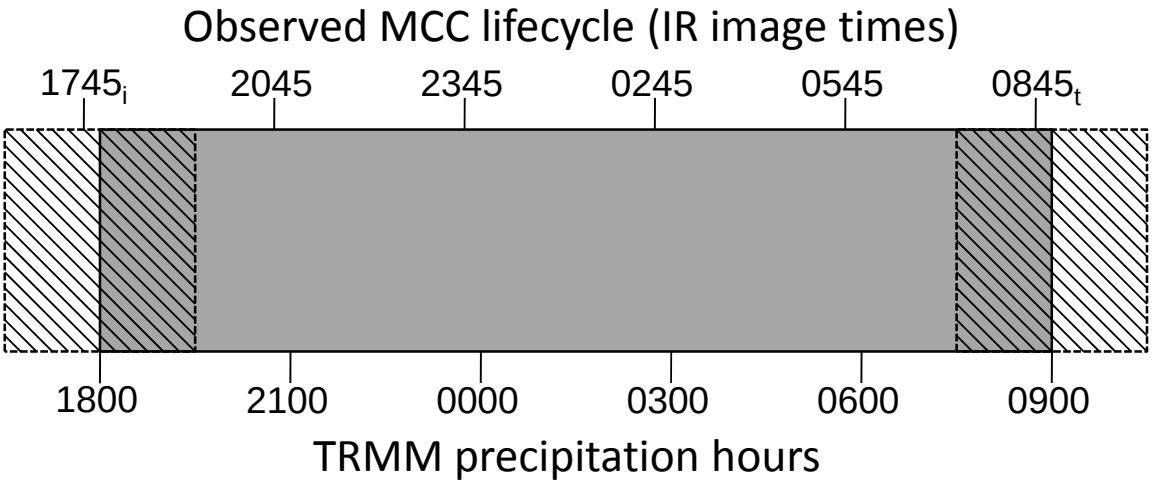

Fig. 3.3. Schematic representation of the precipitation summation for a hypothetical event. Hatched boxes are centered on the synoptic times closest to the event's initiation (subscript 'i') and termination (subscript 't') stages. Precipitation values inside the hatched boxes are assigned a weight of 0.5. Precipitation values inside the solid gray box are assigned a weight of 1.0. Accumulated precipitation is equal to the sum of all weighted observations.

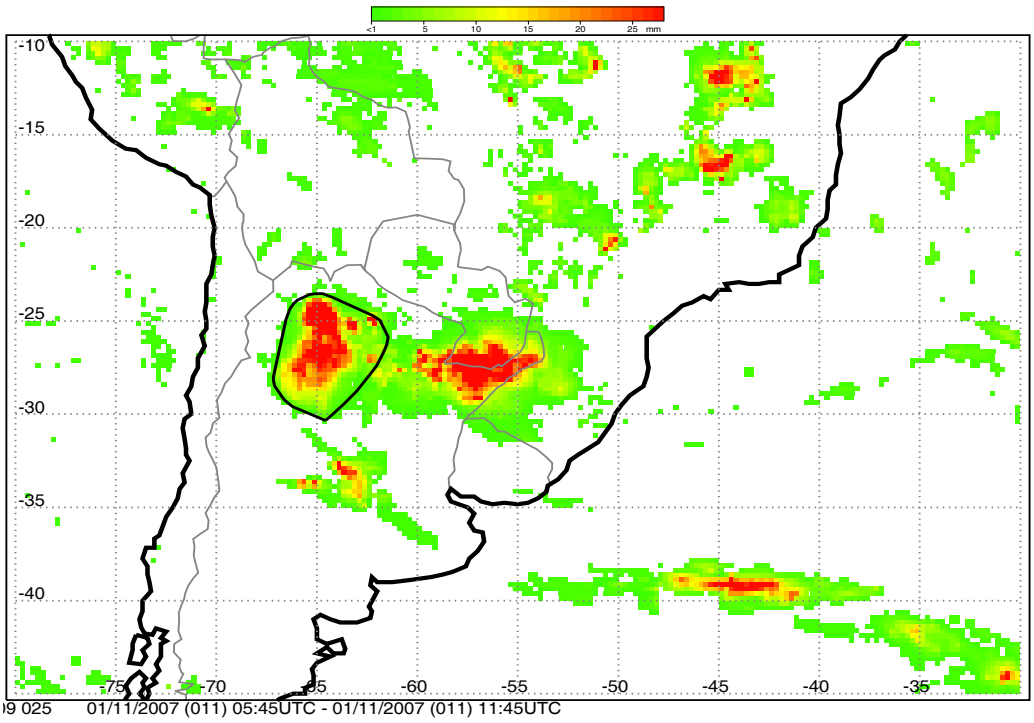

Fig. 3.4. Sample output illustrating the outline of the area (i.e., convex hull) of an MCC storm track overlaid accumulated 3B42 TRMM precipitation.

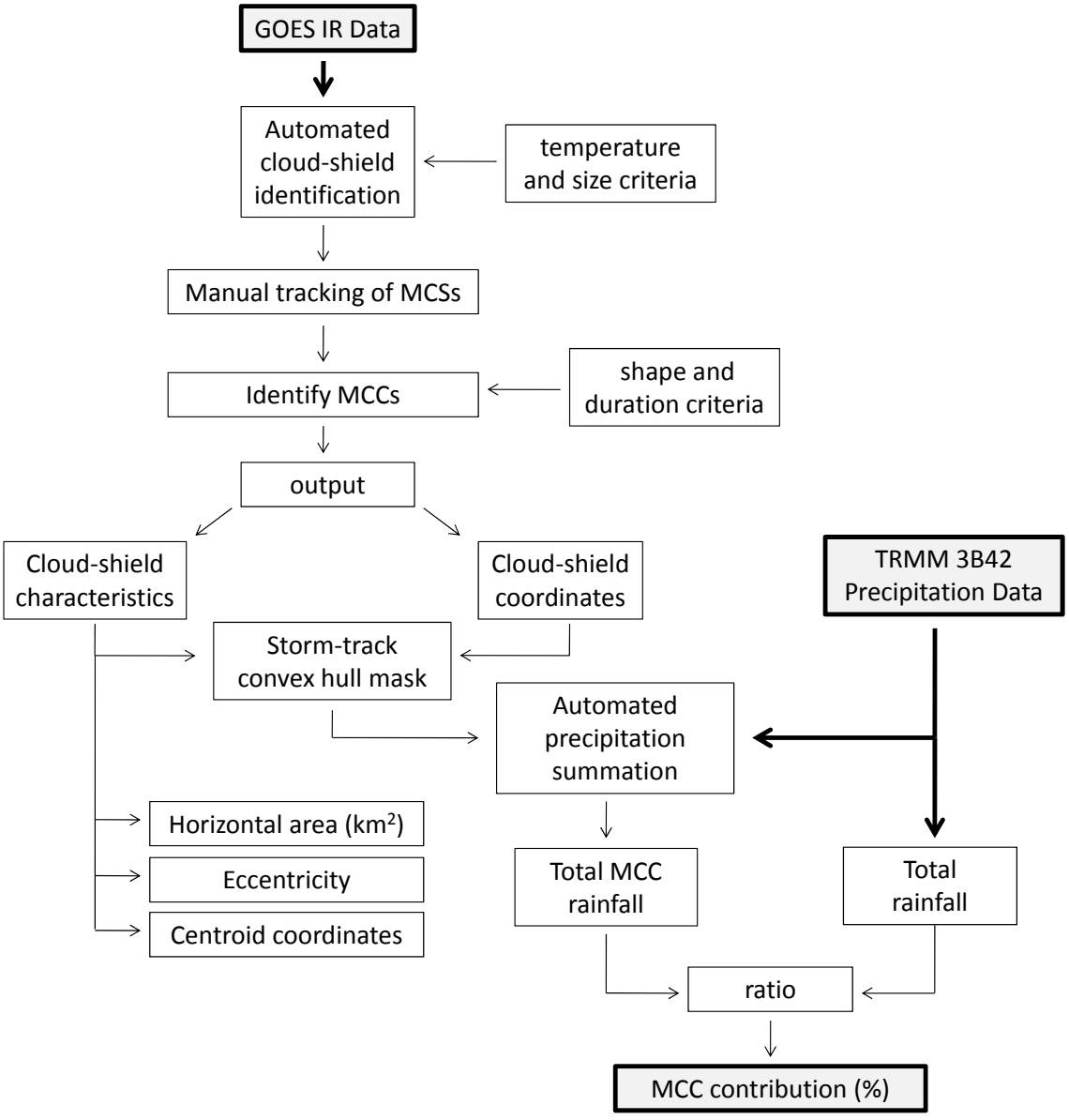

Fig. 3.5. Flow diagram demonstrating the MCC identification and tracking, and precipitation schemes.

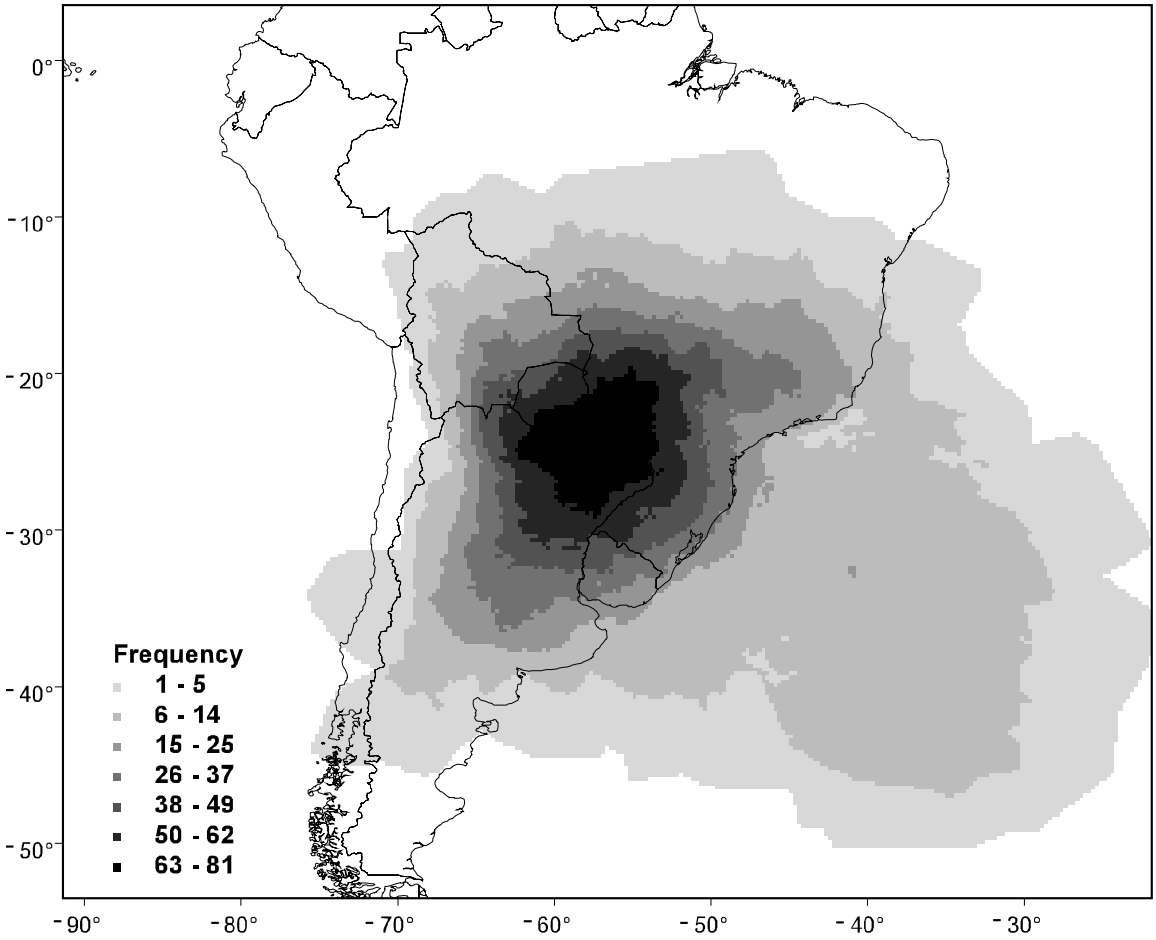

Fig. 3.6. MCC frequency during the warm season (October-May) for 1998-2007 (N = 330) determined by the number of times a grid point was located inside an MCC storm track.

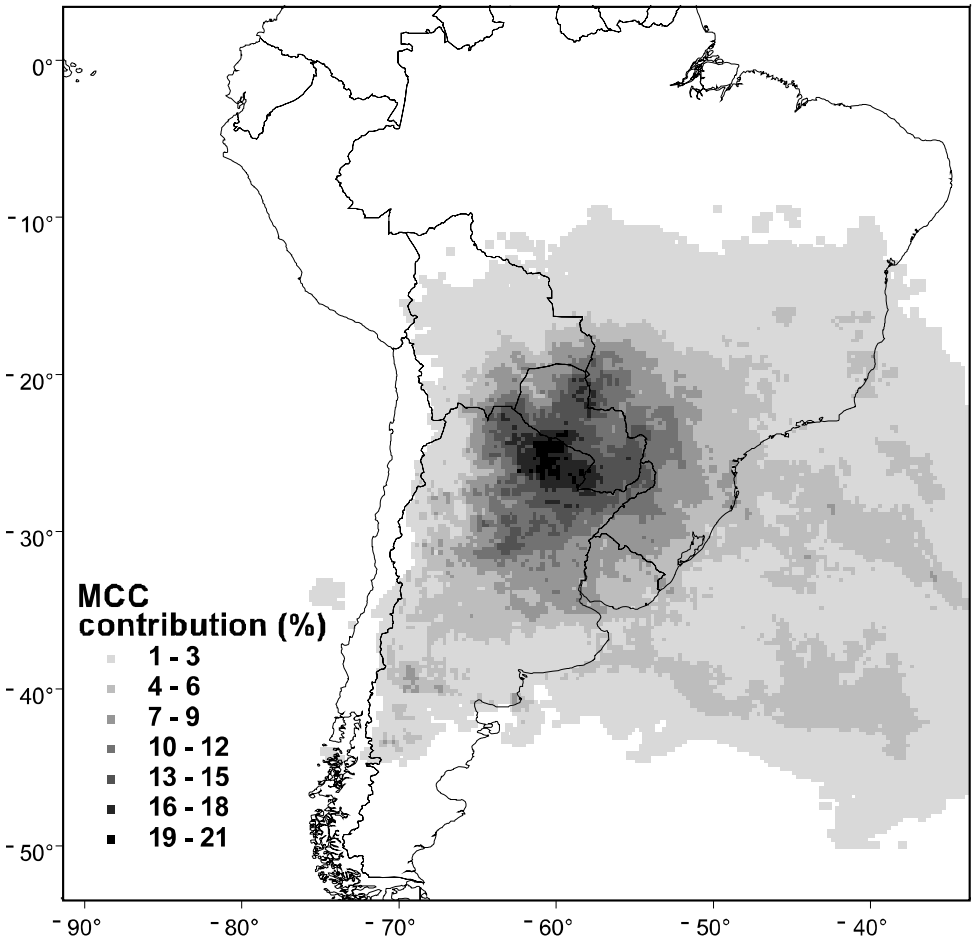

Fig. 3.7. Distribution of the percentage of warm-season rainfall from MCCs during 1998-2007.

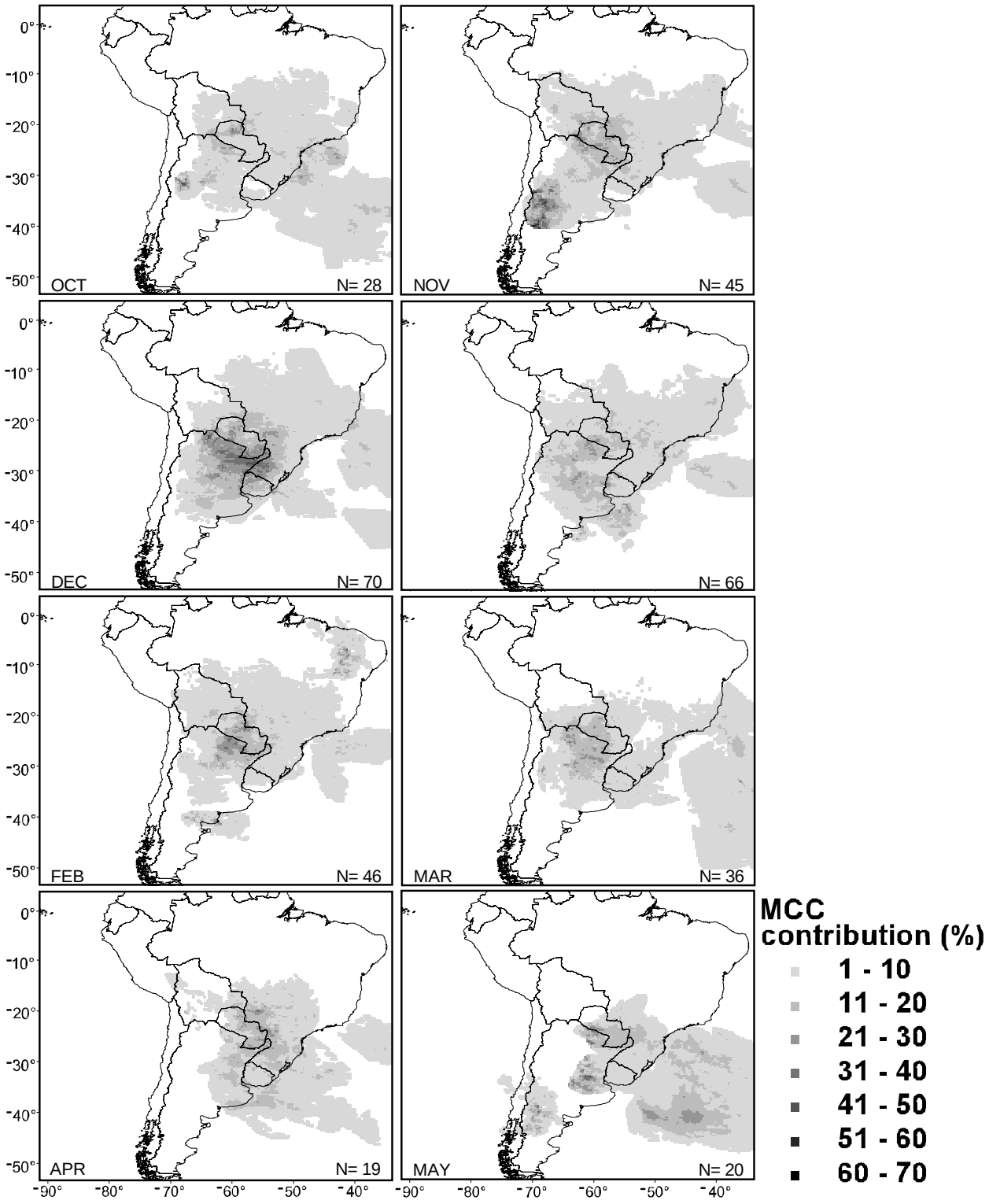

Fig. 3.8. As in Fig. 3.7 except by month.

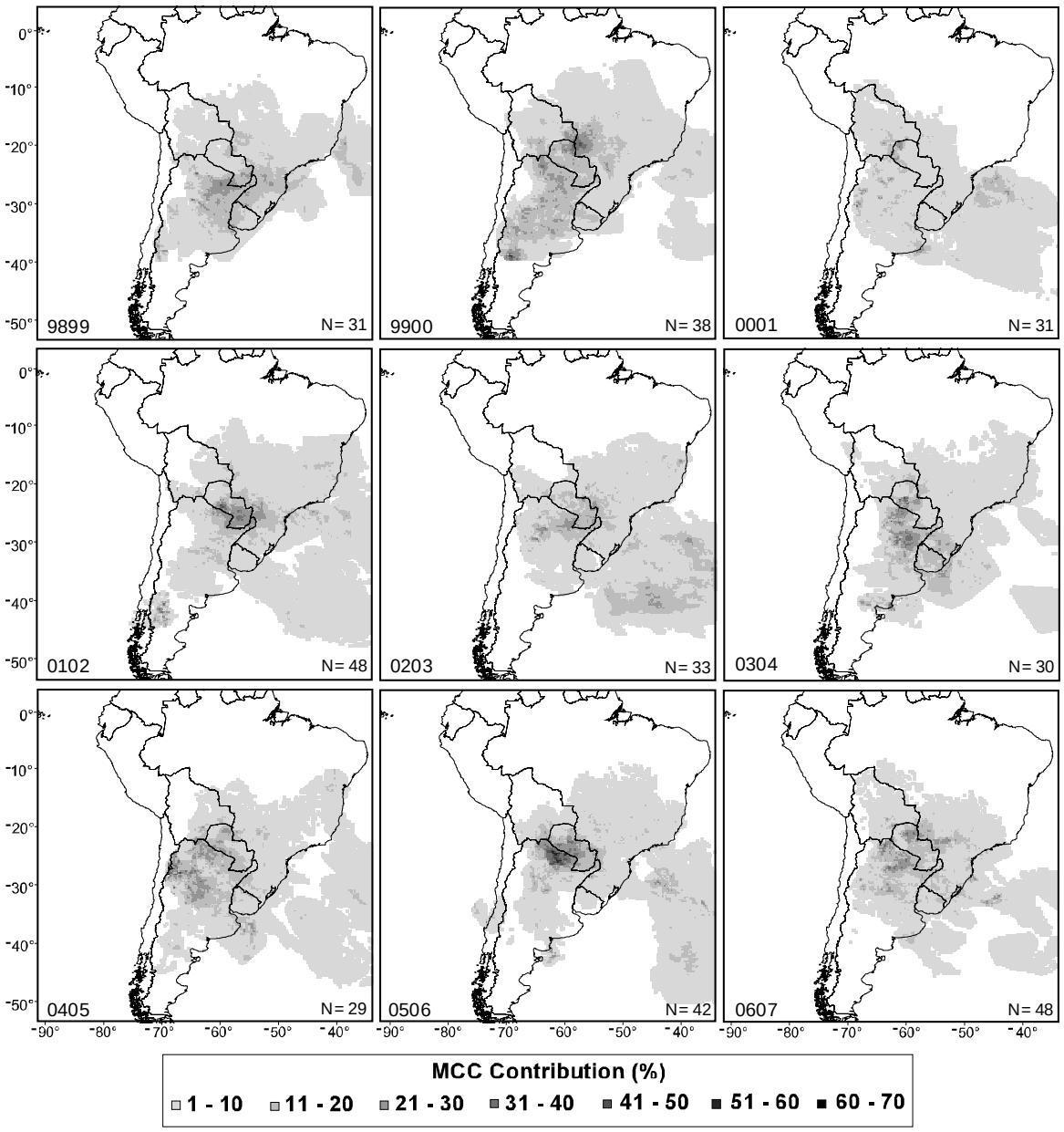

Fig. 3.9. As in Fig. 3.7 except by warm season.

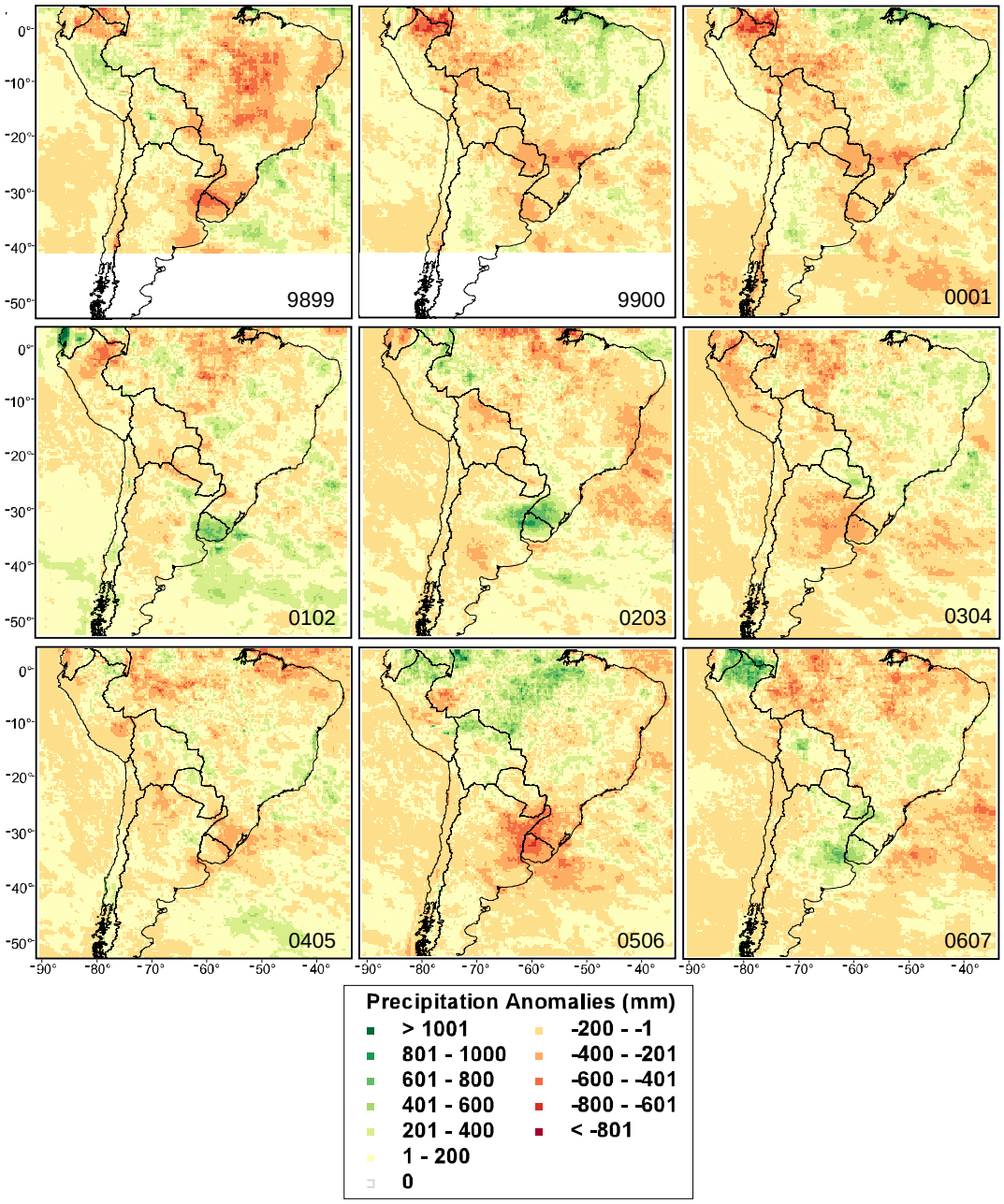

Fig. 3.10. Warm-season precipitation anomalies using 1998-2007 TRMM 3B42 as the baseline

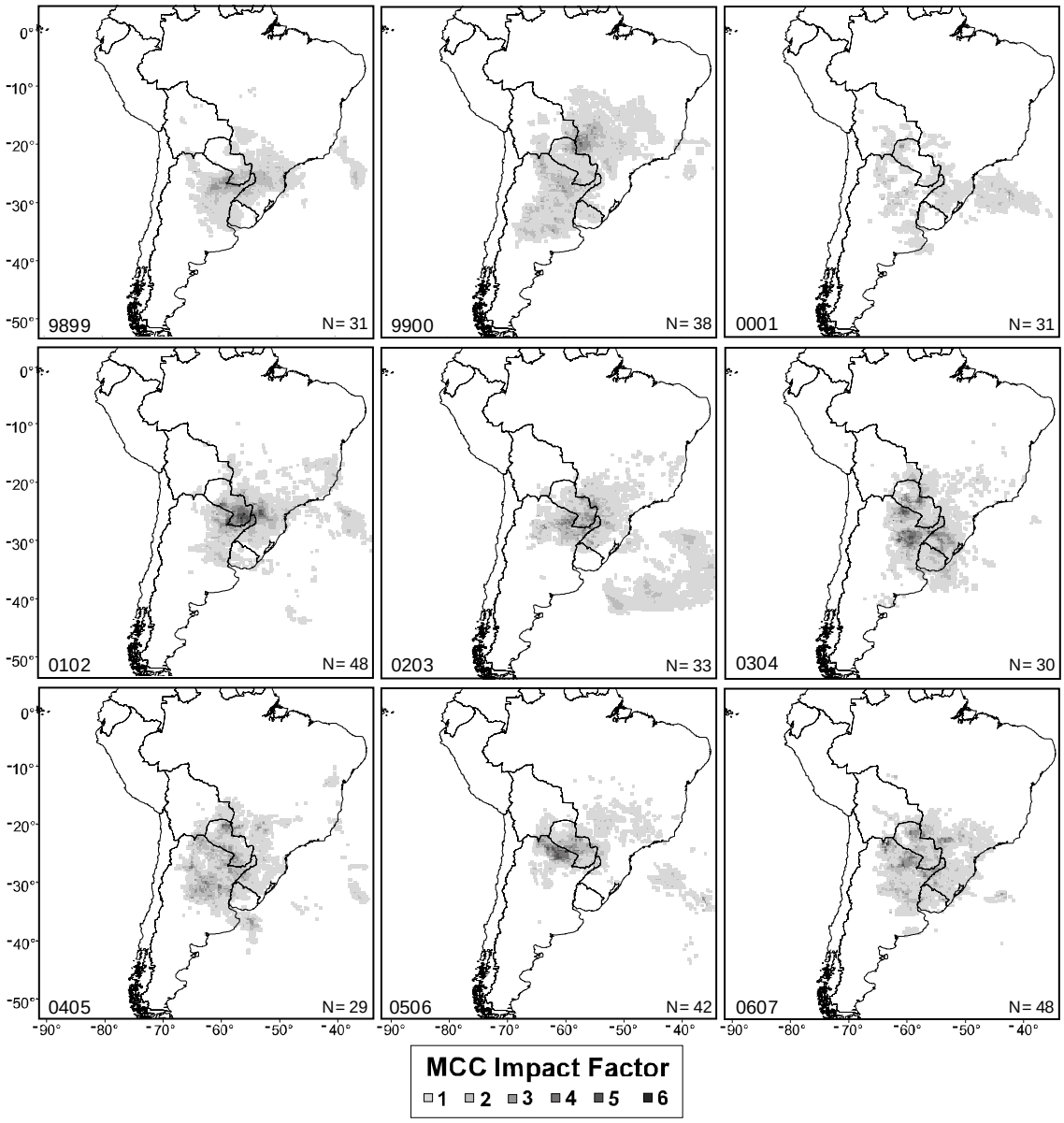

Fig. 3.11. MCC Impact Factors (MIFs) are in 0.5 standard deviation-unit intervals ranging from 1-6. Each grid point represents changes in the anomaly value by ≥ 0.5 standard deviations due to MCC precipitation ($\Delta\sigma_i$).

CHAPTER 4

CHARACTERISTIC CHANGES IN SOUTH AMERICAN MESOSCALE CONVECTIVE COMPLEXES IN RELATION TO THE SOUTH ATLANTIC CONVERGENCE ZONE[5]

[5] Durkee, J. D. and T. L. Mote. To be submitted to *Monthly Weather Review.*

ABSTRACT

Changes in the physical and rainfall characteristics of 291 South American mesoscale convective complexes (MCCs) are compared to variations in large-scale atmospheric circulation, with particular attention given to the South Atlantic Convergence Zone (SACZ), a quasi-stationary band of convection from the Amazon Basin into the Atlantic Ocean. During October-March of 1998-2007, the SACZ occurred during 23% of the warm season days, during which 75 MCCs formed, versus 216 on non-SACZ days. The mean location of MCCs during periods with the SACZ was 240 km to the northeast of the non-SACZ location. The number of MCCs per SACZ and non-SACZ day was 0.18 and 0.17, respectively. Most of the interannual variation (89%) in the number of MCCs during periods of SACZ was simply due to changes in the frequency of SACZ. A composite analysis of several tropospheric data fields shows the large-scale atmospheric patterns favorable for MCCs in preferred areas of the study region during SACZ and non-SACZ periods. This study is unique in showing a link in a preferred region of MCC activity to low-level circulation other than the northerly, tropical low-level jet. Together, the findings show that the SACZ has direct and indirect influences on the development and maintenance of MCCs across portions of tropical and subtropical South America.

4.1 Introduction

The South Atlantic Convergence Zone (SACZ) is an integral component of the austral warm-season monsoonal climate across tropical and subtropical regions (i.e., areas north and south of 20°S, respectively) of South America. A considerable proportion of the intraseasonal precipitation variability across tropical and subtropical South America is explained by changes in low-level circulation when the SACZ is present (Carvalho et al. 2004; Barros et al. 2002; Liebmann et al. 2004 and 1999; Nieto-Ferreira et al. 2003; Barros et al. 2002; Nogués-Paegle and Mo 1997). Therefore, the SACZ is considered one the most important climatological features that plays a key role in the influence of precipitation during the austral warm season (Carvalho et al. 2004).

The SACZ has been subjectively characterized as a distinct warm-season phenomenon, whereby a northwest-southeast oriented quasi-stationary band of convection (persisting $\geq$ 4 days) becomes anchored over the central Amazon Basin and extends into the western South Atlantic Ocean (Liebmann et al. 2004 and 1999; Carvalho et al. 2004 and 2002; Jones and Carvalho 2002; Barros et al. 2002; Lenters and Cook 1999; Nogués-Paegle and Mo 1997; Figueroa et al. 1995; Kodama 1992). The dominant forcing of the SACZ comes from transient mid-latitude westerly Rossby wave trains that aid in the advancement of polar air masses into the tropics. Convergence along surface frontal boundaries triggers the onset of convection, which help create the SACZ region (Liebmann et al. 2004 and 1999). Numerous studies provide evidence that the presence of an active or strong SACZ modulates the low-level wind configuration so that the northerly flow of tropical heat and moisture along the eastern slopes of the Andes (i.e., the low-level jet, LLJ) turns eastward near 20°S into the SACZ region near the Brazilian

states of Goiás, northern Minas Gerais, southern Bahia, and Espírito Santo (Figs. 4.1 and 4.2). Under weak SACZ conditions, or the absence thereof, the Amazonian LLJ feeds convection further south and west into Paraguay, the southeastern and southern Brazilian states of São Paulo, Paraná, Santa Catarina, and Rio Grande do Sul, and northern and central Argentina (Carvalho et al. 2004; Barros et al. 2002; Liebmann et al. 2004 and 1999; Nieto-Ferreira et al. 2003; Barros et al. 2002; Nogués-Paegle and Mo 1997).

Areas of organized convection and precipitation across tropical and subtropical South America have been shown to be closely connected to the location near the exit region of the LLJ (Saulo et al. 2007; Salio et al. 2007; Vera et al. 2006; Silva and Berbery 2006; Liebmann et al. 2004; Zipser et al. 2004; Nieto Ferreira et al. 2003; Marengo et al. 2002; Berbery and Collini 2000; Laing and Fritsch 2000; Nicolini and Saulo 2000, among others). Many of these studies have shown that the influence of the SACZ on the Amazonian LLJ helps explain the sub-monthly variability in the precipitation patterns across the region. Specifically, a dipole precipitation pattern typically occurs with active or intense (weak or absent) SACZ conditions resulting in positive (negative) rainfall anomalies across Goiás, northern Minas Gerais, southern Bahia, and Espírito Santo (São Paulo, Paraná, Santa Catarina, and Rio Grande do Sul in Brazil, Paraguay, and northern Argentina) (see Fig. 4.1).

Despite the abundance of SACZ research, there remains a gap in the literature pertaining to the influence of the SACZ on mesoscale convective complexes (MCCs). MCCs are the largest subset of organized convection (Maddox 1980) (Table 4.1) responsible for contributing substantially to warm-season rainfall totals around the globe (e.g., Chapter 3; Ashley et al. 2003; Laing et al. 1999; Fritsch et al. 1986, among others).

In a global analysis of MCCs, Laing and Fritsch (2000) showed that a LLJ was present in all regions where MCC activity was greatest, especially in South America. Given the relationship documented between the SACZ and the Amazonian LLJ and the relationship shown between the LLJ and MCCs, it is reasonable to question whether the variability of South American MCCs is in part due to the SACZ.

Chapter 2 examined warm-season MCCs (October-May) across subtropical South America (SSA) during 1998-2007. The results from that study showed that the highest frequency of MCCs across SSA was centered over northern Argentina, Paraguay, and southern Brazil during November-March. Additionally, a large majority of MCC cloud-shields ($\leq$ -52°C in infrared satellite imagery) reached their maximum horizontal extent during the nocturnal hours in SSA. Chapter 2 established that MCCs account for 30-50% of the total rainfall across much of the same area between November-March. While neither of the two studies provided an overview of the favorable synoptic environments conducive to MCCs across SSA, the timing and location of the systems documented in Chapter 2 were collocated with the mean location of the Amazonian LLJ (Saulo et al. 2007; Salio et al. 2007; Vera et al. 2006; Nieto-Ferreira et al. 2003). The proximity of MCCs to the mean location of the Amazonian LLJ supports the findings of Velasco and Fritsch (1987) and Laing and Fritsch (2000). Chapter 2 also showed that the timing and location of maximum rainfall contributions from MCCs are collocated with the nocturnal warm-season precipitation maximum found by Berbery and Barros (2002). Furthermore, Carvalho et al. (2004) and Liebmann et al. (2004) showed areas encompassing northeast Argentina, southeast Paraguay, Uruguay, and southern Brazil experience above-average rainfall under anomalous northerly flow from the LLJ. When the LLJ is weak, the same

area experiences below average precipitation, while positive anomalies are found over central-western and southeastern Brazil.

The intimate interaction of MCCs and the LLJ, combined with the influence of the SACZ on the position and direction of the low-level moisture flux, suggests that a connection may exist between MCC activity and the SACZ. In this study, one hypothesis is that when the SACZ is active, MCC activity follows the LLJ further north and east into closer proximity of the SACZ region. However, Barros et al. (2002) also showed when the SACZ is active, low-level anti-cyclonic flow originating off the subtropical coast near 35°S, 45°W provides an influx of moisture into west-central Argentina, leading to positive precipitation anomalies across that area. Under optimal conditions, it is therefore possible for the Amazonian LLJ to aid in convective development near the SACZ region concurrent with oceanic moisture flux feeding convection at higher latitudes in the subtropics. Perhaps this convective signal is evident in MCC activity during active SACZ periods. Because MCCs have been shown to contribute substantially to rainfall totals across the subtropics and portions of the tropics, important questions about these South American systems need to be addressed. Such questions include:

- How do the frequency and location of MCCs across SSA change during the presence of the SACZ?
- Are there significant differences in MCC physical characteristics between active and non-active SACZ episodes?
- How do MCC rainfall characteristics change during the SACZ?

- How does the tropospheric circulation conducive for MCC formation, particularly the Amazonian LLJ, change relative to the presence of the SACZ.

The current study is motivated by these unanswered questions.

4.2 Data and Methods

The MCC databases used in this study were those developed in Chapters 2 and 3. The former used a hybrid automated/manual technique to identify and track the physical characteristics of 330 warm-season MCCs (October-May) spanning 1998-2007 using GOES-8 and GOES-12 digital 4km infrared satellite imagery, provided by the National Oceanic Atmospheric Administration Comprehensive Large-array data Stewardship System (NOAA 2007). Data on MCC physical characteristics included information on storm duration, cloud-shield areas, area during maximum extent, and the timing and location of cloud-system centroids throughout their lifecycles.

To determine MCC precipitation characteristics, data from Chapter 2 were combined with rainfall data provided by the Tropical Rainfall Measuring Mission Multi-Satellite Precipitation Analysis 3B42 version 6 (Huffman et al. 2007). This product provides global 3-hourly rain rate estimates with latitudinal coverage between 50°N-S (0.25° x 0.25° grid) since 1998 January. MCC rainfall data for SSA includes information on aerially-averaged rainfall volumes, precipitation areas, volumetric rain-rate, and MCC rainfall contributions (given by the ratio of MCC rain to the total rainfall). The methods used to determine the physical and rainfall characteristics of the 330 MCCs are discussed in detail in Chapters 2 and 3. The current study utilizes the data from both studies to

examine the influence of the SACZ on MCC activity during October-March for 1998-2007.

Within the Brazilian Ministry of Science and Technology's National Institute for Space and Research (INPE), the Center for Weather Forecast and Climatic Studies (CPTEC) provide archived monthly climate bulletins (*Climanálise*) that detail daily occurrences of SACZ episodes between October-March (CPTEC 2008). The seasonal period in this study was chosen based on the INPE/CPTEC SACZ observational period, which denotes the typical seasonal onset and demise of the SACZ. CPTEC classifies SACZ episodes from the following criteria: 1) at least a four-day duration of a northwest-southeast oriented quasi-stationary band of convection that extends from the central Amazon Basin toward the western South Atlantic Ocean; 2) the presence of an upper-level Bolivian High and a trough over northeast Brazil, with anti-cyclonic vorticity over the convective band; 3) a northwest-southeast oriented 500 hPa trough axis located east of the Andes; 4) relatively cool air located on the poleward side of the convective band; and 5) at least a four-day duration of ongoing low-level moisture flux convergence within the SACZ region. Other information that may be included in these archived summaries includes infrared satellite imagery, a brief synoptic analysis, and notes pertaining to hazardous outcomes (e.g., record rainfall totals, flooding, mudslides, property or crop damages, etc.). It is important to note that the exact location and magnitude of each SACZ episode is not included.

Daily composites of atmospheric data, including sea-level pressure, 850 hPa winds and specific humidity, 700 hPa geopotential height, 500 hPa geopotential height and vertical velocities, and 200 hPa geopotential height and winds, were extracted from

National Centers for Environmental Prediction – National Center for Atmospheric Research (NCEP-NCAR) reanalysis data version 1 on a 2.5° latitude by 2.5° longitude grid (Kalnay et al. 1996). Composites of MCC characteristics and atmospheric data were constructed for MCCs that occurred during SACZ and during non-SACZ periods. The criteria used in the composite analyses are described in detail in section 4.4.

4.3 Statistical analysis

a. Composite assessment of MCCs during SACZ and non-SACZ periods

During October-March of 1998-2007, the average locations for 291 MCCs were identified across subtropical and tropical South America (Fig. 4.3). Table 4.2 summarizes the interannual frequencies of SACZ and non-SACZ periods, including MCC frequencies during each period. On average, SACZ and non-SACZ periods constitute 23% and 77% of the total warm-season days between October-March, respectively. MCC frequency per SACZ or non-SACZ day, given by the ratio of the number of MCCs to the number of days in each period, shows that for the period of record MCC frequency was nearly the same regardless of the presence or absence of the SACZ (0.18 vs. 0.17 MCCs per SACZ and non-SACZ day, respectively).

A summary of the composite physical and precipitation characteristics of MCCs during SACZ periods and during non-SACZ periods is given in Table 4.3. MCCs during SACZ periods were smaller, shorter-lived systems that distributed less rain across smaller areas when compared to non-SACZ MCCs. The mean location for MCCs during SACZ periods was also found to the north and east of the non-SACZ MCC location. Results

from a Student's *t*-test show that there were significant differences in the maximum extent ($p = 0.03$), latitude, and longitude ($p = 0.01$).

Based on these findings, it appears that differences in the frequency of MCCs were not affected by the presence of the SACZ. Further inspection revealed while the differences in each of the characteristics were consistent (i.e., smaller, shorter-lived and MCCs producing less rainfall during SACZ periods compared to non-SACZ periods), most were not statistically significant. However, while the shift in the composite MCC position between SACZ and non-SACZ periods may appear small, considering the large size of the clouds-shields, it is also important to consider the distribution of MCC rainfall beneath the cloud shields. McAnelly and Cotton (1989) and Kane et al. (1987) found for the United States, the area with the heaviest rainfall is typically found within the southern flank of an MCC. Both studies suggested that the LLJ plays a role in this asymmetric precipitation pattern. The northeast shift in the mean MCC position during SACZ periods may be indicative of the changing position and direction of the low-level transport of heat and moisture.

b. Interannual and intraseasonal MCC variability during SACZ and non-SACZ periods

This study also examined the variability in MCC frequency relative to the number of SACZ and non-SACZ days for each season, in order to ascertain whether MCCs were preferentially occurring during SACZ or non-SACZ days. The preference for MCCs to occur in either period was determined by calculating the difference between the number of MCCs per SACZ day and non-SACZ day for each warm season (Table 4.4). Positive (negative) values of this difference indicate more MCCs per non-SACZ day (SACZ day).

While the numbers of MCCs per SACZ and non-SACZ day were nearly identical over the period of this study, the results showed there was substantial interannual variability in the occurrence of MCCs in between both periods. Specifically, four of the nine years had a preponderance of events during non-SACZ periods, while the other five had a greater portion occur during SACZ periods. This further suggests that MCCs appear no more likely to form in the presence or absence of the SACZ.

Next, the interannual variability in the number of MCCs and the number of days in each period were analyzed (Fig. 4.4). It is apparent that seasons with greater (lesser) numbers of SACZ days have increased (decreased) MCC frequency during the SACZ. In contrast, the number of MCCs that occurred during periods without the SACZ appears to be unrelated to the number of days without the SACZ. Linear regressions for both scenarios confirm that only a significant correlation exists between the number of MCCs and SACZ days ($p = 0.01$) (Fig. 4.5). Specifically, 89% of the variability in warm-season MCC frequency during SACZ periods is explained simply by the number of SACZ days during the season. In other words, warm seasons with longer periods of the SACZ experience an increase in MCC activity during these periods. While this may seem obvious, there was no statistical correlation between the number of days without the SACZ and the number of MCCs during periods without SACZ.

However, it could be possible for a given season to have a large number of MCCs in a season during a relatively small number of SACZ days, compared to a relatively higher number SACZ days without MCCs. This situation would introduce a bias in the relationship between the number of SACZ days and SACZ MCC frequency, if one were to examine only the seasonal totals. Considering the possibility of situations like the one

just described, proportions of *simultaneous* SACZ days and MCC days were quantified throughout each season (Table 4.5). Results show that there are relatively few instances of SACZ periods without MCCs, thereby reducing concerns over the lack of intra-seasonal overlap between the two variables. This finding lends further evidence of the robustness of the relationship shown in Figs. 4.4 (a) and 4.5.

With the connection between SACZ frequency and SACZ MCCs established, the next step was to spatially segregate the linear regression analysis in order to determine where the response is greatest. The study region was divided into quadrants centered on the geographic mean (see Fig. 4.3). MCC frequencies were similar for three of the four quadrants (northwest, 24; northeast, 22; southwest, 23; southeast, 6). The linear regression analysis shown in Fig. 4.5 was repeated for each quadrant between the number of MCCs and SACZ days. Only the northwest and southwest quadrants had significant positive correlations ($p = 0.01$ for both), with the greater response in the northwest quadrant ($R^2 = 0.89$ and 0.70, respectively) (Fig. 4.6; only significant plots are shown). Given such a small sample size of MCCs in the southeast quadrant (6 events), a linear regression with few degrees a freedom would inflate the threshold for statistically significant findings. Therefore, an additional regression was calculated for all events east of the geographic center to increase the sample size from 6 to 28 MCCs (i.e., the total in the merged northeast and southeast quadrants). Again, no statistically significant relationship was found.

Overall, the linear regression analysis suggests that a large proportion of the variability in MCC activity across particular areas within South America is explained by the presence of the SACZ. This geographic preference suggests that there may be certain

changes in the synoptic environment that are particularly conducive to MCC development across Bolivia and northwestern Paraguay, and central Argentina.

4.4 Synoptic analysis

In order to ascertain how the synoptic environment that produces MCCs changes in relation to position with respect to the SACZ, or the absence of the SACZ, the tropospheric circulation across South America were examined for six different subsets of MCCs. The areas that were examined for the first two subsets were chosen based on relationship between MCCs and the SACZ west of the 55°W meridian (hereafter, NW and SW, referring to the northwest and southwest quadrants shown in Fig. 4.6). Additionally, recall that Barros et al. (2002) also show positive precipitation anomalies can occur in the SACZ region and at higher subtropical latitudes during SACZ periods. These anomalies occur as a result of thunderstorms that feed from the influx of oceanic moisture that is advected from a coastal low-level anti-cyclonic circulation. It is possible that MCCs can develop inside the SACZ region, as well as the southern region of SSA during SACZ periods; thus comparisons of low and high latitude MCCs (hereafter, North-SACZ and South-SACZ) during SACZ periods were explored. Lastly, MCCs located in the core MCC region during SACZ periods and during non-SACZ periods (hereafter, $Core_{SACZ}$ and $Core_{non\text{-}SACZ}$, respectively) were considered.

A composite analysis was used to identify differences in the synoptic environment conducive to MCC activity in each of the locations described above. In an attempt to control for differences in the location and magnitude of the SACZ, as well as other indirect influences on the variability in large-scale atmospheric circulation including

teleconnections (e.g., El Niño/Southern Oscillation), MCCs in each composite analysis were selected based on the following criterion:

- For each subset (i.e., NW, SW, North, South, $Core_{SACZ}$, and $Core_{non\text{-}SACZ}$):
    - MCCs occurred in reasonably close proximity (i.e., MCCs in each subset were at least $\leq 5°$ of latitude and longitude from each other during some point of their lifecycles).
    - Based on the previous criterion, each composite analysis was performed only for MCCs that occurred in the same warm seasons.

Based on these criteria, each composite analysis for the subsets of NW, SW, $Core_{SACZ}$, and $Core_{non\text{-}SACZ}$ contained three MCCs, each during 1999-2000, 2005-2006, and 2006-2007. The North-SACZ and South-SACZ subsets contained four MCCs during the same seasons. MCC locations for each subset used in the composite analysis are shown in Fig. 4.7.

NCEP-NCAR reanalysis data version 1 (Kalnay et al. 1996) were used to create composites of the synoptic environments conducive to NW and SW MCCs during SACZ periods. The NW, SW, North-SACZ, South-SACZ, and $Core_{SACZ}$ composites were constructed from 21, 40, 41, 45, and 30 SACZ days, respectively. The North-SACZ and South-SACZ composite analysis was constructed from 15 SACZ days. The final composite analyses included MCCs during non-SACZ periods, consisting of nine days. Figs. 4.8 and 4.9 illustrate conceptual models of the synoptic environments for the MCCs that occurred during SACZ and non-SACZ periods, which were subjectively determined from analyses of the daily NCEP-NCAR reanalysis data.

a. MCCs during SACZ periods

In general, the composite analysis of MCCs during SACZ periods exhibited similar large-scale atmospheric patterns. The conceptual diagram of the atmospheric composite is summarized in Fig. 4.8. Starting at the surface, the mean position of the subtropical high in the Atlantic was located near 20°S, 22°W (not shown) with surface ridging extending from this high pressure center southwest into the coastal area near eastern Argentina and Uruguay. A coastal high was evident with anti-cyclonic low-level flow, advecting oceanic moisture into central and western Argentina. The 850 hPa winds showed a low-level core of maximum northwesterly winds (≥ 4 m s^{-1}) along the Andes Mountains in northwestern South America, which typically turned eastward in central Bolivia toward the vicinity of the Brazilian states of Minas Gerais and São Paulo. Specific humidity values at 850 hPa (not shown) typically increased across much the tropical region and western portions of SSA, when compared to normal. A shortwave trough at 700 hPa (not shown) was evident across central SSA. At 500 hPa, there was a moderately amplified wave pattern with a ridge over northwest Argentina and a negatively tilted trough centered over the SACZ region. A tripole pattern of the 500 hPa vertical velocities of upward vertical velocities (UVV) was found across the SACZ region, downward VV (DVV) over Paraguay, northeast Argentina, Uruguay, and southeast Brazil, and UVV over much of central Argentina. Lastly, a 200 hPa winds showed a high above Bolivia (known as the Bolivian High) and a trough over northeast Brazil, with a jet streak centered over north-central Argentina, Uruguay, and Rio Grande do Sul, Brazil.

The response of increased MCC activity in NW during active SACZ periods is a likely result of the superimposition of strong, low-level heat and moisture flux, mid-level differential vorticity advection and UVV, speed divergence within the descending branch of a mid-level trough, and the vicinity of the left entrance region of an upper-level jet streak. To the south, MCCs in central Argentina likely developed from the superimposition of the low-level oceanic moisture flux from a coastal anti-cyclone, mid-level differential vorticity advection, diffluent mid-level winds, and the right exit region of the upper-level jet streak. It is also possible that ascent of warm moist air is enhanced from the up-sloping terrain.

The composite analysis for MCCs in the SACZ region shows these systems were influenced by converging 850 hPa winds from the northwesterly tropical corridor and the Atlantic subtropical high pressure center, strong mid-level differential vorticity advection and UVV, and upper-level divergence. The SACZ summary from *Climanálise* states that there were intense rains found across the states of Minas Gerais and São Paulo ranging from 287-439 mm during the eight-day SACZ episode 2000. During a seven-day SACZ episode in 2006, there were positive rainfall anomalies of 50 mm across northern Rio de Janeiro. Intense 24-hour rain totals were associated with moisture convergence in the states São Paulo, Rio de Janeiro, and southern Minas Gerais during a 21-day SACZ episode in 2007. Each of these heavy rainfall events were collocated in time and location with MCCs.

b. MCCs during non-SACZ periods

The final composite analysis is of three MCCs in the core MCC region, but in the absence of the SACZ (i.e., non-$SACZ_{CR}$) (Fig. 4.9). The synoptic pattern varies from the conceptual SACZ models described above. One of the primary differences included a more northerly component to the 850 hPa wind corridor near the MCC region. The 500 hPa longwave pattern was less amplified with the descending branch of the trough in the vicinity of the MCC region. The 500 hPa vertical velocity tripole pattern was no longer evident. The area with UVVs extended from central and eastern Brazil into western-central areas of SSA. Finally, a stronger 200 hPa jet streak was located further east centered over southeastern Uruguay, with the left entrance region of the jet streak over the MCC region.

As with *most* MCCs, prime synoptic conditions for system development and maintenance includes ample low-level heat and moisture flux via the LLJ into a surface frontal boundary zone with the presence of a shortwave trough in the mid-levels (Laing and Fritsch 2000; Smull and Augustine; Augustine and Howard 1991; Cotton et al. 1989; Kane et al. 1987; Velasco and Frisch 1987; Maddox 1983). The superimposition of these features characterizes the low-level baroclinic environment conducive to MCCs. The primary difference is that some MCCs in South America, particularly the events from the composite analysis, are not as dependent on heat and moisture flux from the Amazon Basin. As this study shows, this is particularly the case for some MCCs at higher latitudes of the subtropics. Figs. 4.10 and 4.11 show 925 hPa wind circulation during the leading hours prior to achieving MCC classification, and the locations of North-SACZ and South-SACZ MCCs during the SACZ, respectively. MCCs located in the SACZ

region are positioned in the area of relatively strong converging west/northwesterly and northeasterly winds. Notice in Fig. 4.11 the pre-storm anti-cyclonic circulation with easterly and northeasterly flow from the Atlantic into central Argentina where the MCCs later developed.

While the results presented here differ from the composite analysis presented by Laing and Fritsch (2000), these findings are supported by the conceptual SACZ synoptic model shown in Barros et al. (2002). This does not imply that MCCs at higher latitudes of the subtropics rarely interact with the Amazonian LLJ. Rather, some proportion of MCCs across central Argentina develop more in response to low-level subtropical easterly and northeasterly circulation from the Atlantic rather than tropical northerly flow from the Amazon region, which is in part influenced by the SACZ.

4.5 Summary and Conclusions

The purpose of this study was to determine characteristic changes in South American MCCs as they relate to the presence of the SACZ. Previous studies have shown that the SACZ modulates the synoptic circulation in a manner that results in a precipitation dipole pattern across portions of tropical and subtropical South America. During active (non-active) SACZ periods, positive (negative) precipitation anomalies are found across Goiás, northern Minas Gerais, southern Bahia, and Espírito Santo in Brazil (São Paulo, Paraná, Santa Catarina, and Rio Grande do Sul in Brazil, Paraguay, and northern Argentina). This dipole pattern is largely a result due to the shift in the location and direction of the low-level heat and moisture flux via the Amazonian LLJ. Previous studies found that the development and maintenance of MCCs are closely connected to

the location of the exit region of the LLJ. Results from this study demonstrate that some MCCs in South America, particularly at higher subtropical latitudes, are not as dependent on the Amazonian LLJ.

Between October-May during 1998-2007 there were 291 MCCs, 75 of which occurred during active SACZ periods. On average, the SACZ occurs during 23% of the warm season. The mean rate of MCCs per SACZ day compared to MCCs per non-SACZ day was nearly the same (0.18 and 0.17, respectively). While these findings indicate that during the study period, MCC *frequency* was not influenced by the presence of the SACZ, statistically significant differences in the mean MCC *location* in each period were determined. Specifically, the mean location for MCCs during the SACZ period was located 240 km northeast of the mean location of non-SACZ MCCs. Following the hypothesis that the mean MCC location during SACZ periods should be located further north and east, in part as a result of the position of the Amazonian LLJ, was supported by the findings in this study.

In terms of composite physical and rainfall characteristic differences between MCCs, SACZ systems were shorter-lived, smaller, with smaller rainfall areas, and less rainfall production and intensity compared to non-SACZ MCCs. However, the only significant difference was for the horizontal area the cloud shield at the time of maximum extent. Given that the majority of MCCs during active SACZ periods occur near 20°S, it is possible that MCCs at this latitude (i.e., more tropical) are in closer proximity to other convective systems competing for moisture. In this situation, MCCs are smaller and less efficient at producing precipitation.

Another approach taken in this paper was to examine the variability in the number of MCCs and SACZ and non-SACZ days on interannual and intraseasonal time scales. A linear regression analysis comparing MCC frequency with the number of days in each period shows warm seasons with longer periods of the SACZ experience significant increases in MCC activity during these periods ($R^2 = 0.89$). In support of this relationship, the timing of the SACZ was collocated with MCCs throughout the majority each season. In contrast, there was little relationship between the number of days without the SACZ and MCC frequency during periods without the SACZ. These findings suggest that the synoptic environment during SACZ periods is conducive to the development of MCCs

With the evidence of the positive relationship between the SACZ and MCCs on interannual and intraseasonal time scales, the next step was to determine where the response was located within the study region. The linear regression analysis was repeated for MCCs located in four quadrants centered on the geographic center of MCC activity. Results show significant positive relationships between the number of SACZ days and MCC frequency were located in the northwest ($R^2 = 0.89$) and southwest ($R^2 = 0.70$) quadrants of the study region. These results helps support the connection between the SACZ and MCCs established in this study.

In order to determine the physical link between the atmosphere and MCCs for various locations during SACZ and non-SACZ periods, a composite analysis of large-scale atmospheric fields was conducted. The composite analysis revealed that there are certain lower and middle tropospheric circulation patterns conducive to the development of MCCs during SACZ and non-SACZ periods. For SACZ MCCs, a coastal high

pressure center induces low-level anti-cyclonic flow of oceanic moisture flux inland toward central and western Argentina. The resultant moisture pooling and increased instability has the potential to interact with the sloping terrain along the eastern slopes of the Andes to induce lift of this warm moist air. Dynamical features found in the middle and upper levels such as differential vorticity advection and jet streak circulations commonly traverse the region to provide enhanced ascent. Together, these features provide the trigger for the onset of MCC development at higher subtropical latitudes. Further north, the convergence of northwesterly and northeasterly winds along a slow moving cold or quasi-stationary frontal boundary induces a low-level baroclinic zone, which provides the optimal low-level conditions for MCC initiation.

The findings for the composite analysis for non-SACZ MCCs are in agreement with results from previous studies of common synoptic regimes conducive to MCC development. The presence of a relatively weak shortwave disturbance rotating through a low amplified mid-level longwave pattern is commonly present. The low-level wind maximum in the tropics has a more northerly component providing ample low-level heat and moisture into the subtropics. The interaction of these features within a deep wind-shear layer provides a classic setup for MCCs.

Laing and Fritsch (2000) found in their global analysis of MCC synoptic environments that the LLJ was present in all regions. Numerous other studies have demonstrated the close connection between thunderstorm formation and the exit region of the LLJ. However, this study is unique in that it demonstrates a scenario, whereby an area common to MCCs may often form 15°-20° south of the exit region of the Amazonian LLJ. In this situation MCCs thrive in part from the strength and position of

the coastal high, and are far removed from interactions with the Amazonian LLJ. Its strength and position may vary in part, as a function of the presence of the SACZ. The Amazonian LLJ has been shown to penetrate higher subtropical latitudes (i.e., south of 25°S –known as Chaco Jet Events; see Nicolini and Saulo 2000), aiding in the initiation of convection across central Argentina. It is possible that the northerly flow from Chaco Jet Events merges with the coastal anti-cyclone to enhance moisture flux into this region, particularly during non-SACZ periods. However, the current study demonstrates that at least some proportion of MCCs in central Argentina develops in the absence of northerly low-level winds. It is therefore possible that overall convection and resultant precipitation patterns across central Argentina during the warm season are modulated by the presence of both Chaco Jet Events and a coastal anti-cyclone, which have been shown to be strongly influenced by the SACZ.

Lastly, it is important to consider that the SACZ exhibits large geographic variability in the magnitude, extent, and location. Carvalho et al. (2004) classified the SACZ based on oceanic vs. continental locations and weak vs. intense version of each category. Differences in the magnitude and location of the SACZ may lead to considerable variations in the synoptic circulation. It is likely given the small sample set used in the composite analysis in the current study that the variation in both MCCs and the SACZ is not fully represented. For these reasons, future work should include a greater sample size of MCCs or other thunderstorm events, or concentrate on modeling efforts in order to explore the results presented here in greater detail.

4.6 References

Ashley, W. S., T. L. Mote, P. G. Dixon, S. L. Trotter, J. D. Durkee, E. J. Powell, and A. J. Grundstein, 2003: Effects of mesoscale convective complex rainfall on the distribution of precipitation in the United States. *Mon. Wea. Rev.*, **131**, 3003-3017.

Augustine, J. A., and K. W. Howard, 1991: Mesoscale convective complexes over the United States during 1986 and 1987. *Mon. Wea. Rev.,* **119,** 1575–1589.

Barros, V., M. Doyle, M. González, I. Camilloni, R. Bejarán, and R. M. Caffera, 2002: Revision of the South American monsoon system and climate in subtropical South America south of 20° S. *Meteorológica*, **27**, 33-57.

Berbery, E. H., and E. A. Collini, 2000: Springtime and water vapor flux over southeastern South America. *Mon. Wea. Rev.,* **128**, 1328–1346.

Berbery, E. H., and V. R. Barros, 2002: The hydrologic cycle of the La Plata Basin in South America. *J. Hydr. Meteor.,* **3**, 630-645.

Carvalho, L. M. V., C. B. Jones, and B. Liebmann, 2002: Extreme precipitation events in southern South America and large-scale convective patterns in the South Atlantic Convergence Zone. *J. Climate,* **15**, 2377-2394.

Carvalho, L. M. V., C. B. Jones, and B. Liebmann, 2004: The South Atlantic Convergence Zone: Intensity, Form, Persistence, Relationships with Intraseasonal to Interannual Activity and Extreme Rainfall. *J. Climate*, **17**, 88-108.

Cotton, W. R., R. L. McAnelly, and C. J. Tremback, 1989: A composite model of mesoscale convective complexes. *Mon. Wea. Rev.,* **117**, 765 -783.

CPTEC, 2008: Climanálise: Boletim de monitoramento e análise climatica. São José Dos Campos, Sao Paulo, Brazil. [available online: http://www6.cptec.inpe.br/revclima/boletim].

Durkee, J. D. and T. L. Mote, 2008: A climatology of warm-season mesoscale convective complexes in subtropical South America. Submitted to *Int. J. Climatol*.

Figueroa, S. N., P. Satyamurty, and P. L. da Silva Dias, 1995: Simulations of the summer circulation over the South American region with an eta coordinate model. *J. Atmos. Sci.,* **52**, 1573–1584.

Fritsch, J. M., R. J. Kane, and C. R. Chelius, 1986: The contribution of mesoscale convective weather systems to the warm-season precipitation in the United States. *J. Appl. Meteor.*, **25**, 1333-1345.

Huffman, G. J., R.F. Adler, D. T. Bolvin, G. Gu, E. J. Nelkin, K. P. Bowman, Y. Hong, E. F. Stocker, D. B. Wolff, 2007: The TRMM Multi-satellite Precipitation Analysis: Quasi-global, multi-year, combined-sensor precipitation estimates at fine scale. *J. Hydrometeor*., **8**, 38-55.

Jones, C. B., and L. M. V. Carvalho, 2002: Active and break periods in the South America monsoon system. *J. Climate,* **15,** 905–914.

Kalnay, E., and Coauthors, 1996: The NCEP/NCAR 40-Year Reanalysis Project. *Bull. Amer. Meteor. Soc.,* **77,** 437–471.

Kane, R. J., C. R. Chelius, and J. M. Fritsch, 1987: Precipitation characteristics of mesoscale convective weather systems. *J. Appl. Meteor.*, **26**, 1345–1357.

Kodama, Y.-M., 1992: Large-scale common features of sub-tropical convergence zones (the Baiu frontal zone, the SPCZ, and the SACZ). Part II: Conditions of the circulations for generating the STCZs. *J. Meteor. Soc. Japan,* **71,** 581–610.

Laing, A. G., J. M. Fritsch, and A. J. Negri, 1999: Contribution of mesoscale convective complexes to rainfall in Sahelian Africa: Estimates from geostationary infrared and passive microwave data. *J. Appl. Meteor.*, **38**, 957–964.

Laing, A. G., and J. M. Fritsch, 2000: The large-scale environments of the global populations of mesoscale convective complexes. *Mon. Wea. Rev.,* **128**, 2756-2776.

Lenters, J. D., and K. H. Cook, 1999: Summertime precipitation variability over South America: Role of the large-scale circulation. *Mon. Wea. Rev.,* **127,** 409–431.

Liebmann, B., G. N. Kiladis, J. A. Marengo, T. Ambrizzi, and J. D. Glick, 1999: Submonthly Convective Variability over South America and the South Atlantic Convergence Zone. *J. Climate*, **12**, 1877-1891.

Liebmann, B., G. N. Kiladis, C. S. Vera, A. C. Saulo, and L. M. V. Carvalho, 2004: Subseasonal variations of rainfall in South America in the vicinity of the low-level jet east of the Andes and comparison to those in the South Atlantic Convergence Zone. *J. Climate*, **17**, 3829-3842.

Maddox, R. A., 1980: Mesoscale convective complexes. *Bull. Amer. Meteor. Soc*., **61**, 1374-1387.

Maddox, R. A., 1983: Large-scale meteorological conditions associated with mid-latitude mesoscale convective complexes. *Mon. Wea. Rev.* **111**, 1475-1493.

Marengo, J. A., M. W. Douglas, and P. L. Silva Dias, 2002: The South American low-level jet east of the Andes during the 1999 LBATRMM and LBA-WET AMC campaign. *J. Geophys. Res.,* **107,** 8079, doi:10.1029/2001JD001188.

McAnelly, R. L., W. R. Cotton, 1989: The precipitation life cycle of mesoscale convective complexes over the central United States. *Mon. Wea. Rev.*, **117**, 784-808.

National Oceanic Atmospheric Administration, Comprehensive Large-Array Stewardship System, 2007: Silver Spring, MD. [available online: http://www.class.noaa.gov].

Nicolini, M., and A. C. Saulo, 2000: ETA characterization of the 1997–98 warm season Chaco jet cases. Preprints, *Sixth Int.Conf. on Southern Hemisphere Meteorology and Oceanography,* Santiago, Chile, Amer. Meteor. Soc., 330–331.

Nieto Ferreira, R. N., T. M. Rickenbach, D. L., Herdies, and L. M. V. Carvalho, 2003: Variability of South American Convective Cloud Systems and Tropospheric Circulation during January–March 1998 and 1999. *Mon. Wea. Rev*., **131**, 961–973.

Nogués-Paegle, J., and K. C. Mo, 1997: Alternating wet and dry conditions over South America during summer. *Mon. Wea. Rev.,* **125,** 279–291.

Salio, P. and Nicolini M., 2007: Mesoscale convective systems over southeastern South America and their relationship with the South American low-level jet. *Mon. Wea. Rev*., **135**, 1290-1308.

Saulo C., J. Ruiz, and Y. G. Skabar, 2007: Synergism between the low-level jet and organized convection at its exit region. *Mon. Wea. Rev*., **135**, 1310-1326.

Silva, V. B. S. and E. H. Berbery, 2006: Intense rainfall events affecting the La Plata Basin. *J. Hydr. Meteor.,* **7**, 769-787.

Smull, B. F., and J. A. Augustine, 1993: Multi-scale analysis of a mature mesoscale convective complex. *Mon. Wea. Rev.,* **121,** 103–132.

Velasco, I., and J. M. Fritsch, 1987: Mesoscale convective complexes in the Americas. *J. Geophys. Res*., **92**, 9591–9613.

Vera, C., J. Baez, M. Douglas, C. B. Manuel, J. Marengo, J. Meitin, M. Nicolini, J. Nogués-Paegle, J. Paegle, O. Penalba, P. Salio, M. A. Silva Dias, P. Silva Dias, and E. Zipser, 2006: The South American Low-Level Jet Experiment. *Bull. Amer. Meteor. Soc.,* **87**, 63–77.

Zipser, E., P. Salio, and M. Nicolini, 2004: Mesoscale convective systems activity during SALLJEX and the relationship with SALLJ. *CLIVAR Exchanges,* No. 9, International CLIVAR Project Office, Southampton, United Kingdom, 14–16.

Table 4.1. Mesoscale Convective Complex definition based on analyses of infrared satellite imagery.

Mesoscale Convective Complex (MCC) Definition	
Criterion	**Physical Characteristics**
Size	Interior cold cloud region with temperature of ≤ -52°C must have an area 50,000 km^2
Initiation	Size definition first satisfied
Duration	Size definition must be met for a period of ≥ 6 hours.
Maximum Extent	Contiguous cold-cloud shield (IR temperature -52°C) reaches maximum size.
Shape	Eccentricity (minor axis/major axis) ≥ 0.7 at time of maximum extent.
Terminate	Size definition is no longer satisfied
MCC definition originally developed by Maddox (1980)	

Table 4.2. Summary of MCCs, and SACZ and non-SACZ periods during October-March for 1998-2997. The % indicates the frequency proportion of the total number of warm-season days from each period.

Season	SACZ				No SACZ			
	No. of days	**%**	**No. of MCCs**	**MCCs per day**	**No. of days**	**%**	**No. of MCCs**	**MCCs per day**
1998-99	29	16	2	0.07	153	84	27	0.18
1999-00	54	30	14	0.26	129	70	22	0.17
2000-01	18	10	0	0.00	165	90	27	0.16
2001-02	35	19	7	0.20	147	81	32	0.22
2002-03	34	19	8	0.24	148	81	21	0.14
2003-04	31	17	7	0.23	152	83	18	0.12
2004-05	45	25	7	0.16	138	75	17	0.12
2005-06	58	32	13	0.22	124	68	26	0.21
2006-07	75	41	17	0.23	107	59	26	0.24
Total	**379**		**75**		**1261**		**216**	
Mean	**42**	**23**	**8**	**0.18**	**140**	**77**	**24**	**0.17**

Table 4.3. MCC composite characteristics based the presence and absence of the SACZ. The * indicates statistically significant difference of means.

MCC physical characteristics	SACZ	No SACZ
Duration (h)	12.9	13.6
*Maximum extent (km^2)	210,667	261,652
Rainfall Area (km^2)	302,131	361,188
Rainfall Volume (km^3)	4.7	6.3
Rain Rate (km^3 hr^{-1})	0.33	0.39
*Latitude	24.46°S	25.57°S
*Longitude	54.31°W	55.83°W

Table 4.4. The difference between the number of MCCs per SACZ day and non-SACZ day for each warm season. Positive (negative) values indicate more MCCs per non-SACZ day (SACZ day).

Season	MCC rate Difference
1998-99	0.11
1999-00	-0.09
2000-01	0.16
2001-02	0.02
2002-03	-0.10
2003-04	-0.11
2004-05	-0.04
2005-06	-0.01
2006-07	0.01

Table 4.5. Monthly percent of SACZ days (total number of SACZ days/ total number of days in a month) and the percent of MCCs that occurred during SACZ days (total number of MCC SACZ days/total number of SACZ days), respectively, given by the ordered pairs in each cell. Bold underlined values highlight SACZ months with SACZ days and no MCCs. N is the number of SACZ and non-SACZ MCCs in each season, respectively.

OCT	NOV	DEC	JAN	FEB	MAR	
+	**20,0**	+	**42,0**	29,20	+	1998-99 N = 2:27
36,15	23,22	16,58	19,50	21,25	+	1999-00 N=14:22
+	+	**44,0**	**13,0**	+	+	2000-01 N = 0:27
+	13,17	19,40	+	36,23	+	2001-02 N = 7:32
+	+	26,23	36,48	**4,0**	+	2002-03 N = 8:21
+	+	+	48,29	25,30	+	2003-04 N = 7:18
+	7,67	26,36	10,40	32,10	**41,0**	2004-05 N = 7:17
+	30,44	32,17	29,31	14,43	26,20	2005-06 N=13:26
13,0	27,10	36,35	45,42	36,33	**16,0**	2006-07 N=17:26

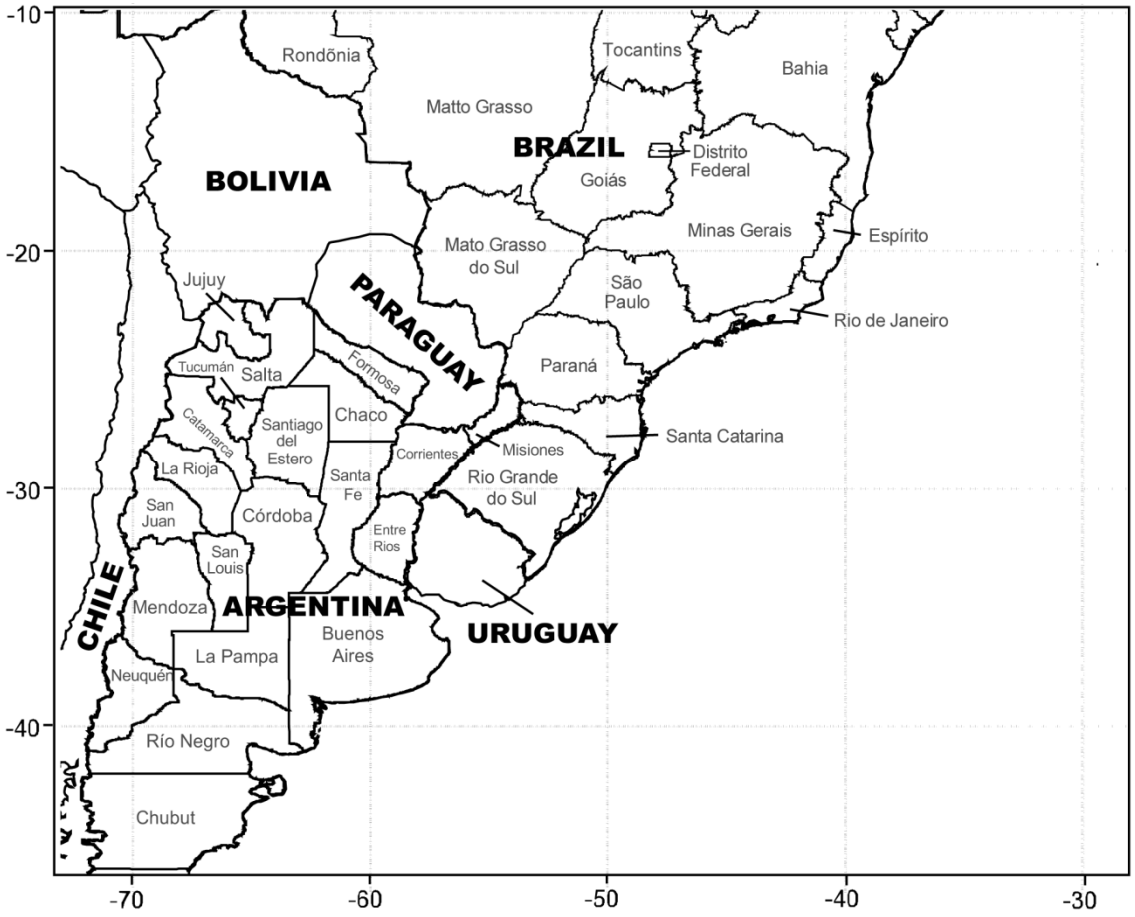

Fig. 4.1. Subtropical South America, including the states of Brazil and the provinces of Argentina.

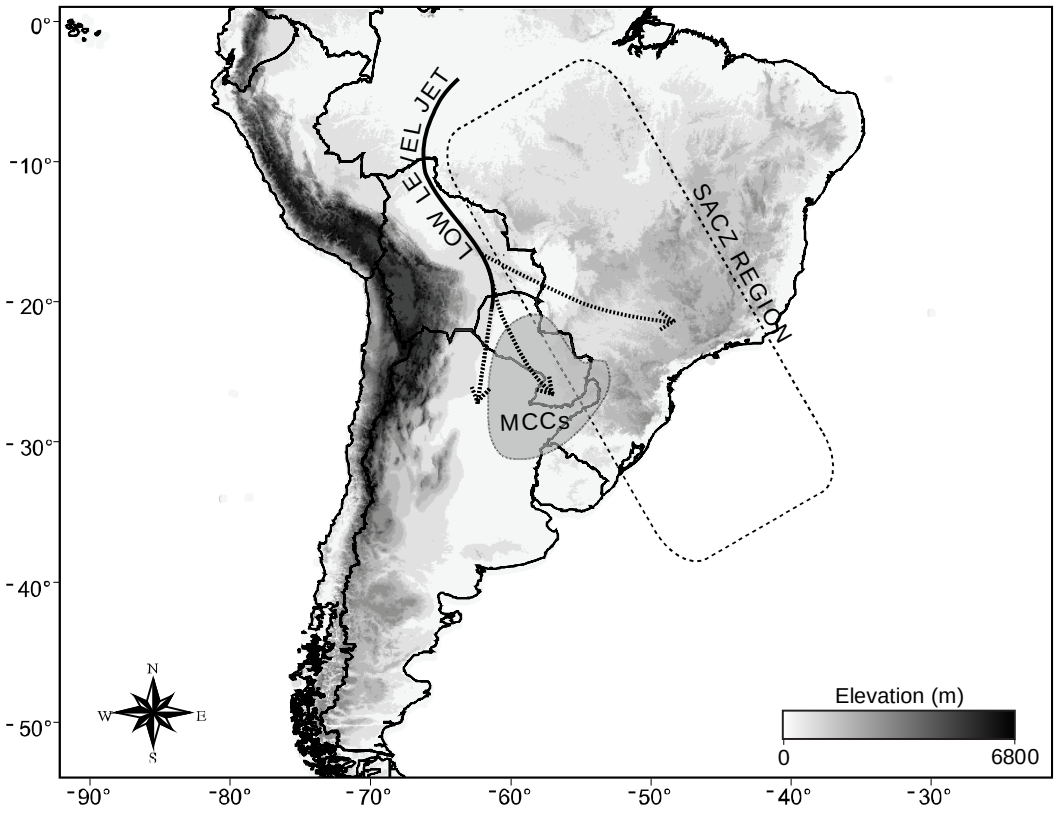

Fig. 4.2. Schematic diagram illustrating the SACZ region (hatched box) across South America. Arrows depict common routes of the northerly LLJ throughout the warm season. The shaded area represents the area with the greatest MCC activity and widespread MCC rainfall contributions ranging between 30-50%.

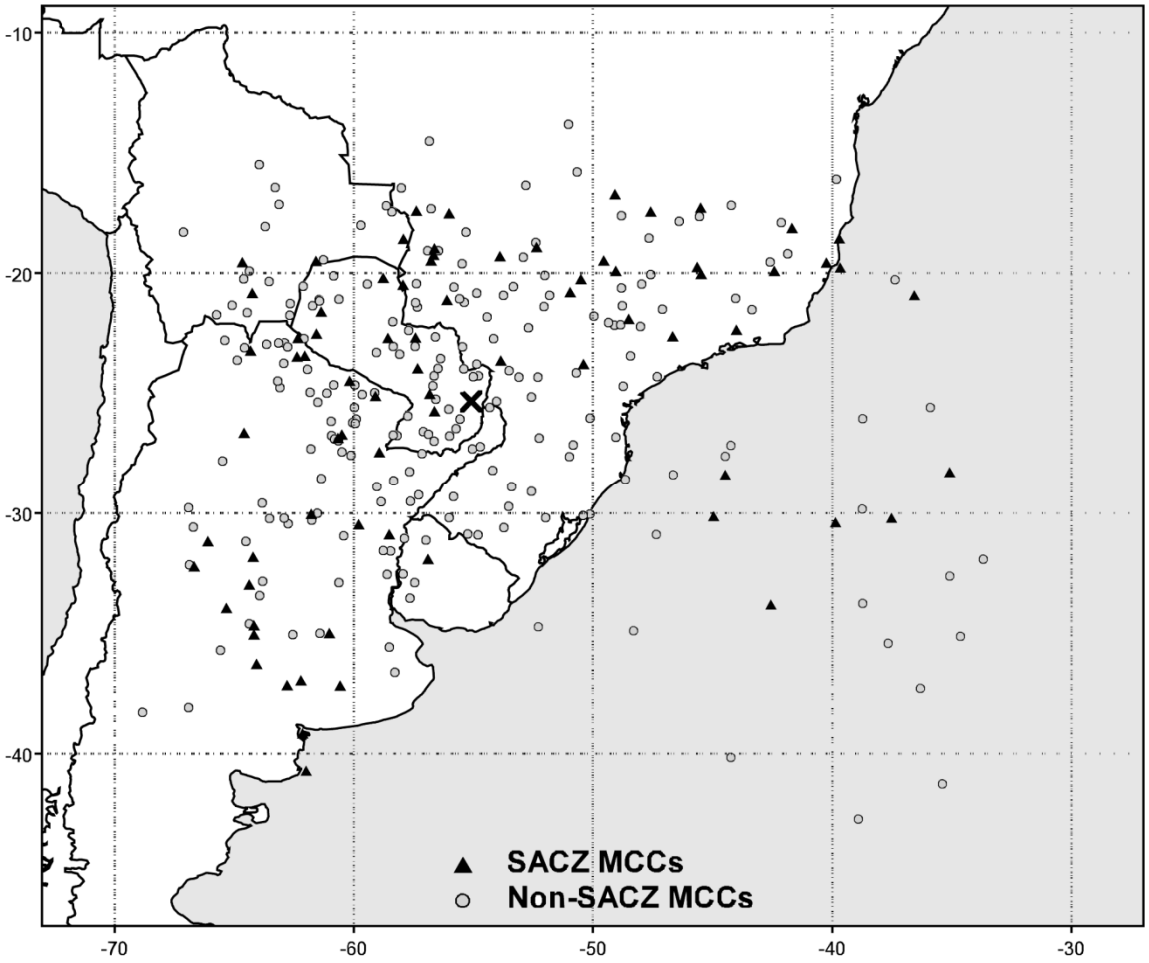

Fig. 4.3. Spatial distribution of the 291 MCCs between October-March for 1998-2007 during the time of maximum extent. Dots indicate MCCs that occurred when the SACZ was not present, whereas triangles indicate MCCs during SACZ days. The "x" located in southeast Paraguay indicates the mean position of all MCCs at the time of maximum extent.

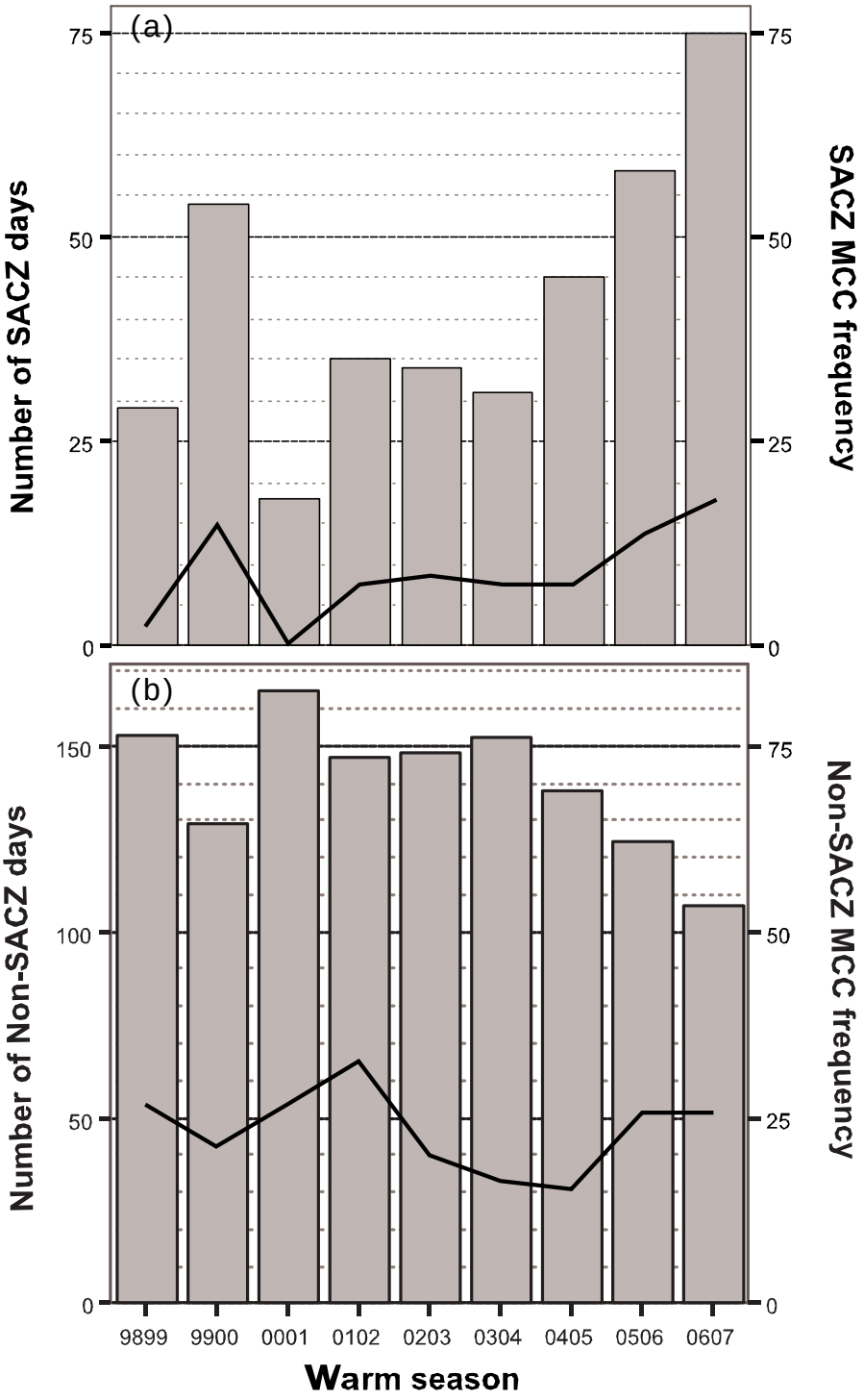

Fig. 4.4. The number of MCCs (bold line) and the number of days during (a) SACZ and (b) non-SACZ periods (bars).

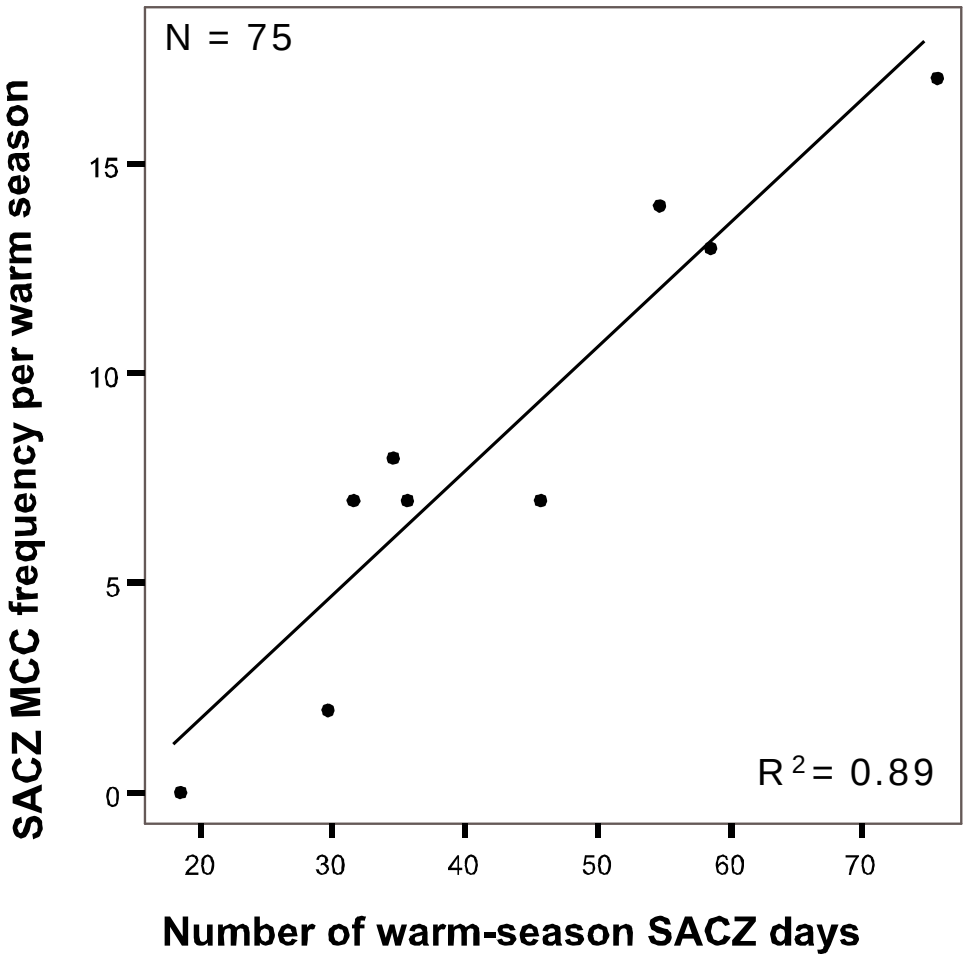

Fig. 4.5. MCC frequency (only during the presence of the SACZ) and the number of SACZ days in each warm season. Line shows the linear regression model fit of these data. N = 75 MCCs that occurred during the SACZ for the nine warm seasons of 1998-2007.

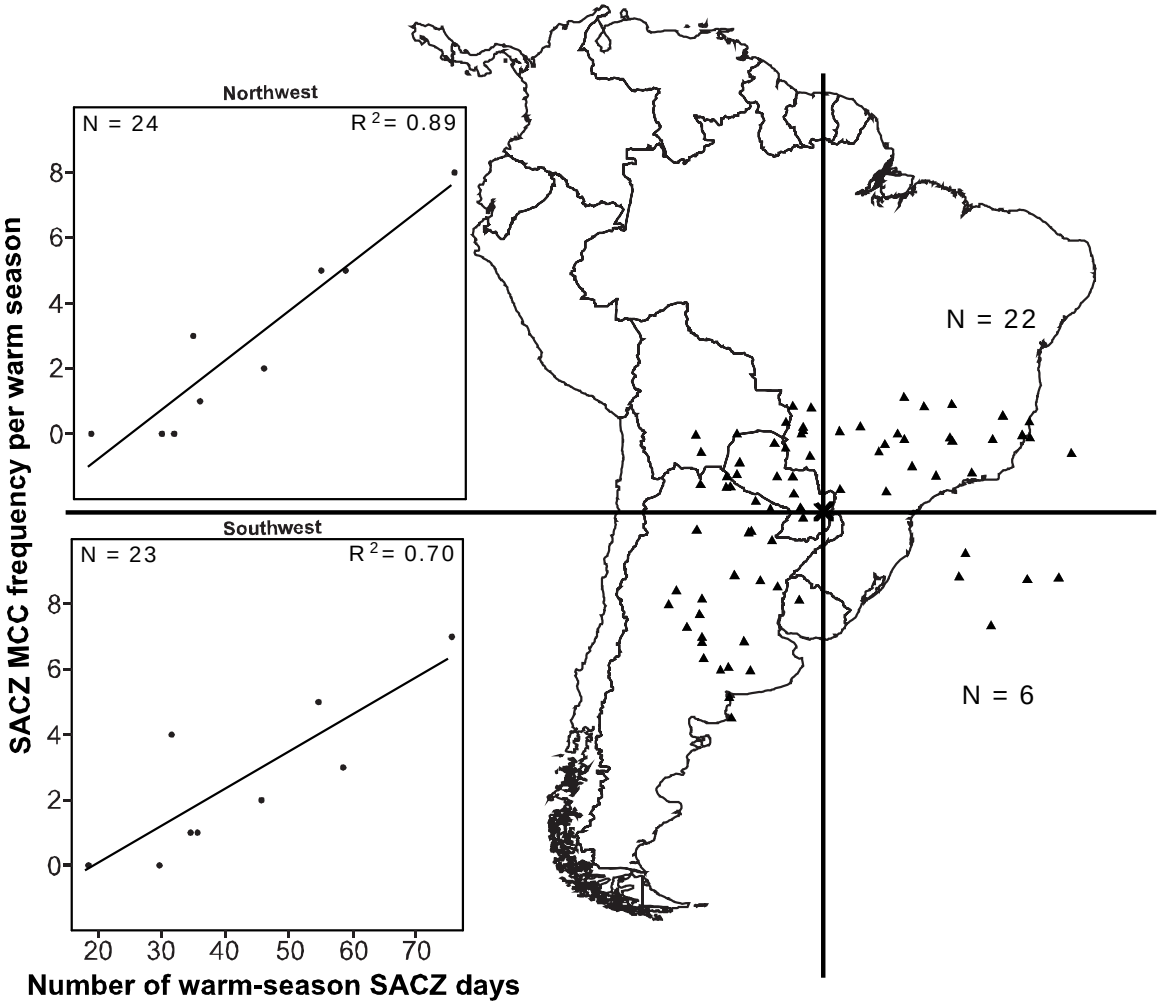

Fig. 4.6. Spatial distribution of MCCs that occurred during SACZ periods. Linear regression models are the same as in Fig. 4.5 except by quadrants centered on the geographic mean (see Fig. 4.1).

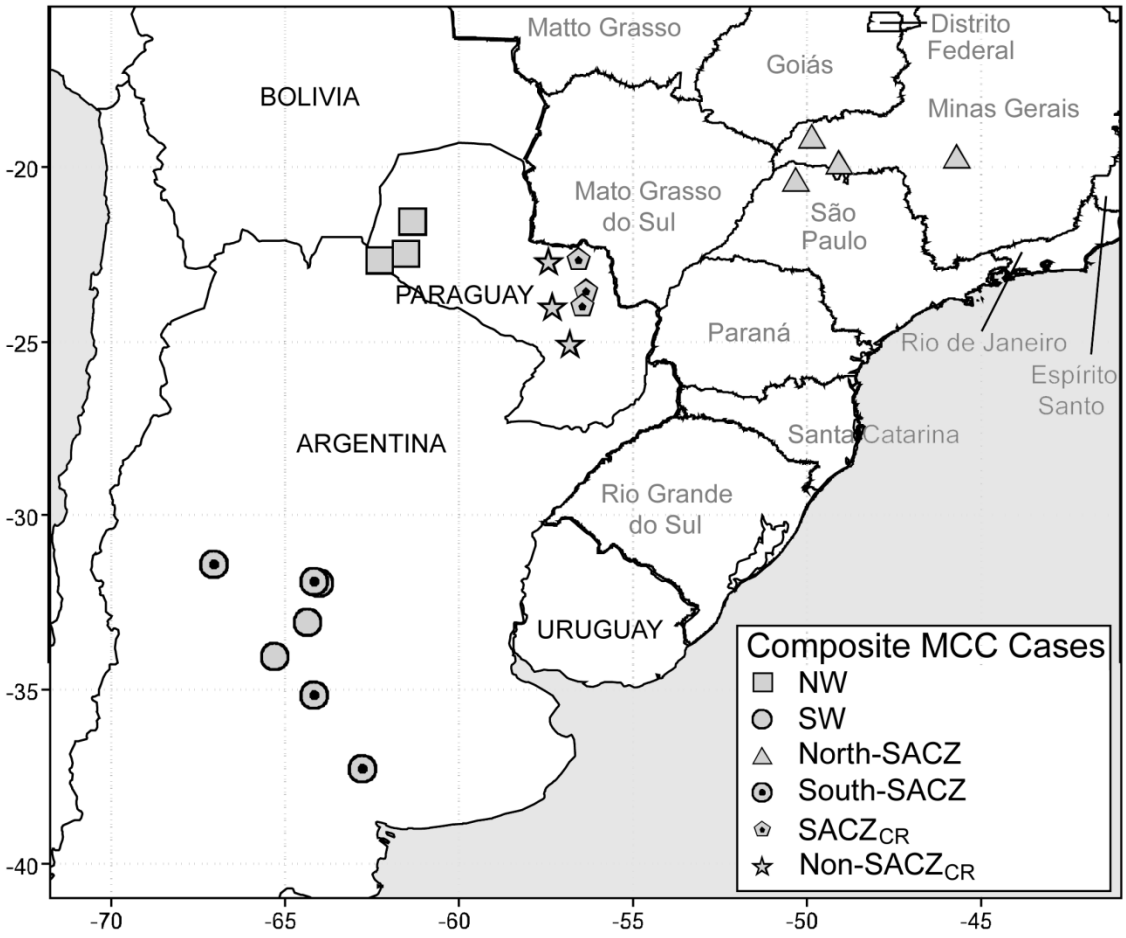

Fig. 4.7. Locations of composite SACZ MCC subsets for the northwest and southwest quadrants (squares and circles, respectively; see Fig. 4.6), SACZ region (North-SACZ, triangles), high-latitude region (South-SACZ, circles with dots), and core MCC region (pentagons with dots), and non-SACZ MCCs in the core region (stars) and systems located inside the primary MCC region (see Fig. 4.2).

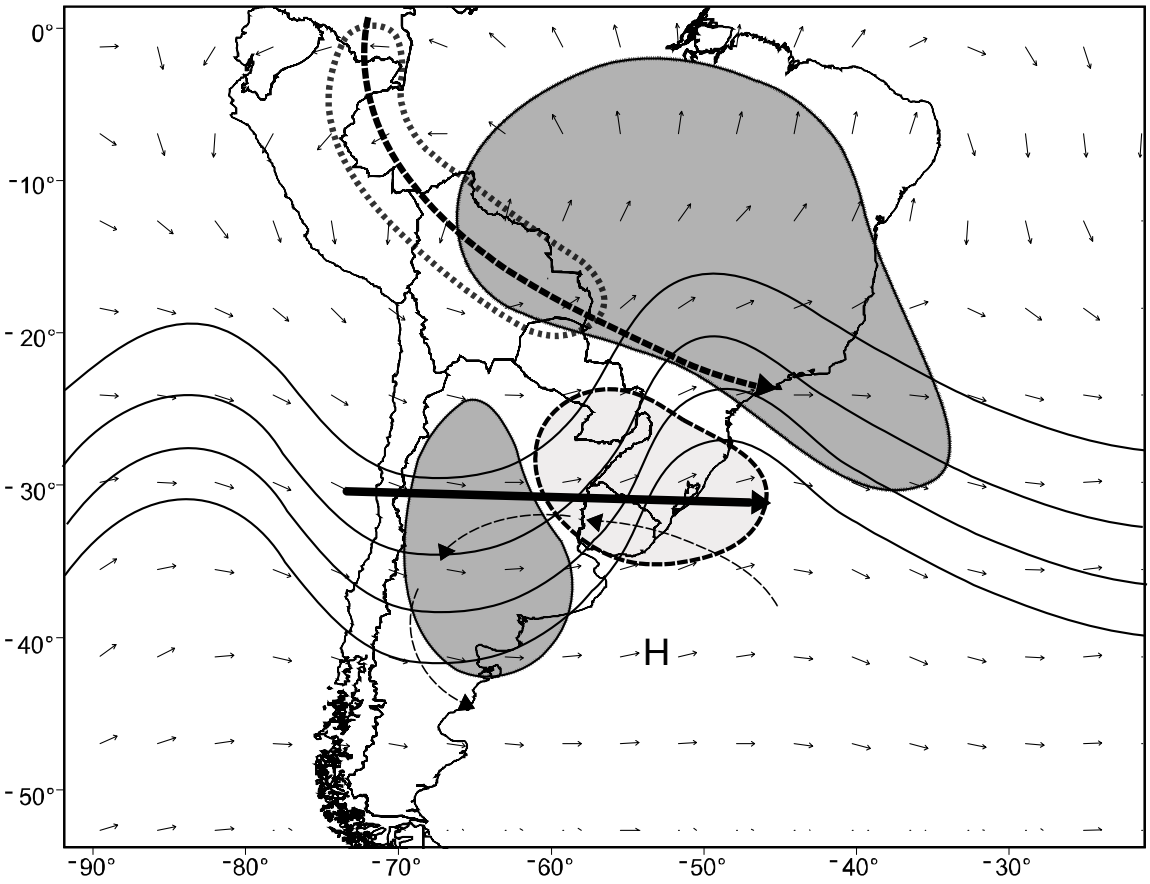

Fig. 4.8. Schematic diagram illustrating composite synoptic environment for MCCs that occurred during SACZ periods. Surface anticyclone is shown by the bold "H"; Bold dashed arrow with hatched circle indicates the direction and location of the strongest 850 hPa winds; long thin arrows near 30°S indicate 850 hPa-wind circulation; thin-line wave pattern shows 500 hPa geopotential height configuration; dark (light) shaded regions show areas of upward (downward) 500 hPa vertical velocity; small thin arrows are 200 hPa wind directions; long bold arrow is the axis of the 200 hPa jet streak.

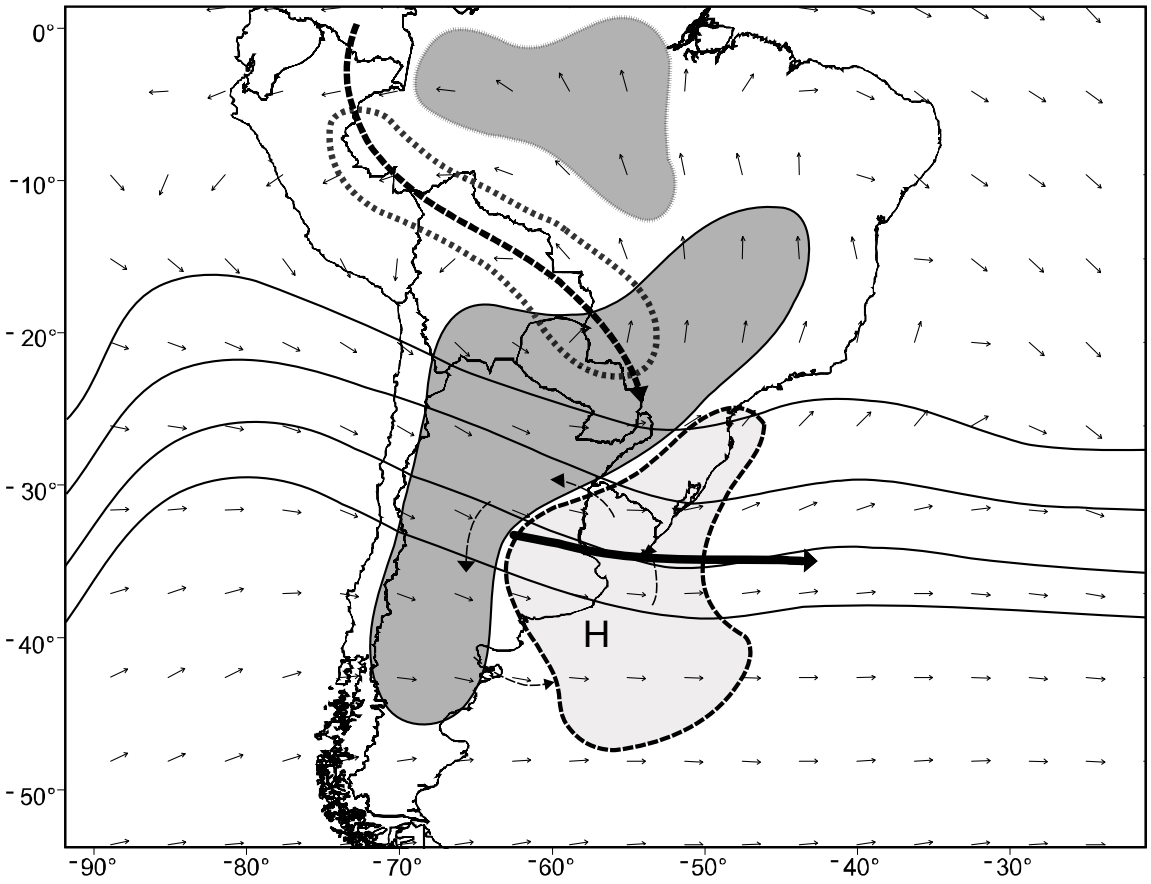

Fig. 4.9. As in Fig. 4.8 except for systems located inside the MCC region (see Fig. 4.1) during non-SACZ days.

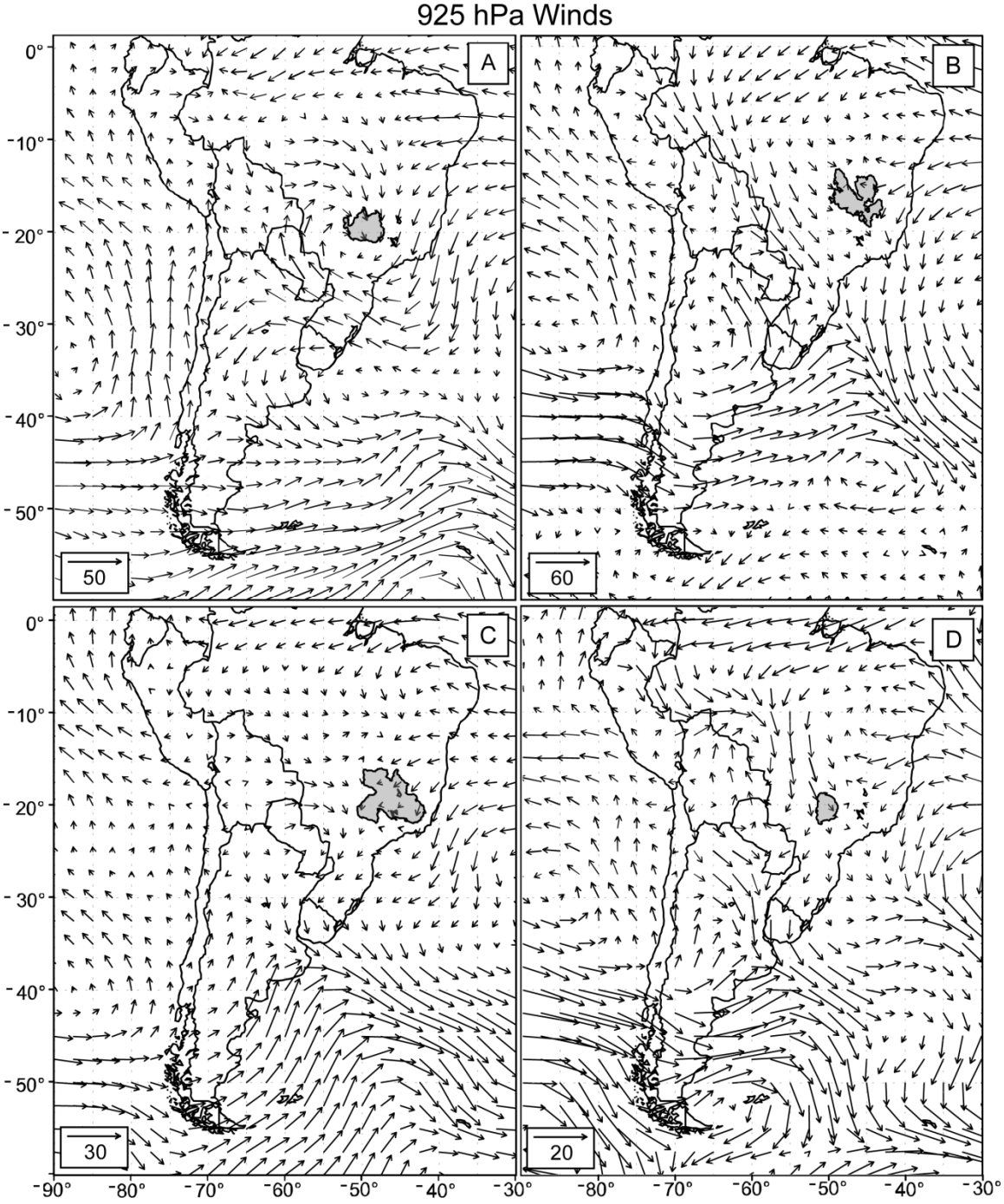

Fig. 4.10. 925 hPa wind vectors and the locations of MCCs (shaded areas) that occurred during (a) 1-8 January 2000, (b) 24-28 November 2005, (c), 27 January-2 February 2006, and (d) 27 December 2006-16 January 2007 SACZ periods.

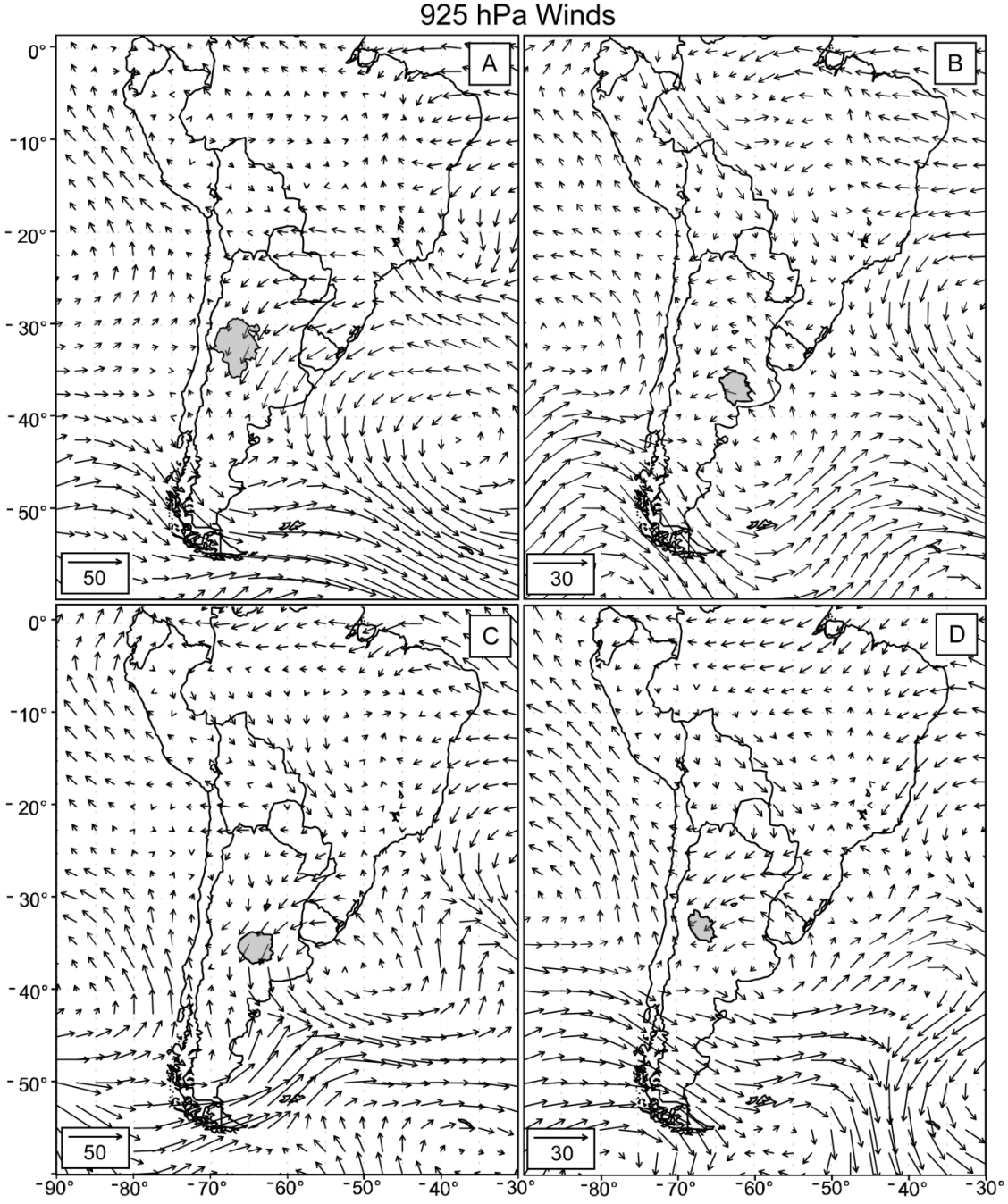

Fig. 4.11. As in Fig. 12 except for "South" MCCs that took place during (a) 17-25 November 1999, (b) 1-8 January 2000, (c) 27 January-2 February 2006, and (d) 27 December 2006-16 January 2007 SACZ periods.

CHAPTER 5

SUMMARY AND CONCLUSIONS

5.1 Overview

South American weather and climate are driven by the combination of complex physiographic landscapes, diverse land-cover, and the position of the continent with respect to prevailing large-scale atmospheric circulation and adjacent ocean bodies. The abundance of heat and moisture transported from both the Amazon rainforest and Atlantic Ocean fuel some the world's largest, most intense thunderstorms, particularly in the subtropics (Zipser et al. 2006). The impact of the rainfall from these thunderstorms on the communities within subtropical South America (SSA) varies from beneficial to perilous. Much of the rainfall from large, long-lived thunderstorms across SSA helps to sustain the economy as a natural resource for agricultural industries (Mechoso et al. 2001). However, intense prolonged rainfall from organized thunderstorms often leads to floods that result in the spreading of diseases, property and crop damages, injuries, and deaths (IPCC 2007; Jonkman 2005; Carvalho et al. 2002; Mechoso et al. 2001; Velasco and Fritsch 1987). Given the wide range of impacts from heavy rainfall events in SSA, the overarching goal of this dissertation was to assess the climatology, rainfall characteristics, and the influence of large-scale atmospheric circulation on the largest thunderstorm class of mesoscale convective systems, the mesoscale convective complex (MCC).

MCCs are often associated with prodigious rainfall totals, distributed over sizeable areas that account for large fractions of the total rainfall for various regions around the world (e.g., Ashley et al. 2003; Laing et al. 1999; McAnelly and Cotton 1989; Fritsch et al. 1986). While some studies focusing on South American convection and precipitation have included investigations of the characteristics of large, long-lived thunderstorms, there is a paucity of research on MCC over South America. Some studies of South American MCCs focused only on specific events or concentrated on MCCs across relatively smaller areas within the continent (e.g., Figueiredo and Scolar 1996; Duquia and Silva Dias 1994; Rocha 1992; Scolar and Figueiredo 1990; Silva Dias 1987; Guedes 1985; Guedes and Silva Dias 1984). In one of the pioneering investigations of South American MCCs, Velasco and Frisch (1987) found MCC activity was highly concentrated within the subtropical region (20°S-40°S) during their study period (1981-1983). Results from their study also showed that MCCs in South America were larger and longer-lived than MCCs in the United States. Based on their limited sample of two years, it was hypothesized that MCCs in SSA were significant in terms of size, duration, and rainfall production and contribution, particularly with respect MCCs in the U.S. Therefore, a longer period of record was necessary in order to better understand and describe the physical characteristics of MCCs in SSA.

5.2 Summary

a. Subtropical South American MCC climatology

The purpose of the first manuscript (Chapter 2) was to improve our understanding of South American MCCs by examining these events during the warm-season (October-May) for the period 1998-2007. During the period of record, 330 MCCs were documented. SSA experienced a mean occurrence of 37 MCCs each warm season with peak frequencies in December and January over northern Argentina, Paraguay, and portions of southern Brazil. Although the mean warm-season frequencies documented in Velasco and Fritsch (1987) and this study are similar, Velasco and Fritsch (1987) found November as the month of peak MCC occurrence. Contrary to the findings in Velasco and Fritsch (1987), this dissertation shows that the variability in MCC frequency throughout the warm season appears to be strongly connected to the seasonal solar cycle. This is apparent given that 80% of all MCCs occurred during November through March. Furthermore, the MCCs examined in this dissertation were predominantly nocturnal events that typically lasted 14 hours and reached maximum cloud-shield sizes of 256,500 km^2. When compared to the MCCs documented by Velasco and Fritsch (1987), the results presented here show that MCCs are 27% larger and 2.5 hours longer than they documented.

While the differences in the findings between Velasco and Fritsch (1987) and this dissertation highlight the importance of examining a longer period of record, both studies showed that MCCs are very large, long-lasting, and frequently occurring events in SSA. This is particularly true when compared to MCCs in the U.S. MCCs in SSA were

hypothesized to contribute substantially to rainfall totals across the region, given their large size and frequent occurrence, which was examined further in the second manuscript (Chapter 3).

b. MCC rainfall

The purpose of the second manuscript (Chapter 3) was to quantify MCC rainfall, determine the contribution of MCCs to the total rainfall across SSA, and assess the impact of MCC rainfall on regional precipitation anomalies. In order to quantify warm-season rainfall in data-sparse areas across SSA, the Tropical Rainfall Measuring Mission Multi-Satellite Precipitation Analysis (TMPA) 3B42 Version 6 data (Huffman et al. 2007) were combined with the MCC dataset developed in the first manuscript (Chapter 2). The result from the second manuscript (Chapter 3) provided a unique perspective on the role of MCC rainfall in South American precipitation variability, which helps extend our global understanding of MCCs.

During 1998-2007, MCCs produced an average of 15.7 mm of rainfall over 381,000 km^2, with a volume of 7.0 km^3. MCCs accounted for 15-21% of the total warm-season rainfall across portions of northern Argentina and Paraguay. When examined on intraseasonal time scales, MCC rainfall contributions ranged from 11-20% during all warm-season months across much of this region. For some areas of northern Argentina and Paraguay, MCCs accounted for 20-30% of the total rainfall between November-February, and 30-50% in December. MCCs contributed 30-66% and 30-40% of the total rainfall across the central-western provinces of Mendoza, Neuquén, and La Pampa in Argentina during November and May, respectively (see Fig. 1.1). When compared to the

monthly analysis, interannual MCC rainfall contributions were higher, accounting for ≥ 50% of the total rainfall across SSA.

These findings reveal the important role MCCs play in monthly and annual rainfall totals across much of SSA. Another way to portray the importance of MCC rainfall is to examine MCC rainfall totals in relation to warm-season precipitation anomalies. In order to determine the magnitude of the effect of MCC rainfall on precipitation anomalies, a MCC Impact Factor (MIF) was developed. The MIF simply identified locations where anomaly values changed by ≥ 0.5 standard deviations due to MCC rainfall, and used a MIF magnitude ranking scale of 1-6 at intervals of 0.5 standard deviations. A comparison of the locations of various MIF magnitudes in relation to the given rainfall anomaly helps identify the impact of MCCs on areas that received above or below average seasonal rainfall totals.

Results from the MIF analysis showed that MCC rainfall had an impact (i.e., ≥ MIF-1) on many areas of SSA in each of the nine warm-seasons. The 2000-01 warm season was unique in that only MIF-1 was observed. However, many locations of MIF-1 were found in areas of below-average rainfall (particularly southern and southeastern Brazil). The extent of the impact was greatest during 1999-2000 with MIF-1 as the dominant magnitude. Anomalously dry conditions were collocated with zero impact of MCC rainfall across Uruguay, northeastern Argentina, and southeastern Brazil during 2005-06. However, MIF-4 and MIF-5 were collocated with near average rainfall just to the northwest, which suggests that the abrupt change from below-average to normal rainfall across this area was largely a result of MCCs. Overall, the MIF analysis

demonstrated that MCC rainfall can help sustain average rainfall conditions, as well as prevent (exacerbate) rainfall deficit (surplus) across many areas within SSA.

c. MCCs and the South Atlantic Convergence Zone

The purpose of the third manuscript (Chapter 4) was to determine characteristic changes in South American MCCs as they relate to the presence of the South Atlantic Convergence Zone (SACZ), a quasi-stationary band of convection from the Amazon Basin into the Atlantic Ocean. The SACZ is closely monitored by the Center for Weather Forecast and Climatic Studies (CPTEC) within the Brazilian Ministry of Science and Technology's National Institute for Space and Research (INPE) between October-March. CPTEC provides archived monthly climate bulletins (*Climanálise*) that detail the timing of the onset and demise of SACZ episodes. The datasets developed in the previous manuscripts (Chapters 2 and 3) were combined with the SACZ data provided by CPTEC to examine alterations in the large-scale atmospheric circulation during the SACZ that were conducive MCC development across the study region.

During October-March of 1998-2007, the SACZ occurred during 23% of the warm season days, during which 75 MCCs formed, versus 216 on non-SACZ days. The number of MCCs per SACZ and non-SACZ day was 0.18 and 0.17, respectively. Although the rate of MCC occurrence in each period was very similar, the mean location of SACZ MCCs was 240 km northeast of the non-SACZ location. This shift toward the SACZ region was expected because of the changing position and direction of the low-level flow of heat and moisture toward the SACZ region that has been shown in previous studies. Furthermore, most of the interannual variation (89%) in the number of MCCs

during periods of SACZ was due to changes in the frequency of SACZ. This relationship was particularly strong across portions of Bolivia and northwest Paraguay, and central Argentina.

Composite analyses of several tropospheric data fields of subsets of SACZ MCCs across the study region (e.g., Bolivia and northwest Paraguay, central Argentina, and the SACZ region) showed the direct and indirect influence of the SACZ on MCCs. During the SACZ, some MCCs located ≤ 20°S developed in the vicinity of the northwesterly low-level corridor of heat and moisture transport. Other systems developed in the SACZ region where the convergence of westerly and northeasterly winds in association with the Amazonian LLJ and subtropical Atlantic high was often observed. Farther south in central Argentina, some MCCs developed in the vicinity of low-level easterly flow from anti-cyclonic circulations off the coast of Argentina and Uruguay. This study is unique in showing a link between an MCC genesis region and low-level circulation other than the northerly, tropical advection of heat and moisture. Much of previous MCC research has shown MCC development and maintenance are connected to the exit region of the LLJ. Contrary to the findings from previous MCC research, the development of some MCCs, particularly higher-latitude systems in South America, is dominated by moisture fluxes from low-level anti-cyclonic flow off the coast in the Atlantic during SACZ periods. Together, these findings demonstrate the direct and indirect influences of the SACZ on the development and maintenance of MCCs across portions of tropical and subtropical South America, through its effect on the synoptic environment.

5.3 Conclusions

Results from this dissertation extend our global understanding of the role of MCCs, particularly with respect to subtropical South American precipitation variability. Prior to this work, South American MCCs were largely un-studied, with the exception of the pioneering research by Velasco and Fritsch (1987). This dissertation has shown that MCCs in SSA are large, long-lived events that produce copious amounts of rainfall over sizeable areas. These events account for large fractions of the total precipitation across SSA, and they have been shown to have a substantial impact on regional precipitation anomalies. Furthermore, this study utilizes innovative techniques to provide a new perspective on monthly and warm-season precipitation patterns across SSA.

However, due to strict MCC classification criteria used in this study, it is likely that the inclusion of other large MCSs would show that even higher rainfall contributions are the result of large mesoscale convective systems. Further investigations should examine differences in fractional rainfall contributions of MCCs and other large MCSs. These types of studies are increasingly important given that the most recent Assessment Report from the Intergovernmental Panel on Climate Change (IPCC 2007) suggests that heavy precipitation events are very likely to increase throughout the next century. The result of the projected increase due to anthropogenic climate change would likely contribute to nearly 20% increased rainfall and up to 40% increased annual runoff across portions of SSA (IPCC 2007). Increases in flood frequency and magnitude from heavy rainfall events, including rainfall resulting from MCCs, will likely contribute to considerable property loss and disruptions of industry and society. Lastly, increases in heavy precipitation events and their resultant flooding will likely lead to an increased risk

of injuries, diseases, and loss of life (IPCC 2007). Perhaps the work presented here will raise the awareness, and harness a better understanding of the characteristics and behavior of heavy precipitation events such as MCCs, so that the people and economy of SSA are less vulnerable to these potential threatening changes in climate across the region.

REFERENCES

Anderson, C. J., and R. W. Arritt, 1998: Mesoscale convective complexes and persistent elongated convective systems over the United States during 1992 and 1993. *Mon. Wea. Rev.*, **126**, 578–599.

Anderson, C. J., and R. W. Arritt, 2001: Mesoscale convective systems over the United States during the 1997-1998 El Niño. *Mon. Wea. Rev.*, **129**, 2443-2457.

Ashley, W. S., T. L. Mote, P. G. Dixon, S. L. Trotter, J. D. Durkee, E. J. Powell, and A. J. Grundstein, 2003: Effects of mesoscale convective complex rainfall on the distribution of precipitation in the United States. *Mon. Wea. Rev.*, **131**, 3003-3017.

Augustine, J. A., 1985: An automated method for the documentation of cloud-top characteristics of mesoscale convective systems. NOAA Tech. Memo. ERL ESG-10, NOAA/FSL, Boulder, CO, 121 pp.

Augustine, J. A., and K. W. Howard, 1988: Mesoscale convective complexes over the United States during 1985. *Mon. Wea. Rev.*, **116**, 685-701.

Augustine, J. A., and K. W. Howard, 1991: Mesoscale convective complexes over the United States during 1986 and 1987. *Mon. Wea. Rev.*, **119,** 1575–1589.

Barber, D. and H. Huhdanpaa, 1996: The quickhull algorithm for convex hulls. ACM Transactions on Mathematical Software, **22**, 469-483.

Barros, V., M. Doyle, M. González, I. Camilloni, R. Bejarán, and R. M. Caffera, 2002: Revision of the South American monsoon system and climate in subtropical South America south of 20° S. *Meteorológica*, **27**, 33-57.

Bartels, D. L., and A. A. Rockwood, 1983: Internal structure and evolution of a dual mesoscale convective complex. Preprints, *Fifth Conf. on Hydrometeorology,* Tulsa, OK, Amer. Meteor. Soc., 97–102.

Berbery, E. H., and E. A. Collini, 2000: Springtime and water vapor flux over southeastern South America. *Mon. Wea. Rev.*, **128**, 1328–1346.

Berbery, E. H., and V. R. Barros, 2002: The hydrologic cycle of the La Plata Basin in South America. *J. Hydr. Meteor.*, **3**, 630-645.

Carvalho, L. M. V., C. Jones 2001: A satellite method to identify structural properties of mesoscale convective systems based on maximum spatial correlation tracking technique (MASCOTTE). *J. Appl. Meteor*., **40**, 1683–1701.

Carvalho, L. M. V., C. B. Jones, and B. Liebmann, 2002: Extreme precipitation events in southern South America and large-scale convective patterns in the South Atlantic Convergence Zone. *J. Climate,* **15**, 2377-2394.

Carvalho, L. M. V., C. B. Jones, and B. Liebmann, 2004: The South Atlantic Convergence Zone: Intensity, Form, Persistence, Relationships with Intraseasonal to Interannual Activity and Extreme Rainfall. *J. Climate*, **17**, 88-108.

Collander, R. S., and E. I. Tollerud, 1993: Characteristics of extreme rainfall in mesoscale convective complexes: a phenomenological study. Preprints, *13th Conference on Weather Analysis and Forecasting*, August 2-6, 1993: Vienna, Virginia, 393-396.

Cotton, W. R., R. L. McAnelly, and C. J. Tremback, 1989: A composite model of mesoscale convective complexes. *Mon. Wea. Rev.,* **117**, 765 -783.

CPTEC, 2008: Climanálise: Boletim de monitoramento e análise climatica. São José Dos Campos, Sao Paulo, Brazil. [available online: http://www6.cptec.inpe.br/revclima/boletim].

Curtis, S., 2008: The El Niño-Southern Oscillation and global precipitation. *Geography Compass*, **2**, 600-619.

Durkee, J. D. and T. L. Mote, 2008: A climatology of warm-season mesoscale convective complexes in subtropical South America. Submitted to *Int. J. Climatol*.

Duquia, C. G. and M. A. F. Silva Dias, 1994: Complexo convectivo de mesoescala: um estudo de caso para o oeste do Rio Grande do Sul. In: VIII Congresso Brasileiro de Meteorologia, SBMET, **2**, 610-612.

Ebert, E., J. E. Janowiak, and C. Kidd, 2007: Comparison of near real-time precipitation estimates from satellite observations and numerical models. *Bull. Amer. Meteor. Soc.*, **88**, 47-64.

Figueiredo, J. C. and J. Scolar, 1996: Estudo da trajetória dos sistemas convectivos de mesoescala na América do Sul. In: VII Congresso Latino-Americano e Iberico de Meteorologia, Buenos Aires, 165-166.

Figueroa, S. N., P. Satyamurty, and P. L. da Silva Dias, 1995: Simulations of the summer circulation over the South American region with an eta coordinate model. *J. Atmos. Sci.,* **52**, 1573–1584.

Fritsch, J. M., R. J. Kane, and C. R. Chelius, 1986: The contribution of mesoscale convective weather systems to the warm-season precipitation in the United States. *J. Appl. Meteor.*, **25**, 1333-1345.

Grimm, A. M., S. E. T. Ferraz, and J. Gomes, 1998: Precipitation anomalies in Southern Brazil associated with El Niño and La Niña events. *J. Climate,* **11,** 2863–2880.

Grimm, A. M., V. R. Barros, and M. E. Doyle, 2000: Climate variability in southern South America associated with El Niño and La Niña events. *J. Climate,* **13,** 35–58.

Guedes, R. L. and M. A. F. Silva Dias, 1984: Estudo de tempestades severas associadas com o jato subtropical na América do Sul. In: III Congresso Brasileiro de Meteorologia, SBMET. Belo Horizonte, MG, 3-7 Dezembro, **1**, 289-296.

Guedes, R. L., 1985: Condições de grande escala associadas a sistemas convectivos de mesoescala sobre a região central da América do Sul**.** Dissertação de Mestrado. São Paulo, SP, IAG/USP, 89 pp.

Houze, R. A., B. F. Smull, and P. Dodge, 1990: Mesoscale organization of springtime rainstorms in Oklahoma. *Mon. Wea. Rev.,* **118**, 613-654.

Huffman, G. J., R.F. Adler, D. T. Bolvin, G. Gu, E. J. Nelkin, K. P. Bowman, Y. Hong, E. F. Stocker, D. B. Wolff, 2007: The TRMM Multi-satellite Precipitation Analysis: Quasi-global, multi-year, combined-sensor precipitation estimates at fine scale. *J. Hydrometeor*., **8**(1), 38-55.

Huffman, G. J., and D. T. Bolvin, 2007: Real-time TRMM multi-satellite precipitation analysis data set documentation. Laboratory for Atmospheres, NASA Goddard Space Flight Center and Science Systems and Applications, Inc. [available online: ftp://meso.gsfc.nasa.gov/pub/trmmdocs/3B42_3B43_doc.pdf].

IPCC, 2007: Climate Change 2007: Synthesis report. Contribution of Working Groups I, II, and III to the Fourth Assessment Report of the Intergovernmental Panel on Climate Change. IPCC, Geneva, Switzerland, 104 pp. [available online: http://www.ipcc.ch/ipccreports/ar4-syr.htm].

James, J., 1992: A preliminary study of mesoscale convective complexes over the mid-latitudes of eastern Australia. Tech. Report 66, Bureau of Meteorology, Melbourne, Australia, 30 pp.

Jackson, J. E., 1991: A user's guide to principal component analysis. Wiley-Interscience, 569 pp.

Jones, C. B., and L. M. V. Carvalho, 2002: Active and break periods in the South America monsoon system. *J. Climate,* **15,** 905–914.

Jonkman, S. N., 2005: Global perspectives on loss of human life caused by floods. *Nat. Hazards*., **34**, 151-175.

Kalnay, E., and Coauthors, 1996: The NCEP/NCAR 40-Year Reanalysis Project. *Bull. Amer. Meteor. Soc.,* **77,** 437–471.

Kane, R. J., 1985: The temporal and spatial characteristics of precipitation from mesoscale convective weather systems. M.S. thesis, The Pennsylvania State University, 152 pp.

Kane, R. J., C. R. Chelius, and J. M. Fritsch, 1987: Precipitation characteristics of mesoscale convective weather systems. *J. Appl. Meteor.*, **26**, 1345–1357.

Kodama, Y.-M., 1992: Large-scale common features of sub-tropical convergence zones (the Baiu frontal zone, the SPCZ, and the SACZ). Part II: Conditions of the circulations for generating the STCZs. *J. Meteor. Soc. Japan,* **71,** 581–610.

Kummerow, C., J. Simpson, O. Thiele, W. Barnes, A. T. C. Chang, E. Stocker, R. F. Adler, A. Hou, R. Kaka, F. Wentz, P. Ashcroft, T. Kozu, Y. Hong, K. Okamoto, T. Iguchi, H. Kuroiwa, E. Im, Z. Haddad, G. Huffman, B. Ferrier, W. S. Olson, E. Zipser, E. A. Smith, T. T. Wilheit, G. North, T. Krishnamurti, and K. Nakamura, 2000: The status of the Tropical Rainfall Measuring Mission (TRMM) after two years in orbit. *J. Appl. Meteor*., **39**, 1965–1982.

Laing, A. G., and J. M. Fritsch, 1993a: Mesoscale convective complexes in Africa. *Mon. Wea. Rev.,* **121,** 2254–2263.

Laing, A. G., and J. M. Fritsch, 1993b: Mesoscale convective complexes over the Indian monsoon region. *J. Climate*, **6**, 911–919.

Laing, A. G., and J. M. Fritsch, 1997: The global population of mesoscale convective complexes. *Quart. J. Roy. Meteor. Soc.,* **123**, 389–405.

Laing, A. G., J. M. Fritsch, and A. J. Negri, 1999: Contribution of mesoscale convective complexes to rainfall in Sahelian Africa: Estimates from geostationary infrared and passive microwave data. *J. Appl. Meteor.*, **38**, 957–964.

Laing, A. G., and J. M. Fritsch, 2000: The large-scale environments of the global populations of mesoscale convective complexes. *Mon. Wea. Rev.,* **128**, 2756-2776.

Lau, K. M. and J. Zhou, 2003: Anomalies of the South American summer monsoon associated with the 1997-99 El Niño-Southern Oscillation. *Int. J. Climatol.*, **23**, 529-539.

Lenters, J. D., and K. H. Cook, 1999: Summertime precipitation variability over South America: Role of the large-scale circulation. *Mon. Wea. Rev.,* **127,** 409–431.

Liebmann, B., G. N. Kiladis, J. A. Marengo, T. Ambrizzi, and J. D. Glick, 1999: Submonthly Convective Variability over South America and the South Atlantic Convergence Zone. *J. Climate*, **12**, 1877-1891.

Liebmann, B. and J. A. Marengo, 2001: Interannual variability of the rainy season and rainfall in the Brazilian Amazon Basin. *J. Climate*, **14**, 4308-4318.

Liebmann, B., G. N. Kiladis, C. S. Vera, A. C. Saulo, and L. M. V. Carvalho, 2004: Subseasonal variations of rainfall in South America in the vicinity of the low-level jet east of the Andes and comparison to those in the South Atlantic Convergence Zone. *J. Climate*, **17**, 3829-3842.

Machado, L. A. T., W. B. Rossow, R. L. Guedes, and A. W. Walker, 1998: Life cycle variations of mesoscale convective systems over the Americas. *Mon. Wea. Rev.,* **126**, 1630-1654.

Maddox, R. A., 1979: A methodology for forecasting heavy convective precipitation and flash flooding. *Natl. Wea. Dig.*, **4**, 30-42.

Maddox, R. A., 1980: Mesoscale convective complexes. *Bull. Amer. Meteor. Soc.*, **61**, 1374-1387.

Maddox, R. A., 1983: Large-scale meteorological conditions associated with mid-latitude mesoscale convective complexes. *Mon. Wea. Rev.* **111**, 1475-1493.

Marengo, J. A., M. W. Douglas, and P. L. Silva Dias, 2002: The South American low-level jet east of the Andes during the 1999 LBATRMM and LBA-WET AMC campaign. *J. Geophys. Res.,* **107,** 8079, doi:10.1029/2001JD001188.

Marengo, J., W. R. Soares, C. Saulo, and M. Nicolini, 2004: Climatology of the LLJ east of the Andes as derived from the NCEP reanalyses: characteristics and temporal variability. *J. Climate,* **17,** 2261–2280.

McAnelly, R. L., W. R. Cotton, 1986: Meso-β-scale characteristics of an episode of meso-α-scale convective complexes. *Mon. Wea. Rev.*, **114**, 1740-1770.

McAnelly, R. L., W. R. Cotton, 1989: The precipitation life cycle of mesoscale convective complexes over the central United States. *Mon. Wea. Rev.*, **117**, 784-808.

Mechoso, R. C., P.S. Días, W. Baetghen, V. Barros, E.H. Berbery, R. Clarke, H. Cullen, C. Ereño, B. Grassi and D. Lettenmaier, 2001: Climatology and Hydrology of the La Plata Basin. *Document of VAMOS/CLIVAR document*, 56 pp. [available online: http://www.clivar.org/organization/vamos/index.htm].

Merritt, J. H., and J. M. Fritsch, 1984: On the movement of the heavy precipitation areas of mid-latitude mesoscale convective complexes. Preprints, *10th Conf. Weather Forecasting and Analysis,* AMS, Tampa, FL, 529, 536.

Miller, D. and J. M. Fritsch, 1991: Mesoscale convective complexes in the western Pacific region. *Mon. Wea. Rev.*, **119**, 2978–2992.

Mota, G. V., 2003: Characteristics of rainfall and precipitation features defined by the Tropical Rainfall Measuring Mission over South America. Ph.D. dissertation, University of Utah, 215 pp.

NOAA, Comprehensive Large-Array Stewardship System, 2007: Silver Spring, MD. [available online: http://www.class.noaa.gov].

Nesbitt, E., J. Zipser, and D. J. Cecil, 2000: A census of precipitation features in the tropics using TRMM: radar, ice scattering, and lightning observations. *J. Climate*, **13**, 4087-4106.

Nicolini, M., and A. C. Saulo, 2000: ETA characterization of the 1997–98 warm season Chaco jet cases. Preprints, *Sixth Int.Conf. on Southern Hemisphere Meteorology and Oceanography,* Santiago, Chile, Amer. Meteor. Soc., 330–331.

Nieto Ferreira, R. N., T. M. Rickenbach, D. L., Herdies, and L. M. V. Carvalho, 2003: Variability of South American Convective Cloud Systems and Tropospheric Circulation during January–March 1998 and 1999. *Mon. Wea. Rev.*, **131**, 961–973.

Nogués-Paegle, J., and K. C. Mo, 1997: Alternating wet and dry conditions over South America during summer. *Mon. Wea. Rev.,* **125,** 279–291.

Orlanski, I., 1975: A rational subdivision of scales for atmospheric processes. *Bull. Amer. Meteor. Soc.*, **56**, 527-530.

Rocha, R. P., 1992: Simulação numérica de sistema de mesoescala sobre a América do Sul. Dissertação de Mestrado. São Paulo. IAG/USP.

Rodgers, D. M., K. W. Howard, and E. C. Johnston, 1983: Mesoscale convective complexes over the United States during 1982. *Mon. Wea. Rev.,* **111**, 2363-2369.

Ropelewski, C. F., and M. S. Halpert, 1987: Global and regional scale precipitation patterns associated with the El Niño/Southern Oscillation. *Mon. Wea. Rev.,* **115**, 1606–1625.

Salio, P. and Nicolini M., 2007: Mesoscale convective systems over southeastern South America and their relationship with the South American low-level jet. *Mon. Wea. Rev.*, **135**, 1290-1308.

Sapiano, M. R. P. and P. A. Arkin, (2008): An inter-comparison and validation of high resolution satellite precipitation estimates with three-hourly gauge data. Submitted to *J. Hydr. Meteor.*

Saulo C., J. Ruiz, and Y. G. Skabar, 2007: Synergism between the low-level jet and organized convection at its exit region. *Mon. Wea. Rev*., **135**, 1310-1326.

Scolar, J. and J. C. Figueiredo, 1990: . Análise das condições sinóticas associadas à formação de Complexos Convectivos de Mesoescala. In: VI Congresso Brasileiro de Meteorologia, SBMET, **2**, 457-461.

Silva, V. B. S. and T. Ambrizzi, 2006: Inter-El Niño variability and its impact on the South American low-level jet east of the Andes during austral summer –two case studies. *Advances in Geosciences*, **6**, 283-287.

Silva, V. B. S. and E. H. Berbery, 2006: Intense rainfall events affecting the La Plata Basin. *J. Hydr. Meteor.,* **7**, 769-787.

Silva Dias, M. A. F., 1987: de Mesoescala e Previsão de Tempo à Curto Prazo. *Revista Brasileira de Meteorologia*, **2**, 133-150.

Smull, B. F., and J. A. Augustine, 1993: Multi-scale analysis of a mature mesoscale convective complex. *Mon. Wea. Rev.,* **121,** 103–132.

Thompson, M. V., B. Palma, J. T. Knowles, and N. M. Holbrook, 2003: Clima multiannual en el Parque Nacional Pan de Azúcar, Desierto de Atacama, Chile. *Revista Chilena de Historia Natural*, **76**, 235-254.

Tollerud, E. I., D. Rodgers, and K. Brown, 1987: Seasonal, diurnal, and geographic variations in the characteristics of heavy-rain-producing mesoscale convective complexes: A synthesis of eight years of MCC summaries. Preprints, *11th Conf. Weather Modification*. Edmonton, Alta., Canada, 143-146.

Tollerud, E. I. and D. M. Rodgers, 1991: The seasonal and diurnal cycle of mesoscale convection and precipitation in the central United States: Interpreting a 10-year satellite-based climatology of mesoscale convective complexes. Preprints, *7th Conference on Applied Meteorology*. Salt Lake City, Utah, 63-70.

Tollerud, E. I. and R. S. Collander, 1993: Mesoscale convective systems and extreme rainfall in the central United States. *Extreme Hydrological Events: Precipitation, Floods and Droughts, International Association of Hydrological Sciences* Number *213*, 11-19.

Velasco, I., and J. M. Fritsch, 1987: Mesoscale convective complexes in the Americas. *J. Geophys. Res*., **92**, 9591–9613.

Vera, C., J. Baez, M. Douglas, C. B. Manuel, J. Marengo, J. Meitin, M. Nicolini, J. Nogués-Paegle, J. Paegle, O. Penalba, P. Salio, M. A. Silva Dias, P. Silva Dias, and E. Zipser, 2006: The South American Low-Level Jet Experiment. *Bull. Amer. Meteor. Soc.,* **87**, 63–77.

Viana, D. R., 2006: Avaliação da precipitação e desastres naturais associados a complexos convectivos de mesoescala no Rio Grande Do Sul entre Outubro e Dezembro de 2003. M. S. thesis, Universidade Federal do Rio Grande Do Sul, 136 pp.

Zipser, E., P. Salio, and M. Nicolini, 2004: Mesoscale convective systems activity during SALLJEX and the relationship with SALLJ. *CLIVAR Exchanges,* No. 9, International CLIVAR Project Office, Southampton, United Kingdom, 14–16.

Zipser, E. J., D. J. Cecil, C. Liu, S. W. Nesbitt, and D. P. Yorty, 2006: Where are the most intense thunderstorms on Earth?. *Bull. Amer. Meteor. Soc*., **87**, 1057–1071.